Role of eIF4A in mRNA recruitment to the initiating ribosome

By
Paul Yourik

A dissertation submitted to Johns Hopkins University in conformity with the requirements for the degree of Doctor of Philosophy

Baltimore, MD
May 2017

Abstract

Control of protein synthesis is a fundamental process necessary for life and energetically one of the most expensive phases of gene expression. The majority of translational control takes place during the initiation step. To start the process, the methionyl-initiator tRNA (Met-tRNAi), along with a dozen eukaryotic initiation factors (eIF), forms a 43S pre-initiation complex (PIC) with the small (40S) subunit of the ribosome and an mRNA intended for translation. At this point the PIC is in an "open" conformation and is poised to bind an mRNA in a process referred to as mRNA recruitment. eIFs 4A, 4B, 4E, and 4G – collectively referred to as mRNA recruitment factors – orchestrate this process and are all critical for efficient translation initiation. During the last decade great progress was made toward understanding the mechanisms governing eukaryotic translation initiation; however, many questions, old and new, surrounding mRNA recruitment remain unanswered.

We developed and implemented various kinetic assays, together with an *in vitro* reconstituted *S. cerevisiae* translation initiation system to dissect the roles of eIF4 factors in mRNA recruitment with a particular focus on eIF4A. We demonstrated that eIF4A ATPase activity is faster in the presence of the PIC, suggesting a previously unreported functional interaction, which we dissected using *in vitro* biochemistry and biophysics. Next, we attempted to connect eIF4A ATPase with mRNA unwinding but despite numerous approaches, we could not directly monitor eIF4A helicase activity in the context of the PIC. In contrast, addition of other similar helicases resulted in robust helicase activity detected well by radiometric and photometric assays. This prompted us to holistically monitor how eIF4A promotes recruitment of mRNAs to the PIC ranging in length, degree of structure, position of structure with respect to the 5'-end, and the effect of the 5'-7-methylguanosine

cap. eIF4A significantly accelerated the rate of recruitment for every mRNA tested, including a 50-mer comprising CAA repeats $(CAA)_n$ expected to lack any substantial secondary structure. Our findings also show that global mRNA structure, rather than the 5'-UTR alone, is the primary determinant of kinetics governing eukaryotic translation initiation. We propose that eIF4A serves to relax global mRNA structure, engages the PIC, and may even directly modulate the PIC as is the case for other DEAD-box ribonucleoprotein complexes in biology.

Thesis Advisor: Dr. Jon Lorsch

Thesis Reader: Dr. Rachel Green

Acknowledgements

As I was preparing to leave my job in Cincinnati to attend Johns Hopkins in August of 2011, my technical manager was giving me some final advice and equated the mind to a piece of metal, which with time and hard work can be shaped into a more elegant object. As expected, the "hard work and time" is definitely applicable to the process of obtaining a PhD but I could never have done it without all of the people in my life.

First, I am grateful to Jon for his fantastic mentorship over the years. At the beginning of graduate school, I was greatly intimidated by the constant question of what experiment am I to perform next and the general feeling of being "lost in the lab." In retrospect, Jon's style of mentorship and our move to the NIH in the summer of 2013 was exactly what I needed. As I was getting comfortable in the lab and living in Baltimore, the announcement came that we were moving to the National Institutes of Health. I am particularly thankful for Jon's patience with me during that time – allowing me to weigh all of my options – and him finding a way for me to be able to come to the NIH with minimal disruption to my studies. As we set up our lab at the NIH and got back to work, Jon's style of mentorship was not the easiest for a graduate student, especially at a place where everyone else had a PhD. He allowed me to figure things out while making sure that I didn't stray too far. Third year of graduate school was particularly tough but I have never walked away from a meeting with Jon without an encouraging comment and support. Lastly, I would like to thank Jon for allowing me to pursue various career development opportunities, including pausing my work in his lab and leaving for a full time internship the summer before my sixth year. During my time in the lab, I feel that I learned a lot more than I bargained for, including how to set up a new lab and move a -80°C freezer (containing 15 years of work) in the middle of the summer. Importantly, Jon's mentorship allowed me to become a more

independent thinker; something that I feel was my biggest challenge when I first walked into the Lorsch lab at Hopkins.

I am also greatly indebted and thankful to all of my colleagues who mentored me on a daily basis and made my graduate experience an enjoyable five years of my twenties. The first months in the lab Sarah and Vaishnavi patiently taught me lab protocols and the basics of translation initiation. Also, Jagpreet, Tony, Shardul, Neha, Daoming, and Fujun were great colleagues, always provided sound advice in scientific and general discussions, and have all become my friends. Jagpreet might be one of the most approachable people I have ever met in my professional life. After Vaishnavi left the lab, I became closer with Colin who over the years became like a second PI to me. Colin taught and challenged me to improve my presentation style, writing, and experimental approach for which and I am extremely thankful (although at this point I am convinced that I just don't have it in me to independently pick pretty colors when making a figure and avoid heavy use of passive voice in my writing). In addition to our lab members, I would also like to thank all the members of our "NIH Supergroup" including the labs of Alan Hinnebusch, Tom Dever, and Nick Guydosh. I feel truly lucky to have had so many leaders in our field present at every lab meeting. Finally, I would like to thank Rachel Green, James Stivers, and James Berger for being on my thesis committee and providing guidance over the years as I matured as a scientist.

My graduate education would not have been possible without the hard work of the staff at Johns Hopkins and the NIH. At Hopkins, I am particularly thankful to Jess, Arhonda, Sharon, and Christina in BCMB, as well as Carolyn – our fearless BCMB program director – and Teri in the Department of Biophysics. Also, Nancy Richman and Brenda Hanning did a tremendous job helping us move to the NIH.

Finally, I would like to thank my incredible and supportive family and my friends for being there for me, celebrating my successes, and keeping me sane during the tough times. I feel that an entire chapter of this thesis can be dedicated to the sacrifices, love, and support people close to me have provided over the years. In the next seven years I hope to develop my career as well as my personal and professional relationships. At that point I will be 37 years old and will have been friends with certain people for 20 years or more. Also, I hope my career will be developing quite well by then. At the age of 37, my parents reset their lives and left Russia (when they were doing just fine) to give me a chance at a better future.
This is for you.

Table of Contents

List of Figures

Chapter 1

Introduction: mRNA recruitment to the ribosome in eukaryotic translation initiation

Paul Yourik[1,2] and Jon R. Lorsch[2]

[1] Johns Hopkins University School of Medicine

Baltimore, MD

[2] Laboratory on the Mechanism and Regulation of Protein Synthesis

The Eunice Kennedy Shriver National Institute of Child Health and Human Development

Bethesda, MD

Introduction

Despite dramatic differences among various life forms, protein synthesis – catalyzed by the ribosome (translation) – is conserved in all living organisms on Earth. In fact, a famous study relied on the ribosomal RNA sequence to define the three main domains of life (Woese & Fox, 1977). Translation is critical (and depending on the research focus, is central) for cellular gene expression requiring large energetic investments and precise regulation (Roux & Topisirovic, 2012). The four main steps of translation are initiation, elongation, termination, and recycling (Dever & Green, 2012; Hinnebusch & Lorsch, 2012). Initiation is marked by assembly of the translational apparatus at the start codon of an mRNA – usually an AUG – with the methionyl initiator tRNA (tRNAi) in the peptidyl site of the ribosome. The small subunit (40S) is bound by the large subunit (60S) together forming an 80S ribosome poised for protein synthesis. Successive rounds of elongation add amino acids, one at a time, to the growing polypeptide chain. The message encoded in the mRNA dictates the order of tRNAs delivering amino acids to the nascent protein chain. This process continues until the machinery reaches a stop signal (stop codon), triggering the third step: termination. At this point the assembled polypeptide chain is released from the 80S complex. The last step of translation, recycling, splits the 80S back into 40S and 60S subunits and prepares the machinery to start another round of protein synthesis.

Translation Initiation

The first step of translation is initiation. The main goal of this process is to assemble the translational apparatus on the start codon of an mRNA with the tRNAi in the P-site of the ribosome. In bacteria, Shine-Dalgarno (SD) sequence complementarity between the 16S

ribosomal RNA within the small subunit of the ribosome (30S) and a region of mRNA upstream of the start codon, positions the ribosome at the start codon (Milón & Rodnina, 2012). In addition, bacterial translation initiation requires three initiation factors (IF) IF1, IF2, and IF3. IF2 is a GTPase that delivers the initiator tRNA charged with *N*-Formylmethionine (fMet-tRNA(fMet)) to the complex. IF1 binds in the A-site of the 30S and stabilizes the binding of IF2 and IF3, meanwhile IF3 ensures proper joining of the large (50S) subunit to the complex (Gualerzi & Pon, 2015; Laursen, Sørensen, Mortensen, & Sperling-Petersen, 2005). Together, these factors facilitate proper translation initiation and start site selection for protein synthesis in bacteria.

In contrast to bacteria, eukaryotes do not rely on a SD sequence, and eukaryotic mRNAs are often more complicated; some have extremely long 5'-untranslated regions (5' UTRs) and varying degrees of structural complexity. Accordingly, a host of 12 eukaryotic translation initiation factors (eIF) – comprising over 20 polypeptides – orchestrates translation initiation in eukaryotes (Figure 1.1). To start, eukaryotic translation initiation factors bind to the 40S small subunit of the ribosome, forming a translation preinitiation complex (PIC). tRNAi, critical for recognition of the start codon, is delivered to the 40S as a ternary complex comprising eIF2, tRNAi, and GTP (Kolitz & Lorsch, 2010; Lorsch & Herschlag, 1999). eIF2 (stimulated by eIF5) hydrolyzes GTP to GDP•Pi; however, the gamma phosphate is not released until the later steps of translation initiation (Algire, Maag, & Lorsch, 2005). Ternary complex binding is stabilized by eIF1, which binds near the P site; eIF1A, an ortholog of bacterial IF1 which binds in the A site; and eIF3 (Majumdar, Bandyopadhyay, & Maitra, 2003), which binds on the opposite (solvent) side of the 40S subunit and is thought to extend its arms to the channel in the PIC occupied by the mRNA (Aitken et al., 2016; des Georges et al., 2015; Hashem et al., 2013). At this point the PIC is in

an "open" conformation, poised to bind an mRNA (Passmore et al., 2007). The mRNA binds the PIC in a process called mRNA recruitment, facilitated by mRNA recruitment factors eIF4A, 4G, 4E, and 4B (Mitchell, Walker, Rajagopal, Aitken, & Lorsch, 2011). Subsequently, the 5'-UTR of the mRNA is scanned for the start codon. Upon start codon recognition, eIF1 is released, allowing the hydrolyzed gamma phosphate to dissociate from the TC and the PIC adopts a "closed" conformation, irreversibly committing the complex to the codon in the P-site of the ribosome (Maag, Fekete, Gryczynski, & Lorsch, 2005). Subsequently, eIF2, GDP, and eIF5 are released from the complex and another GTPase, eIF5B (an ortholog of bacterial IF2) promotes joining of the 60S large subunit of the ribosome. Finally, eIF1A is evicted from the complex allowing elongation to begin (Acker et al., 2009).

Translation initiation has been studied for many years. Various genetic and biochemical approaches led to numerous important results and recent high resolution structural work provided unprecedented insights into the organization of the bacterial (Yusupov et al., 2001) and then eukaryotic ribosomes (Ben-Shem et al., 2011). In the last several years structures of the PIC provided additional details of the mechanisms of translation initiation (Aylett, Boehringer, Erzberger, Schaefer, & Ban, 2015; Llacer et al., 2015; Simonetti et al., 2016) and at this point it is clear that initiation is a dynamic and highly regulated process. Perhaps due to it its dynamic nature, mRNA recruitment to the ribosome remains among less understood steps of the pathway.

mRNA recruitment factors

mRNA recruitment is promoted by a subset of eIFs – collectively referred to as mRNA recruitment factors – namely, eIFs 4A, 4G, 4E, and 4B (Mitchell et al., 2011). eIF4A is a DEAD-box RNA helicase (P Linder & Slonimski, 1989; Patrick Linder & Fuller-Pace, 2013; G. W. J. Rogers, Komar, & Merrick, 2002). It forms a heterotrimeric complex with eIF4G, a large RNA-binding scaffold and eIF4E, the 5'-7-methylguanosine (m7G) cap-binding protein (Merrick, 2015). Collectively the heterotrimer is referred to as eIF4F. The fourth mRNA recruitment factor, eIF4B, is thought to enhance the eIF4A catalytic cycle (Alexandra Zoi Andreou, Harms, & Klostermeier, 2017; George W. Rogers, Richter, Lima, & Merrick, 2001).

eIFs 4G, 4E, and 4B are critical for efficient translation initiation but eIF4A is essential for life (P Linder & Slonimski, 1989). The helicase is the founding member of the DEAD-box ATP-dependent RNA helicase family (part of the larger helicase Super Family 2) named for the D-E-A-D motif necessary for catalysis (P Linder et al., 1989). There are three eIF4A paralogs in mammals: eIF4AI (also known as DDX2A), eIF4AII (DDX2B), and eIF4AIII (DDX48) (Lu, Wilczynska, Smith, & Bushell, 2014). Mammalian eIF4AI and eIF4AII have ~90% amino acid sequence but are thought to perform slightly different, perhaps specialized, roles during translation initiation. eIF4AIII is only ~65% similar and despite the name is better known as a component of splicing within the exon junction complex (EJC) rather than translation initiation (Andersen et al., 2006; Shibuya, Tange, Sonenberg, & Moore, 2004). For all isoforms of eIF4A, the catalytic cycle is marked by cooperative binding of ATP and RNA, removal of RNA structure, hydrolysis of ATP to ADP, and dissociation of the complex (Figure 1.2). Subsequent ATP hydrolysis causes a decrease in affinity for RNA and ATP (Lorsch & Herschlag, 1998) and is thought to facilitate the enzyme recycling from the complex (Liu, Putnam, & Jankowsky, 2008). In

yeast, two genes TIF1 and TIF2, possessing identical sequence encode eIF4A (~80% similar to mammalian eIF4AI and eIF4AII) and there is no known yeast homolog of eIF4AIII. Akin to other DEAD-box helicases, eIF4A has a core comprising two RecA-like domains connected by a short linker (Caruthers, Johnson, & McKay, 2000). It has been demonstrated that eIF4A can unwind short annealed RNA oligomers but it is generally considered a weak helicase and of low processivity (G. Rogers, Richter, & Merrick, 1999; G W Rogers, Lima, & Merrick, 2001). However, in a recent study mammalian eIF4A unwound long hairpins under tension at the 5'- and 3'-end and this activity was enhanced by other mRNA recruitment factors (Garcia-Garcia, Frieda, Feoktistova, Fraser, & Block, 2015).

eIF4G is a large scaffold-like protein that binds RNA and stimulates eIF4A activity (Schütz et al., 2008). Mammals and yeast both have two paralogs – eIF4G1 and eIF4G2 – in yeast encoded by genes *TIF4631* and *TIF4632* (Das & Das, 2016). It is thought that eIF4G promotes eIF4A catalysis by stimulating the RecA-like domains to adopt a catalytic conformation (Hilbert, Kebbel, Gubaev, & Klostermeier, 2011; Oberer, Marintchev, & Wagner, 2005). Mammalian eIF4G (meIF4G) has two eIF4A binding sites, thought to work together to promote eIF4A activity, while yeast eIF4G (yeIF4G) has one binding site for eIF4A. Also, meIF4G binds mammalian eIF3 (meIF3), suggesting a possible interaction with the rest of the PIC (LeFebvre et al., 2006). No interaction between eIF4G and eIF3 has been reported in yeast; however, yeIF4G tightly binds eIF5 (Mitchell et al., 2010), which may bridge the eIF4G-PIC interaction.

Figure 1.1. Model of eukaryotic translation initiation. Translation initiation begins with eIFs 1, 1A, 3, and 5 binding the 40S small subunit together with TC comprising eIF2, GTP, and tRNAi. Together the factors form a PIC in an "open" conformation. The PIC binds the mRNA near the 5'-end – facilitated by eIFs 4A, 4G, 4E, and 4B –n a process called mRNA recruitment. Subsequently, the mRNA is scanned by the PIC for the start codon (usually an AUG). Recognition of the translational start site causes irreversible commitment of the PIC, adopting a "closed" conformation, followed by 60S joining, release of eIF1A, and start of elongation.

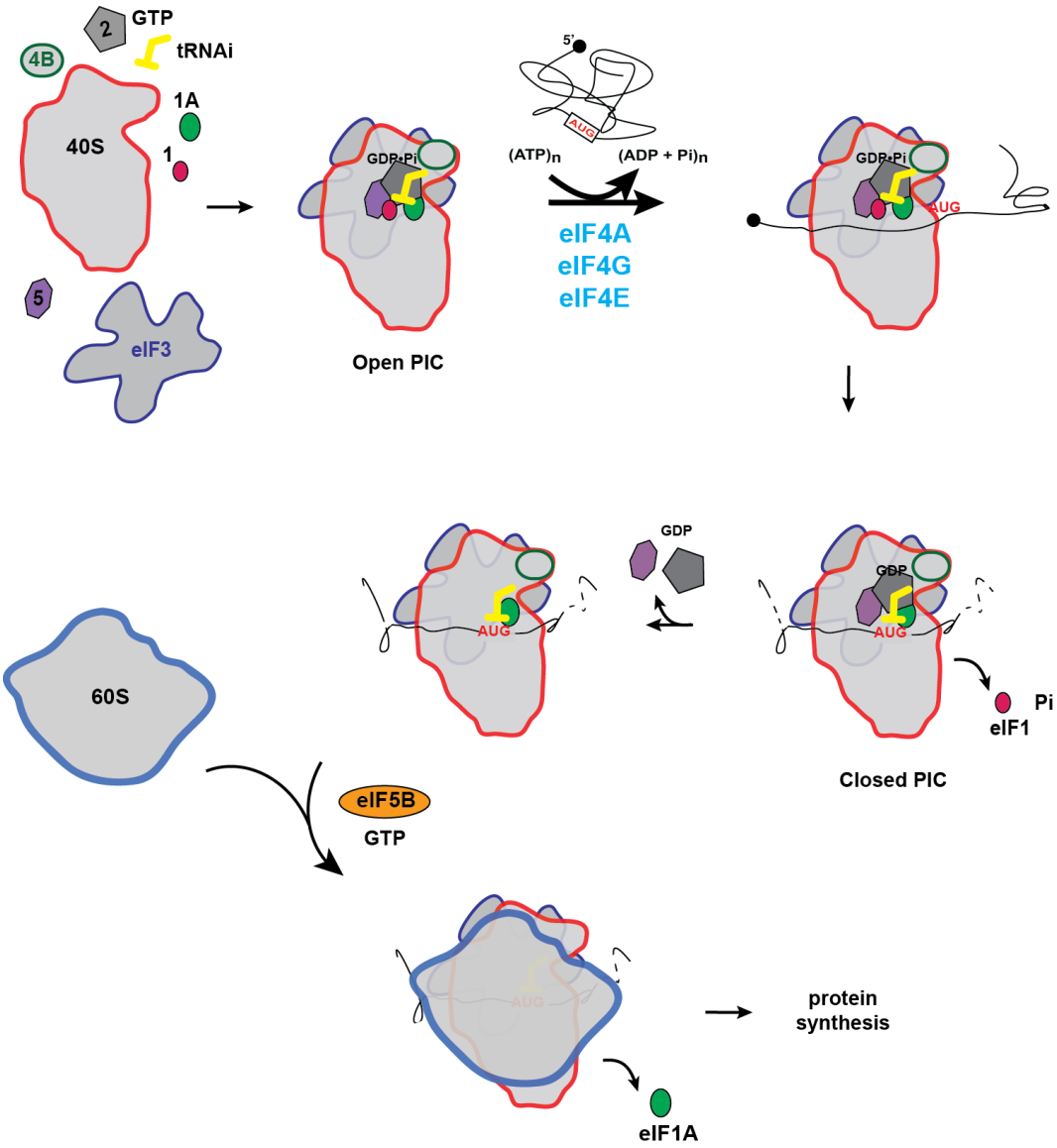
GTP
2
tRNAi
4B
1A
40S
1
5
eIF3
GDP•Pi
Open PIC
5'
AUG
(ATP)n
(ADP + Pi)n
eIF4A
eIF4G
eIF4E
GDP•Pi
AUG
60S
AUG
GDP
GDP
AUG
Pi
eIF1
Closed PIC
eIF5B
GTP
AUG
protein
synthesis
eIF1A

eIF4G, eIF4A, and eIF4E form the heterotrimeric complex eIF4F, which together with the Poly-A Binding Protein (Pab1) is thought to circularize the mRNA. eIF4E binds the 5'-m7G cap and localizes eIF4F to the 5'-end of the mRNA (Lindqvist, Imataka, & Pelletier, 2008). While certain components of translational machinery are highly abundant in the cell (e.g. eIF4A, 40S) eIF4E is substoichiometric (von der Haar & McCarthy, 2002) and has emerged as one of the key regulatory points of translation initiation (Pelletier, Graff, Ruggero, & Sonenberg, 2015). In fact, increased expression of eIF4E – resulting in increased translation – is often associated with cancer (Bitterman & Polunovsky, 2012; Jackson, Hellen, & Pestova, 2010). In addition to the interaction with the 5'-end of an mRNA, eIF4F also interacts with the 3'-end of an mRNA via the interaction between eIF4G and Pab1, effectively circularizing the mRNA (Wells, Hillner, Vale, & Sachs, 1998). Circularization is not essential but is thought to create a more stable complex and facilitate multiple rounds of translation; however, abrogating eIF4G interactions with both eIF4E and Pab1 is synthetically lethal (Park et al., 2011).

eIF4B was considered to be an auxiliary RNA-binding protein (Nielsen et al., 2011; Özeş, Feoktistova, Avanzino, & Fraser, 2011) but recent work in yeast demonstrated that it is critical for efficient translation initiation (Mitchell et al., 2010; Walker et al., 2013). Yeast eIF4B (yeIF4B) and mammalian eIF4B (meIF4B) share only 26% sequence identity and possess rather different domain architecture (Altmann et al., 1993) but both act as a coupling factor for eIF4A, increasing efficiency of helicase activity (Alexandra Z Andreou & Klostermeier, 2014; Alexandra Zoi Andreou et al., 2017; Özeş et al., 2011). Notably, in a study using an *in vitro* reconstituted yeast system, yeIF4B bound to the head of the 40S subunit with a dissociation constant (K_d) that was an order of magnitude lower than that for mRNA (Walker et al., 2013). The same study also showed that in the absence of eIF4B, in

Figure 1.2. Mechanism of eIF4A. eIF4A has two RecA-like domains connected by a linker. It cooperatively binds mRNA and ATP. It is thought that eIF4A twists a region of double stranded mRNA, causing it to adopt an unfavorable conformation, thus "melting" the duplex mRNA. ATP hydrolysis to ADP results in a decrease in affinity, causing the enzyme to dissociate.

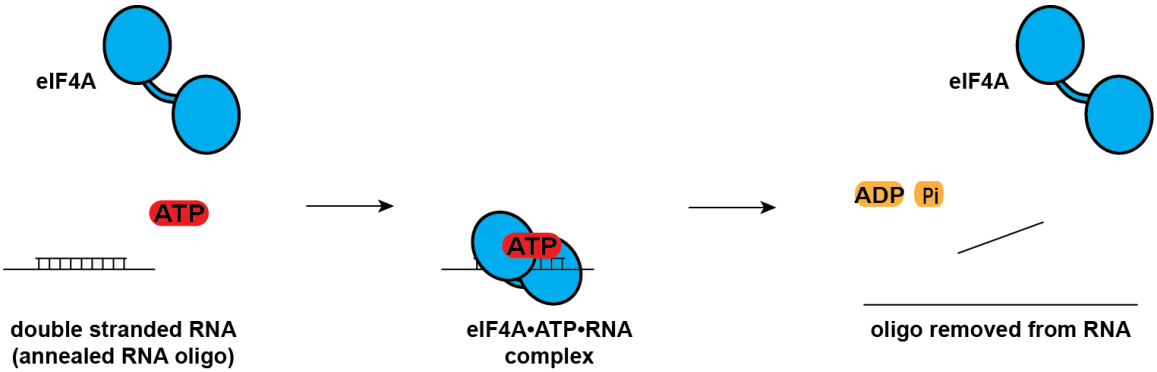

addition to a dramatically lower rate of mRNA recruitment to the PIC, a higher concentration of eIF4A was required to achieve efficient mRNA recruitment. Also, work *in vivo* demonstrated that yeIF4B enhances complex formation between eIF4G and eIF4A (Park et al., 2013). Taken together a growing body of evidence shows that yeIF4B binds the PIC and has a functional interaction with eIF4A, suggesting a possible interaction between eIF4A or eIF4F and the PIC during translation initiation.

Unanswered questions of mRNA recruitment in translation initiation

The mechanism of how an mRNA is bound by the ribosome has been studied for over thirty years but many questions still remain. An mRNA has Watson-Crick (WC) and non-WC interactions, which form local structure (hairpins) as well as interactions with parts of the RNA that are not close in primary RNA sequence (Halder & Bhattacharyya, 2013). These structural elements are inhibitory to mRNA recruitment and must be bypassed by the PIC (Mitchell et al., 2011). Work in the 1970s and 1980s demonstrated that ATP was required for the 40S to bind a structured mRNA (Kozak, 1991; Kramer, Konecki, Cimadevilla, & Hardesty, 1976) and subsequent purification of eIF4F and eIF4A (Grifo, Tahara, Morgan, Shatkin, & Merrick, 1983; P Linder & Slonimski, 1989) allowed biochemical characterization, demonstrating that eIF4A is an ATP-dependent RNA helicase that is stimulated by eIF4G (Korneeva, First, Benoit, & Rhoads, 2005)

The prevailing model for mRNA recruitment (Figure 1.3) suggests that eIF4F is localized to the 5'-end of an mRNA and unwinds inhibitory mRNA hairpins – in an ATP-dependent manner – facilitating PIC attachment (Hinnebusch, 2014). This model is derived from a large body of work contributed by various groups; however, there are other findings

that are challenging to rationalize with this model. Earlier work showed that eIF4A stimulated cell free *in vitro* translation of all mRNAs tested, including an RNA with a 5'-UTR that was eight nucleotides in length (Blum et al., 1992), thus unlikely to form significant structural elements in the 5'-UTR. Later studies also demonstrated that eIF4A promotes formation of a PIC complex at an AUG (48S) on an mRNA with minimal structure in the 5'-UTR (Pestova & Kolupaeva, 2002). More recent work in yeast, holistically examined the role of eIF4A with respect to global translation. Ribosomal profiling (Sen, Zhou, Ingolia, & Hinnebusch, 2015) and *in vivo* titration of eIF4A (Firczuk et al., 2013; von der Haar & McCarthy, 2002) show that the protein affects global translation rather than specific, (e.g. highly structured structured) mRNAs. Taken together, these findings suggest that our understanding of the role of eIF4A in translation initiation is not complete. Accordingly, it is difficult to envision how a notoriously slow helicase, eIF4A, is able to support *in vivo* rates of translation initiation. It is tempting to speculate that eIF4A may have other functions beyond removal of specific RNA hairpins near the 5'-UTR.

eIF4F is referred to as the nexus of cancer development (Bitterman & Polunovsky, 2012; Pelletier et al., 2015) and received much attention in recent years as an attractive therapeutic target (Bhat et al., 2015). However, the exact mechanism of eIF4A and eIF4F in mRNA recruitment and translation initiation is yet to be described. eIF4A is present in large excess to all other components of the translational apparatus (Firczuk et al., 2013) but it is not clear how that is beneficial to translation initiation. Also, cells contain other robust RNA helicases that are capable of efficiently unwinding RNA structure, so why is a slow helicase like eIF4A essential? Furthermore, if the main function of eIF4A is to remove structure near the 5'-end, how is the mRNA subsequently transferred to the PIC? Given previously reported functional interactions between eIF4B and eIF4A (Walker et al., 2013), it is

conceivable that eIF4F or eIF4A may work together with the PIC to facilitate mRNA recruitment.

The *S. cerevisiae in vitro* reconstituted translation initiation system can be utilized to investigate the mechanisms of mRNA recruitment (Acker, Kolitz, Mitchell, Nanda, & Lorsch, 2007; Mitchell et al., 2010). The eIFs and the 40S subunit are expressed in yeast or bacteria and are individually purified. Also, the tRNAi and mRNA are *in vitro* transcribed and gel purified. Together these components can be reconstituted to study the kinetics of translation initiation *in vitro* and can be corroborated by various genetic approaches. The system can be adapted, improved, and combined with other assays to ask mechanistic questions about the pathway. In this work, using the aforementioned *in vitro* approaches we were able to shed light on several questions surrounding the roles of eIF4A and eIF4F in mRNA recruitment.

Here, we used a modified ATPase assay to study eIF4A and eIF4F activity, alone and in the context of the PIC. This activity was then compared with the effect of eIF4A on the overall process of mRNA recruitment for mRNAs of different length and degree of structure (Chapter 2). The ATPase assay adapted for our studies is a useful tool and we describe its development in complete detail (Chapter 3). We conclude with a series of experiments examining the dependence of mRNA recruitment on ATP and the role of the coupling factor eIF4B (Appendix A) and show that eIF4A is a poor RNA helicase in the context of the PIC, while the PIC is capable of removing a short annealed RNA oligomer in the absence of eIF4A (Appendix B). This work provided us with novel insights into the role of eIF4A in translation initiation and allowed us to propose a revised model of mRNA recruitment to the PIC (see Chapter 2 Discussion).

Figure 1.3 Prevailing model for mRNA recruitment to the PIC. eIF4A, together with eIF4F is thought to remove mRNA structure near the 5'-end and the mRNA is subsequently bound by the PIC.

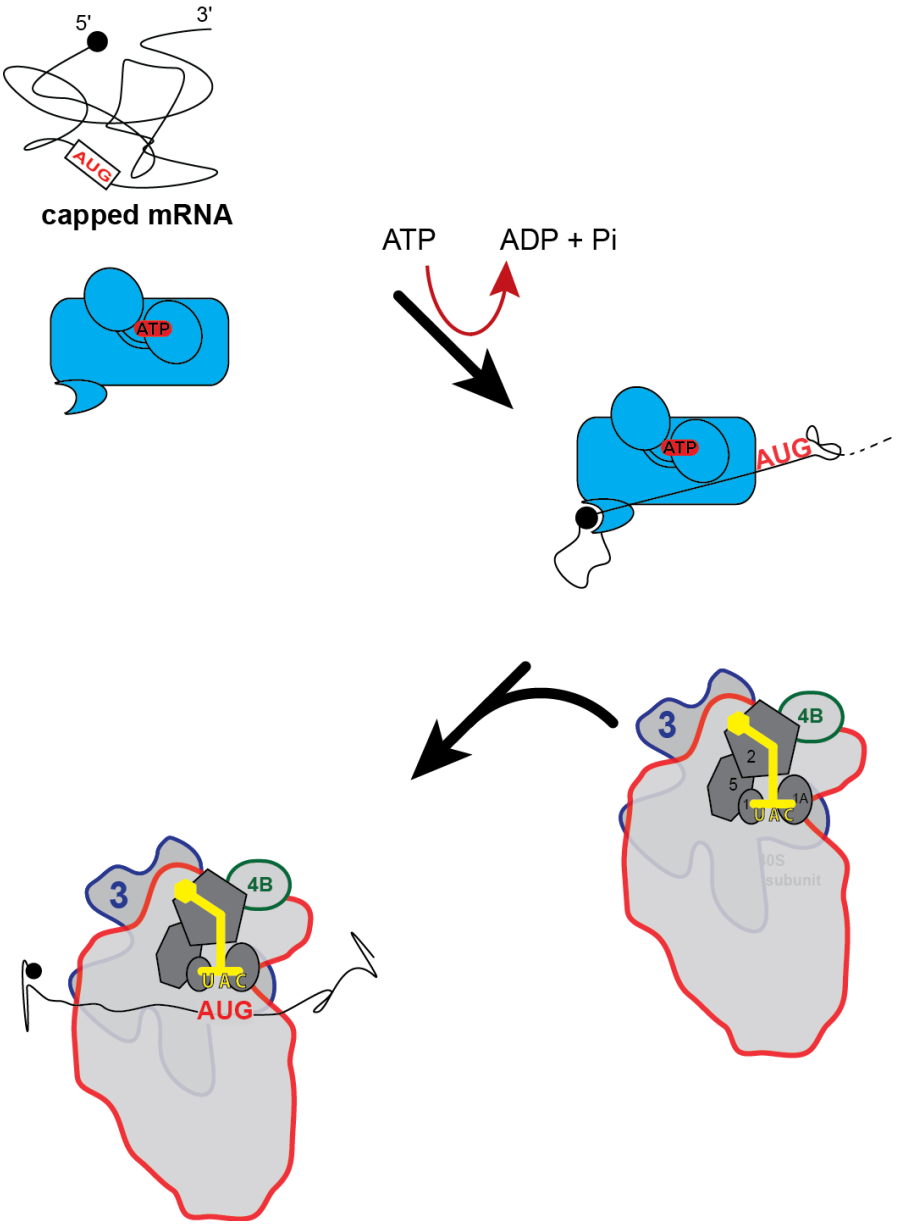

Chapter 2

eIF4A is stimulated by the translation pre-initiation complex and promotes the rate of recruitment of mRNAs regardless of their structural complexity

Paul Yourik[1,2], Colin Echeverría Aitken[2], Fujun Zhou[2], Neha Gupta[2], Alan G. Hinnebusch[2], Jon R. Lorsch[2]

[1] Johns Hopkins University School of Medicine, Baltimore, MD

[2] Laboratory on the Mechanism and Regulation of Protein Synthesis, Eunice Kennedy Shriver National Institute of Child Health and Development, National Institutes of Health, Bethesda, MD

Abstract

eIF4A is a DEAD-box RNA-dependent ATPase thought to unwind RNA secondary structure in the 5'-untranslated regions (UTRs) of mRNAs to promote their recruitment to the eukaryotic translation pre-initiation complex (PIC). We show here that the PIC stimulates the ATPase activity of eIF4A, indicating that the factor acts in association with initiating ribosomal complexes rather than exclusively on isolated mRNAs. ATP hydrolysis by eIF4A accelerates the rate of recruitment for all mRNAs tested, regardless of their degree of secondary structure, indicating that the factor plays important roles beyond unwinding mRNA structure. Structures in the 5'-UTR and 3' of the start codon synergistically inhibit mRNA recruitment, in a manner relieved by eIF4A, suggesting that the factor resolves global mRNA structure rather than just secondary structures in the 5'-UTR. We propose that eIF4A might break the many weak interactions formed within an mRNA that occlude the 5'-UTR and facilitates engagement of the 5'-UTR with the PIC.

Introduction

The goal of translation initiation is to assemble the ribosome containing the initiator tRNA (tRNAi) at the translation start site on an mRNA, indicating the first amino acid of the encoded protein. The process begins when the small subunit of the ribosome (40S) binds eukaryotic translation initiation factors (eIF) 1, 1A, 2, 3, 5 as well as GTP and tRNAi, to assemble the 43S eukaryotic translation initiation complex (PIC) (Mitchell & Lorsch, 2008). eIF1 and eIF1A bind near the P site and in the A site of the 40S, respectively, and promote binding of the ternary complex (TC) comprising eIF2, GTP, and tRNAi. eIF5 is the GTPase-activating protein (GAP) for eIF2 and promotes GTP hydrolysis (Nanda et al., 2009; Nanda, Saini, Muñoz, Hinnebusch, & Lorsch, 2013); however, irreversible release of the gamma phosphate is inhibited at this stage of the pathway (Algire et al., 2005). The complex is also joined by eIF3, which has multiple interactions within the PIC and is involved in nearly every step of translation initiation (Hinnebusch, 2006; Valásek, 2012).

The 43S PIC is assembled in an "open" conformation (Llacer et al., 2015) and binds an mRNA in a process called mRNA recruitment. eIF3 and a set of mRNA recruitment factors – eIF4A, eIF4E, eIF4G, and eIF4B – facilitate this step (Mitchell et al., 2011). In yeast, eIF4B binds directly to the 40S (Walker et al., 2013) while eIF4A, eIF4E, and eIF4G together form a heterotrimeric complex called eIF4F, which is localized to the 5'-end of the mRNA via an interaction between eIF4E and the 5'-7-methylguanosine (m7G) cap (Hinnebusch, 2014). After initial mRNA recruitment, the PIC remains in an open conformation, promoted by a network of interactions between the TC and the rest of the complex, and scans the 5'- untranslated region (UTR) of the mRNA for the start codon, usually an AUG (Hinnebusch, 2014). Recognition of the start codon by the tRNAi triggers a series of irreversible steps – release of the previously-hydrolyzed GTP gamma phosphate by

eIF2 and subsequent eviction of eIF1 – ultimately shifting the PIC from an "open" to a "closed" conformation (Hussain et al., 2014; Kolitz & Lorsch, 2010; Llacer et al., 2015). The 48S PIC thus formed is committed to the selected start codon and binding of the large (60S) subunit of the ribosome to form the 80S complex (Acker et al., 2009).

Whereas a combination of genetic, biochemical, and structural approaches have illuminated the molecular details of the PIC formation and start-codon selection, the intermediate events of mRNA recruitment and scanning remain poorly understood (Aitken & Lorsch, 2012). We recently demonstrated that the absence of either eIF4A, eIF4B, or eIF3 greatly reduces the extent of mRNA recruited to the PIC *in vitro*, and the combined absence of eIF4G and eIF4E reduces the rate of recruitment (Mitchell et al., 2010). Structural and biochemical work suggests that eIF3 is near the mRNA path in the PIC and distinctly interacts with the mRNA near the entry and exit channels of the ribosome (Aitken et al., 2016; Llacer et al., 2015). Yeast eIF4B has also been demonstrated to bind the 40S subunit and induce changes near the mRNA entry channel, and may have a functional interaction with one or more components of the eIF4F complex (Alexandra Z Andreou & Klostermeier, 2014; Harms, Andreou, Gubaev, & Klostermeier, 2014; Park et al., 2013; Walker et al., 2013).

In contrast, eIF4A has not been shown to bind stably to the PIC and is instead thought to promote mRNA recruitment by interacting with the mRNA – within the context of the eIF4F complex – to prepare it for PIC attachment. mRNA has a natural tendency to form local secondary structures but also participates in global interactions, allowing it to adopt an energetically stable but entangled conformation (Halder & Bhattacharyya, 2013). Hairpins in the 5'-UTR are inhibitory to translation initiation and it is thought that eIF4A – localized to the 5'-end via the eIF4G–eIF4E-5'-m7G-cap chain of interaction – unwinds

these hairpins to allow PIC attachment (Merrick, 2015; Pelletier & Sonenberg, 1985; Y. Y. V Svitkin et al., 2001).

eIF4A is a DEAD-box ATP-dependent RNA helicase (Alexandra Z Andreou & Klostermeier, 2013; Patrick Linder & Fuller-Pace, 2013). It cooperatively binds RNA and ATP with no apparent RNA sequence specificity, and is thought to disrupt structures by local strand separation possibly due to bending of the RNA duplex (Henn, Bradley, & De La Cruz, 2012; Patrick Linder & Jankowsky, 2011). Subsequent ATP hydrolysis causes a decrease in eIF4A•RNA•ADP•Pi complex affinity, causing the components to dissociate, thus recycling eIF4A from a high affinity RNA-bound state (Alexandra Z Andreou & Klostermeier, 2013; Jankowsky, 2011; Liu et al., 2008). Several studies have demonstrated that eIF4A is able to disrupt short RNA duplexes (Rajagopal, Park, Hinnebusch, & Lorsch, 2012; G. Rogers et al., 1999) and more recent work suggests that eIF4A can unwind a large hairpin when the RNA is stretched between two tethers (Garcia-Garcia et al., 2015). Also, others have demonstrated that mRNAs with a higher degree of secondary structure in the 5'-UTR are more sensitive to inhibition of translation by a dominant negative mutant of eIF4A and conclude that mRNAs with a higher degree of structure may require more eIF4A for translation initiation (Y. Y. V Svitkin et al., 2001).

Nonetheless, eIF4A is a notoriously slow and unprocessive helicase (Lorsch & Herschlag, 1998; Rajagopal et al., 2012; G. Rogers et al., 1999), and its helicase activity alone is not likely to support *in vivo* rates of translation initiation in the regime of ~10 min^{-1} (Palmiter, 1975). In fact, several more potent helicases appear to promote translation by resolving defined structural elements (Parsyan et al., 2011), raising the possibility that eIF4A instead performs a distinct role during initiation on all mRNAs (Gao et al., 2016). A study comparing effects of eIF4A versus Ded1p – another robust DEAD-box RNA helicase –

demonstrated that while Ded1p was necessary for efficient translation of mRNAs with 5'-UTRs possessing stable RNA hairpins, eIF4A affected global levels of translation (Sen et al., 2015). In a separate study, minor decreases in the normally high cellular levels eIF4A also resulted in depressed global rates of translation (Firczuk et al., 2013). Consistent with the idea that it acts generally, eIF4A has also been shown to promote translation of an mRNA possessing a short (8 nt) 5'-UTR (Blum et al., 1992) and to stimulate 48S formation on mRNAs with low secondary structure in the 5'-UTR (Pestova & Kolupaeva, 2002). Moreover, a large body of work suggests that the eIF4F complex can be recruited to the 5'-end of mRNAs and is critical for recruitment (J. Chen et al., 2016; Dever, Kinzy, & Pavitt, 2016; Hinnebusch, 2014; Jackson et al., 2010). And yet, how the helicase and ATPase activities of eIF4A contribute to its role in promoting initiation on diverse mRNAs remains unclear.

Here – using an *in vitro* translation initiation system reconstituted from purified *S. cerevisiae* components – we examined how the PIC may be working together with eIF4A and eIF4F in mRNA recruitment. We monitored kinetics of eIF4A ATPase activity in the context of mRNA recruitment to the PIC and asked how that activity is utilized for the recruitment of mRNAs possessing various degrees of structure, ranging from natural (structured) sequences to short model mRNAs, made of CAA repeats, lacking any significant structure (unstructured) (Shirokikh, Agalarov, & Spirin, 2010; Sobczak et al., 2010), other than fluctuations in polymer conformation and transient interactions (H. Chen et al., 2012). We show that the PIC stimulates eIF4A ATPase activity directly and as a component of eIF4F. We further show that eIF4A enhances the rate of recruitment of all mRNAs tested, ranging from the natural *RPL41A* mRNA to short, unstructured model mRNAs or mRNAs only containing structural complexity 3' of the start codon. Notably, while eIF4A was

necessary to promote the recruitment of mRNAs possessing structural complexity – defined as either natural mRNA sequence or inserted secondary structure – throughout their sequence, it was not required to recruit mRNAs containing structural complexity only in their 5'-UTR. We propose that eIF4A, alone or as a part of eIF4F, facilitates PIC attachment by relaxing global mRNA structure within and outside of the 5'-UTR or by remodeling the 40S itself.

Results

ATP, but not non-hydrolyzable analogs, stimulates the rate of recruitment of both a structured natural mRNA and a short unstructured model mRNAs in vitro

The prevailing model of mRNA recruitment to the PIC during translation initiation suggests that eIF4F is recruited, via the 5'-cap-eIF4E interaction, to the 5'-end of the mRNA where eIF4A removes structural elements in the 5'-UTR to facilitate PIC attachment (Hinnebusch, 2014). eIF4A cooperatively binds ATP and mRNA (Lorsch & Herschlag, 1998; G. Rogers et al., 1999). Subsequent ATP hydrolysis to ADP facilitates release of the mRNA substrate, thus recycling the enzyme (Liu et al., 2008). In order to better understand how eIF4A-catalyzed ATP hydrolysis is related to the removal of RNA structure and mRNA recruitment, we compared the kinetics of recruitment of the natural mRNA *RPL41A* (possessing structural complexity throughout its sequence) with an unstructured 50 nucleotide-long model mRNA comprising CAA repeats with an AUG codon at positions 24-26 (CAA 50mer) (Aitken et al., 2016).

mRNA recruitment experiments were performed as described previously, using an *in*

vitro-reconstituted *S. cerevisiae* translation initiation system (Acker et al., 2007; Mitchell et al., 2010; Walker et al., 2013). Briefly, PICs containing 40S and saturating levels of TC, eIF1, eIF1A, eIF5, and eIF3 were formed in the presence of saturating levels of eIFs 4A, 4B, 4E, and 4G (see "30 nM PIC" in Methods). Reactions were initiated by simultaneous addition of ATP and an mRNA labeled with a [^{32}P]-7-methylguanosine (m7G) cap, enabling mRNA recruitment to PICs and formation of 48S complexes. Timepoints were acquired by mixing a reaction aliquot with a 25-fold excess of an mRNA identical to one in the reaction, capped with a non-radioactive m7G, thus capturing the pool of free (not recruited) labeled mRNAs and effectively stopping further recruitment of radiolabeled mRNA. Free mRNA and formed 48S complexes were resolved via gel shift on a native 4 % THEM acrylamide gel (Acker et al., 2007; Mitchell et al., 2010).

We first compared the kinetics of recruitment for *RPL41A* with CAA 50mer in the presence and absence of ATP (Figure 2.1). In the absence of ATP less than 20 % of *RPL41A* mRNA was recruited after 6 hours, indicating a dramatically slower rate, which could not be measured accurately due to the low reaction endpoint (Figure 2.1A). In contrast, the rate of recruitment of *RPL41A* in the presence of ATP was 0.74 ± 0.01 min^{-1} with an endpoint in excess of 90%. The CAA 50mer was recruited in the absence of ATP at a rate of 0.90 ± 0.01 min^{-1}, reaching an endpoint in excess of 80%, likely due to its lack of significant structural elements. Surprisingly, the addition of ATP nonetheless stimulated the rate of recruitment of CAA 50mer 4-fold (3.95 ± 0.06 min^{-1}) without affecting the extent of recruitment (Figure 2.1B).

To determine whether ATP hydrolysis was required for the stimulation we observed, we next measured the rate of recruitment with the non-hydrolyzable ATP analogs ADPCP and ADPNP, as well as with the slowly-hydrolyzable analog ATP-ɣ-S (Peck & Herschlag,

1999). Neither ADPCP nor ADPNP stimulated the recruitment of *RPL41A* and CAA 50mer, as compared to the absence of nucleotide (Figure 2.1). In the presence of ATP-γ-S, recruitment of *RPL41A* and CAA 50mer was 39-fold (0.019 ± 0.001 min^{-1}) and nearly 2-fold (2.28 ± 0.02 min^{-1}) slower, respectively, than in the presence of ATP; however, both reactions achieved endpoints of at least 80%, consistent with previous observations that eIF4A is capable of utilizing ATP-γ-S (Peck and Herschlag, 2003). Taken together, these results suggest that ATP hydrolysis by eIF4A stimulates the recruitment of both structured and unstructured mRNAs.

The steady-state rate of eIF4A and eIF4F ATPase activity is increased by the PIC

Having shown that eIF4A-dependent ATP hydrolysis stimulates the recruitment of *RPL41A* as well as CAA 50mer, we next asked if eIF4A collaborates with components of the PIC to promote mRNA recruitment by monitoring ATPase activity using the *in vitro* reconstituted translation initiation system and an ATPase assay. We measured the rate of ATP hydrolysis using the Pyruvate Kinase (PK) and Lactate Dehydrogenase (LDH)-coupled assay described previously (Bradley & De La Cruz, 2012). Upon eIF4A-catalyzed hydrolysis of ATP to ADP, PK catalyzes the transfer of a phosphate group from phosphoenolpyruvate to ADP, generating ATP and pyruvate. LDH subsequently reduces pyruvate to lactate, in the process oxidizes nicotinamide adenine dinucleotide (NADH to NAD+). Because NADH levels can be monitored via its absorption of light at 340 nm, this assay produces a photometric proxy signal for ATP levels. (Figure 2.2A). Reactions were assembled in a 384-well plate and NADH absorbance at 340 nm was recorded every 20 seconds in a microplate reader at various

Figure 2.1. ATP hydrolysis stimulates recruitment of a natural structured mRNA RPL41A as well as a very low structure synthetic CAA-repeats 50mer containing an AUG start codon 23 nucleoties from the 5'-end (CAA 50mer). Concentration of ATP and analogs was 2 mM. (A) Percent RPL41A recruited to the PIC versus time. Observed rates (kobs) measured with ATP: 0.74 ± 0.01 min-1, ATP-γ-S: 0.019 ± 0.001 min-1, kobs with ADPNP, ADPCP, ADP, or no nucleotide could not be measured accurately due to low endpoints. (B) Percent CAA 50mer recruited to the PIC versus time. The larger plot shows the timecourse up to 7.5 min., for clarity, and the inset is the entire timecourse. kobs measured with ATP: 3.95 ± 0.06 min-1, ATP-γ-S: 2.28 ± 0.02 min-1, ADPNP: 1.35 ± 0.02 min-1, ADPCP: 1.08 ± 0.01 min-1, ADP: 0.86 ± 0.1 min-1, no nucleotide: 0.90 ± 0.01 min-1. All data in the figure are mean values and error bars represent average deviation of the mean.

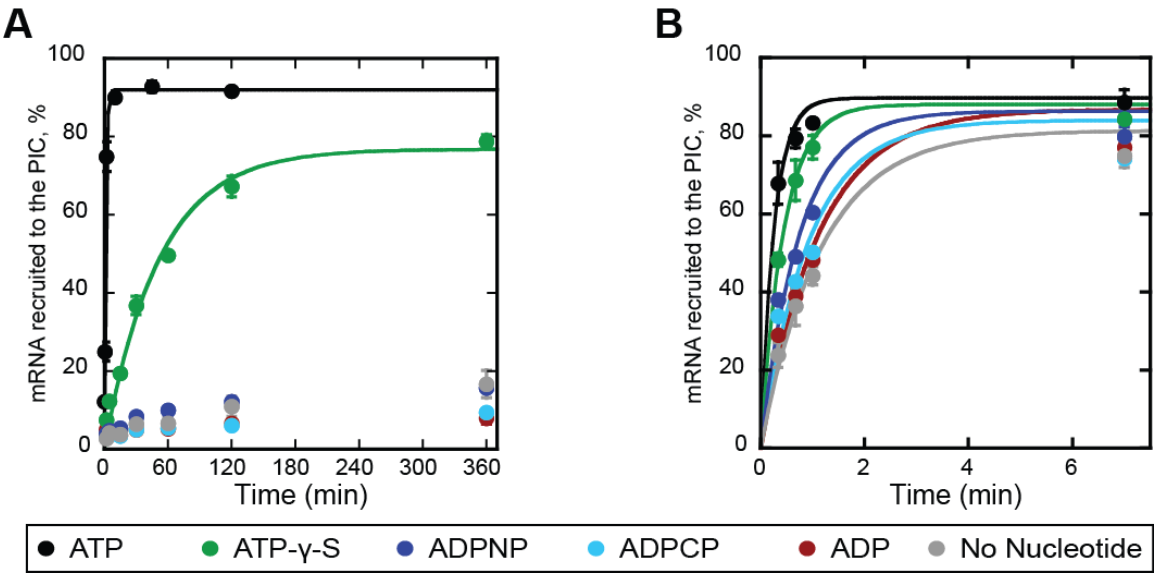

Figure 2.2. eIF4A ATPase activity controls. (A) Controls for NADH coupled enzyme microplate ATPase assay. Decrease in absorbance of 340 nm light was dependent on presence of ATPase activity (5 μM eIF4A, 0.5 μM eIF4G, 0.5 μM eIF4E, together referred to as eIF4F), ATP, and Pyruvate Kinase (900-1400 units/mL)/Lactate Dehydrogenase (600-1000 units/mL) mix from rabbit muscle used as 250x stock solution. (B) Capped RPL41A was titrated in the presence of 5 μM eIF4A and 5 mM ATP. Data were fit with the Michaelis-Menten equation giving a Vmax mRNA of 2.41 ± 0.18 μM/min and Km mRNA of 84 ± 12 μM. (C) ATPase activity and efficiency ($V_{max\ ATP}/K_{m\ ATP}$) with eIF3 and eIF4B in the presecent of saturating capped mRNA RPL41A. In all cases above eIF4A is 5 μM. eIF4E, eIF4G, eIF4B and eIF3, when present, are all 0.5 μM. "All" contains 5 μM eIF4A, 0.5 μM eIF4G, 0.5 μM eIF4E, 0.5 μM eIF4B, 0.5 μM eIF2, 0.5 μM Met-tRNA(Met), 1 mM GDPNP, 0.5 μM eIF3, 0.5 μM eIF5, 1 μM eIF1, 1 μM eIF1A, and 0.5 μM 40S. Data in (B) and (C) are mean values and error is reported as average deviation of the mean.

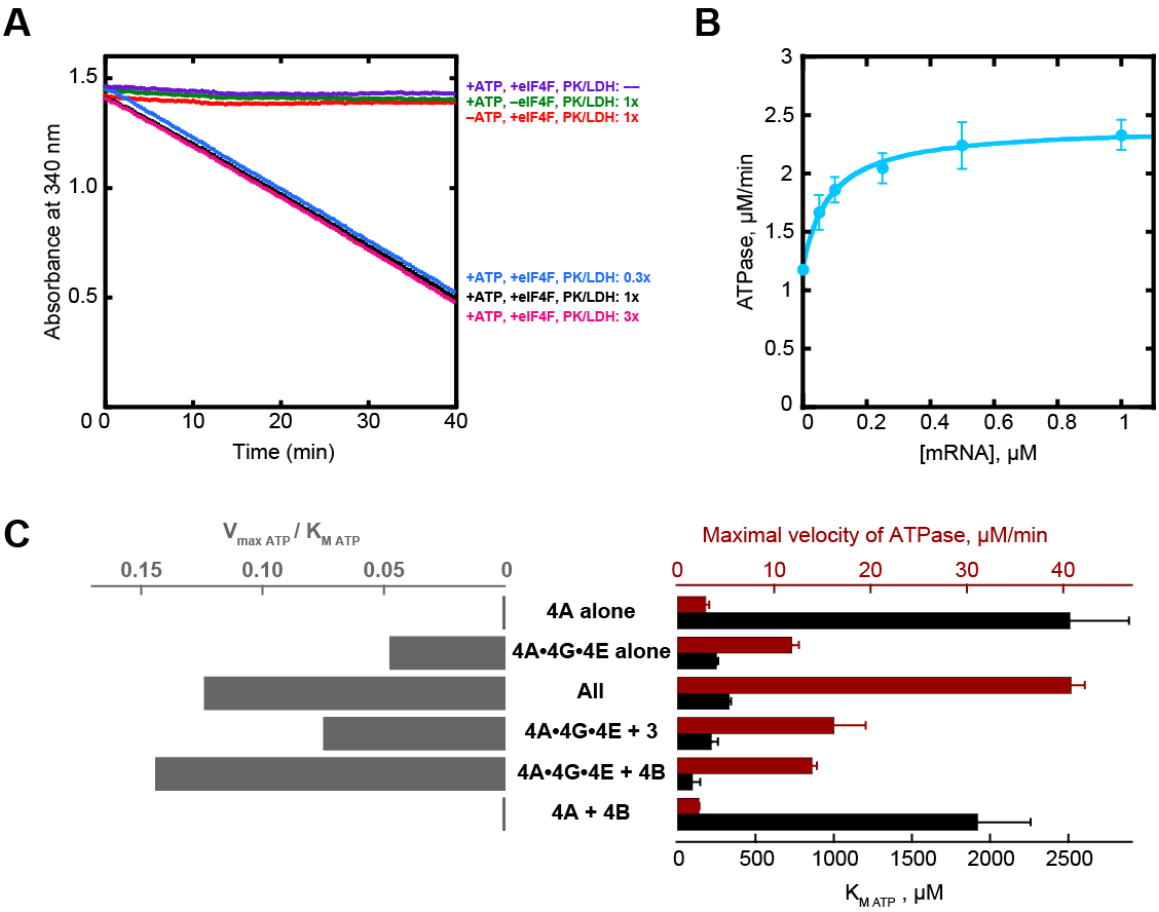
A
Absorbance at 340 nm
Time (min)
+ATP, +eIF4F, PK/LDH: —
+ATP, –eIF4F, PK/LDH: 1x
–ATP, +eIF4F, PK/LDH: 1x
+ATP, +eIF4F, PK/LDH: 0.3x
+ATP, +eIF4F, PK/LDH: 1x
+ATP, +eIF4F, PK/LDH: 3x
B
ATPase, μM/min
[mRNA], μM
C
Vmax ATP / KM ATP
Maximal velocity of ATPase, μM/min
4A alone
4A•4G•4E alone
All
4A•4G•4E + 3
4A•4G•4E + 4B
4A + 4B
KM ATP , μM

concentrations of mRNA in the presence of saturating ATP (5 mM). By titrating mRNA, we determined the maximal velocity of ATP hydrolysis once mRNA has become saturating ($V_{max\ RNA}$), as well as the concentration of mRNA needed to achieve the half-maximal velocity of ATP hydrolysis ($K_{m\ RNA}$). At 5 μM eIF4A the $V_{max\ RNA}$ was measured to be 2.41 ± 0.18 μM/min (or 0.48 ± 0.04 min^{-1}) and the $K_{m\ RNA}$ was 84 ± 13 μM: comparable to previous reports (Figure 2.2B) (Rajagopal et al., 2012). Also, congruent with previous findings (Hilbert et al., 2011; Oberer et al., 2005; Rajagopal et al., 2012), the addition of co-purified full length eIF4G1 and eIF4E (eIF4G•4E) to eIF4A, forming eIF4F, resulted in a 6.5-fold increase in the $V_{max\ RNA}$ and had a $K_{m\ RNA}$ of 102 ± 12 μM (Figure 2.3A).

The addition of the PIC to these reactions (See "0.5 μM PIC" in Methods) increased the observed $V_{max\ RNA}$ an additional 3-fold over the rate observed with eIF4F alone (Figure 2.3A). Leaving out the 40S subunits resulted in a 2-fold decrease of $V_{max\ RNA}$ as compared to the value observed in the presence of the PIC, suggesting that the 40S itself stimulates eIF4A ATPase activity. We observed similar values for $K_{m\ RNA}$ in all instances: 264 ± 39 μM in the presence of a complete PIC; 267 ± 65 μM when all components except the 40S were present; 102 ± 12 μM with eIF4F alone; and 84 ± 13 μM with eIF4A alone (Figure 2.3A). This suggests that the observed differences reflect a stimulation of the rate of eIFA-catalyzed ATP hydrolysis, and not differences in its interaction with mRNA or significant RNA contamination of the PIC components. Because the 5'-cap promotes mRNA recruitment and translation initiation (Kumar, Hellen, & Pestova, 2016; Mitchell et al., 2010) we also measured the rates of ATPase with uncapped mRNAs in the presence or absence of a PIC. The rates of ATP hydrolysis in the presence and absence of the PIC were comparable to ones measured with capped mRNAs under otherwise the same conditions (data not shown). In particular, the observation that the PIC accelerates the maximal rate of eIF4A-catalyzed

ATP hydrolysis, without affecting its apparent interaction with the mRNA, suggest a functional interaction between the PIC and the eIF4F complex.

The rate of eIF4A-catalyzed ATP hydrolysis saturates at levels of eIF4A in excess of the PIC

In vivo eIF4A is in excess of all other components of the translational machinery and the rate of translation is sensitive to minor decreases in eIF4A concentration (Firczuk et al., 2013; von der Haar & McCarthy, 2002). *In vitro,* maximal rate of mRNA recruitment is observed when eIF4A is in excess of the PIC, mRNA, and other initiation factors (Mitchell et al., 2010; Walker et al., 2013). To determine if the relative amounts of eIF4A and the PIC affect the stimulation of eIF4A by the PIC that we observe, we titrated eIF4A relative to the PIC, in the presence of saturating levels of mRNA and ATP. The rate of ATP hydrolysis observed was normalized to the rate observed with eIF4A alone (Figure 2.3B). Increasing the concentration of eIF4A, and thus the relative ratio of eIF4A to the PIC, resulted in increased rates of ATP hydrolysis plateauing at a concentration of eIF4A in 10-fold excess of the PIC, consistent with the requirement of excess eIF4A for mRNA recruitment, both *in vivo* and *in vitro*. Observed stimulation with respect to eIF4A alone decreased when eIF4A was in excess by 24-fold, likely because all available PICs were saturated by eIF4A (Figure 2.3B).

The PIC and eIF4G•4E stimulate eIF4A via distinct mechanisms

Having observed that the PIC increases the rate of eIF4A-catalyzed ATP hydrolysis at saturating ATP levels without affecting the dependence on mRNA, we next investigated

the effects of the PIC and eIF4E•4G on the dependence of eIF4A for ATP. As before, we measured ATPase activity in the presence and absence of the PIC but here performed experiments with saturating capped *RPL41A* mRNA and instead varied the ATP concentration to determine the maximal rate of ATP hydrolysis at saturating ATP levels ($V_{max\ ATP}$) and the concentration of ATP required to achieve half the maximal rate ($K_{m\ ATP}$). We further calculated $V_{max\ ATP}/K_{m\ ATP}$, as a measure of the catalytic efficiency of eIF4A. In the absence of the PIC and other initiation factors, eIF4A alone hydrolyzed ATP at maximal velocity of 2.92 ± 0.38 μM/min and had a $K_{m\ ATP}$ of 2510 ± 379 μM, yielding a $V_{max\ ATP}/K_{m\ ATP}$ value of $1.16 \times 10^{-3} \pm 0.23 \times 10^{-3}$. The addition of eIF4G•4E to eIF4A resulted in a 4-fold increase in the $V_{max\ ATP}$ (11.9 ± 0.6 μM/min) and a 10-fold decrease in $K_{m\ ATP}$ (249 ± 13 μM), thereby increasing $V_{max\ ATP}/K_{m\ ATP}$ 41-fold. The addition of the PIC to eIF4F increased the $V_{max\ ATP}$ another 4-fold but had no additional effect on $K_{m\ ATP}$ (Figure 2.3C, "4A alone," "4A•4G•4E alone," "+"), increasing $V_{max\ ATP}/K_{m\ ATP}$ an additional 2.6-fold. Omitting 40S subunits from reactions containing eIF4F and all other PIC components decreased the $V_{max\ ATP}$ (as compared to reactions containing eIF4F and all PIC components, "+") by a factor of 2 but also had no effect on the $K_{m\ ATP}$ (Figure 2.3C, "-40S"), underscoring the importance of the 40S subunit in promoting ATPase activity. In contrast, the omission of eIF4A from reactions containing all other components resulted in a 67-fold decrease in the rate of ATPase, ruling out any significant ATPase contamination in either the PIC components or other initiation factors (Figure 2.3C, "-4A").

We next asked if the PIC could stimulate eIF4A ATPase directly, in the absence of eIF4G•4E. Addition of the PIC to eIF4A, in the absence of eIF4G•4E, resulted in a 6-fold increase in $V_{max\ ATP}$ over eIF4A alone (Figure 2.3C, "4A alone" vs. "-4G•4E") without any change to the $K_{m\ ATP}$. This, in turn, caused a modest increase in $V_{max\ ATP}/K_{m\ ATP}$, a value

which is nonetheless lower than that observed either in the presence of eIF4F alone or in the presence of eIF4F together with all PIC components (Figure 2.3C, grey bars, "-4G•4E"). eIF4G is thought to position eIF4A domains for binding and catalysis (Hilbert et al., 2011; Oberer et al., 2005), potentially explaining its enhancement of $K_{m\ ATP}$. Whereas eIF4G•4E also stimulated the maximal rate of ATP hydrolysis ($V_{max\ ATP}$), the PIC increased only the $V_{max\ ATP}$ without affecting $K_{m\ ATP}$, consistent with the interpretation that the PIC stimulates ATP hydrolysis without affecting eIF4A ATP binding, whereas eIF4G•4E enhances both.

eIF3 and other components of the PIC are required for full stimulation of eIF4A

To further dissect the functional interactions among eIF4A, eIF4G•4E, and the PIC, we next measured $V_{max\ ATP}$ and $K_{m\ ATP}$ in the absence of each PIC component. In contrast to the absence of either 40S subunits or eIF4G•4E, the absence of either eIF5 or eIF4B had no significant effects on either $V_{max\ ATP}$ or $K_{m\ ATP}$. However, we observed decreases of approximately 30-60 % in $V_{max\ ATP}$ in the absence of either eIF3, eIF2, $tRNA_i$, eIF1, or eIF1A, with the greatest decrease observed in the absence of eIF3 (Figure 2.3C). We did not observe significant differences in $K_{m\ ATP}$ in the absence of these components. Together, these suggest the PIC stimulation of eIF4A that we observe depends on the presence of the majority of PIC constituents.

Figure 2.3 eIF4A and eIF4F activity is stimulated by the PIC. (A) ATPase activity in the presence of saturating ATP, titrating natural capped mRNA RPL41A. "+" contains 5 μM eIF4A, 0.5 μM eIF4G, 0.5 μM eIF4E, 0.5 μM eIF4B, 0.5 μM eIF2, 0.5 μM Met-tRNA(Met), 1 mM GDPNP, 0.5 μM eIF3, 0.5 μM eIF5, 1 μM eIF1, 1 μM eIF1A, and 0.5 μM 40S. Capped mRNA RPL41A concentrations are varied. Black: +, kcat RNA = 45.2 ± 3.9 μM/min, Km RNA 264 ± 39 μM. Red: -40S, kcat RNA = 26.5 ± 0.1 μM/min, Km RNA 267 ± 65 μM. Green: 5 μM eIF4A, 0.5 μM eIF4G, and μM 0.5 μM eIF4E, kcat RNA = 16 ± 1 μM/min, Km RNA 102 ± 12 μM. Cyan: 5 μM eIF4A alone, kcat RNA = 2.4 ± 0.2 μM/min, Km RNA 84 ± 13 μM. (B) ATPase activty versus stoicheometry of eIF4A to the PIC, normalized to eIF4A ATPase alone. Concentrations are same as in "+" in (A) except eIF4A, which are as indicated on the plot. (C) ATPase activity with 0.5 μM PIC. "+" is the same as in (A). Red bars: (top scale) Vmax ATP; Blue bars (bottom scale) Km ATP ; Grey Vmax ATP/Km ATP. Components missing from the PIC are indicated. (D) ATPase with 30 nM PIC. "+" contains 5 μM eIF4A, 0.05 μM eIF4G, 0.05 μM eIF4E, 0.3 μM eIF4B, 0.3 μM eIF2, 0.3 μM Met-tRNA(Met), 0.5 mM GDPNP, 0.3 μM eIF3, 0.3 μM eIF5, 1 μM eIF1, 1 μM eIF1A, 0.03 μM 40S, and 0.015 μM RPL41A (black) or CAA 50mer (green). Red bars (top scale) Vmax ATP; Blue Km ATP (bottom scale). All data presented in the figure are mean values (n≥2) and error bars represent average deviation of the mean.

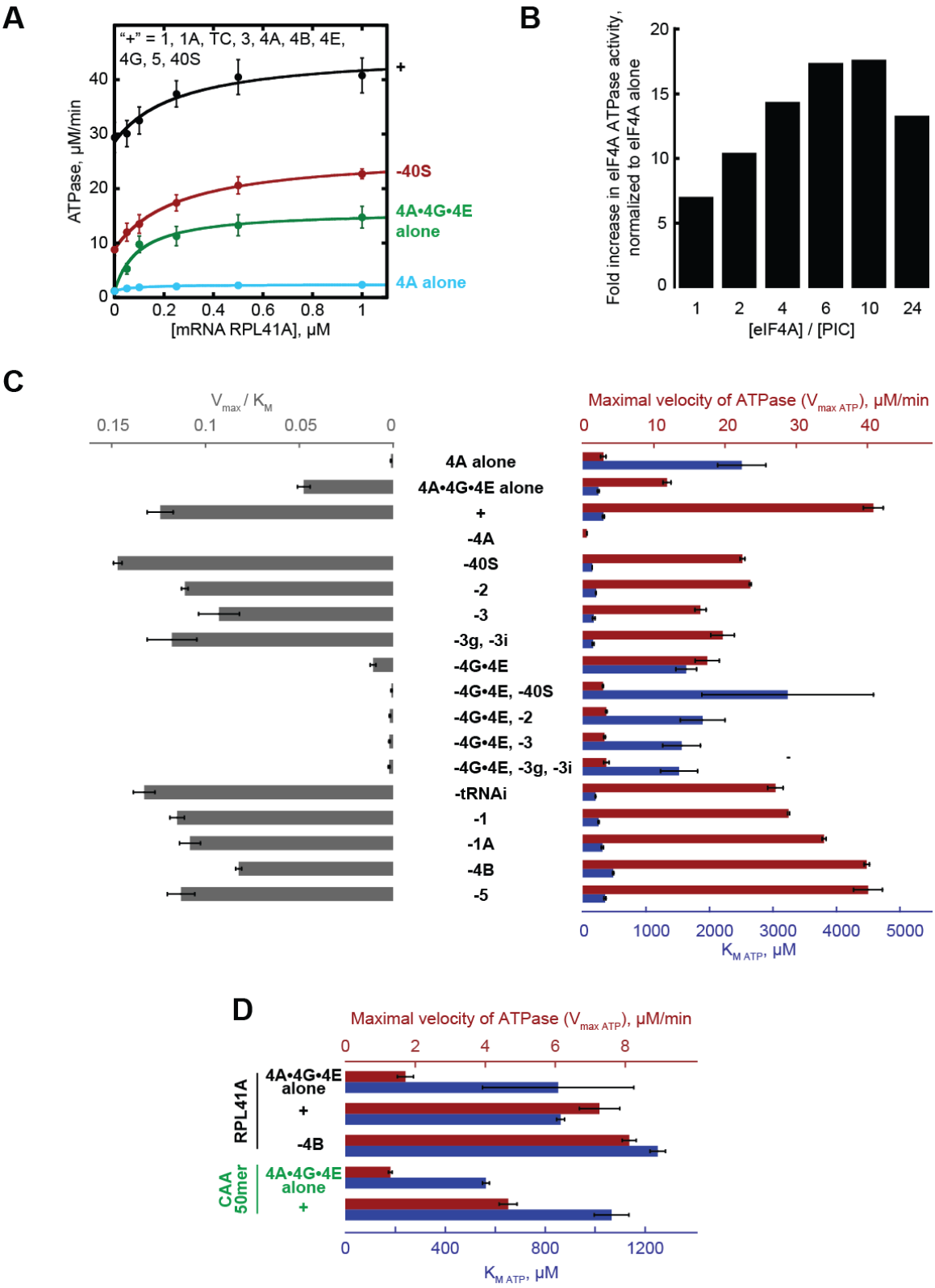
A
"+" = 1, 1A, TC, 3, 4A, 4B, 4E, 4G, 5, 40S
+
-40S
4A•4G•4E alone
4A alone
ATPase, μM/min
[mRNA RPL41A], μM
B
Fold increase in eIF4A ATPase activity, normalized to eIF4A alone
[eIF4A] / [PIC]
C
Vmax / KM
Maximal velocity of ATPase (Vmax ATP), μM/min
4A alone
4A•4G•4E alone
+
-4A
-40S
-2
-3
-3g, -3i
-4G•4E
-4G•4E, -40S
-4G•4E, -2
-4G•4E, -3
-4G•4E, -3g, -3i
-tRNAi
-1
-1A
-4B
-5
KM ATP, μM
D
Maximal velocity of ATPase (Vmax ATP), μM/min
RPL41A
4A•4G•4E alone
+
-4B
CAA 50mer
4A•4G•4E alone
+
KM ATP, μM

Of these effects, one of the strongest defects we observe occurred in the absence of eIF3. eIF3 comprises 5 core subunits and is involved in numerous steps of translation initiation, including mRNA recruitment. We have previously demonstrated that eIF3 is essential for mRNA recruitment within the *in vitro* system (Mitchell et al., 2010), as it is *in vivo* (Jivotovskaya, Valášek, Hinnebusch, & Nielsen, 2006), and that it stabilizes the PIC and functions to promote mRNA recruitment near the PIC entry channel. (Aitken et al., 2016). In particular, the eIF3g and eIF3i subunits have been implicated in scanning and AUG recognition *in vivo* (Cuchalová et al., 2010) and are required for recruitment of *RPL41A in vitro* (Aitken et al., 2016; Valásek, 2012). Both subunits are thought to be located near the mRNA entry channel of the ribosome, at either the solvent or intersubunit face of the 40S subunit (Aylett et al., 2015; des Georges et al., 2015; Llacer et al., 2015). Reactions containing eIF4F and PIC formed with the eIF3 subunits a, b, and c but lacking the g and i subunits produced $V_{max\ ATP}$ and $K_{m\ ATP}$ values similar to those obtained in the absence of the entire eIF3 complex (Figure 2.3C, "-3" vs. "-3g, -3i"). The combined absence of eIF4G•4E and either eIF3 (wild type or mutant lacking 3g and 3i), eIF2, or 40S abrogated all stimulation of ATPase activity and resembled the rate of observed with eIF4A alone (Figure 2.3C), suggesting that an intact PIC and eIF4G•4E together are required for the increased rate of ATP hydrolysis.

In contrast to the absence of eIF3 and other PIC components, we did not observe any effect on the kinetics of ATPase activity by eIF4B in the presence or absence of the PIC (Figure 2.2C and 2.3C). Previous reports demonstrated eIF4B to function as a coupling factor for ATP-dependent RNA unwinding and stimulate eIF4A ATPase in both mammals and yeast (Alexandra Z Andreou & Klostermeier, 2014; Alexandra Zoi Andreou et al., 2017; Özeş et al., 2011). Differences may have resulted from our experimental setup employing a

full-length eIF4G1 co-purified with eIF4E or due to the fact that eIF4A – mimicking the scenario *in vivo* – was in excess of all other factors. The ratio of $V_{max\ ATP}/K_{m\ ATP}$, reporting on the catalytic efficiency of the enzyme, was modestly higher in the presence of eIF4B (Figure 2.3C, grey bars, "+" vs. "-4B") consistent with the idea that eIF4B facilitates more productive ATP hydrolysis. Repeating the experiment under previously reported conditions (Walker et al., 2013) marked by limiting, rather than saturating mRNA, in the presence of saturating concentrations of factors (also used throughout this study – see "30 nM PIC" in Methods) also did not result in a notable difference in the presence or absence of eIF4B (Figure 2.3D, "+" vs. "-4B").

The PIC stimulates ATP hydrolysis by eIF4F in the presence of limiting amounts of both a structured natural mRNA and a short unstructured model mRNA

Our initial observation that eIF4A stimulated the recruitment of both the natural *RPL41A* mRNA and the unstructured CAA 50mer model mRNA was made under conditions of limiting mRNA, whereas our experiments investigating the stimulation of eIF4A ATPase by the PIC and other initiation factors were performed at saturating mRNA levels. To confirm that PIC stimulation of eIF4F we observed is maintained at limiting mRNA levels, we monitored ATP hydrolysis by eIF4A (in the context of the eIF4F complex), and the effect of adding the PIC to these reactions, in the presence of 15 nM *RPL41A* or CAA 50mer (30 nM PIC conditions, as in Figure 2.1). As under saturating mRNA conditions, the addition of the PIC increased $V_{max\ ATP}$ approximately 4-fold in the presence of both the natural *RPL41A* and the unstructured CAA 50mer mRNAs, as compared to eIF4F alone (Figure 2.3D). Together with the observation that eIF4A

accelerates the recruitment of both mRNAs under identical conditions, this suggests a role for eIF4A in translation initiation that may not depend on the degree of mRNA structure (Hinnebusch, 2014; Sen et al., 2015). As compared to the 0.5 μM PIC conditions (Figure 2.3C), the $K_{m\ ATP}$ was higher in all cases with 30 nM PIC conditions, by approximately 3-fold, likely because eIF4A binds RNA and ATP cooperatively (Lorsch & Herschlag, 1998) and mRNA was subsaturating in these experiments (Figure 2.3D) whereas it was saturating in experiments performed under the 0.5 μM PIC conditions (Figure 2.3C).

eIF4A stimulates the recruitment of both unstructured mRNAs and mRNAs containing varying degrees of structure 5'- or 3'- of the start codon

The finding that eIF4A-dependent ATP hydrolysis increases the rate of recruitment of a natural mRNA as well as a short, unstructured 50 nucleotide-long model mRNA prompted us to investigate which features of an mRNA confer dependence on eIF4A for mRNA recruitment. To this end, we created a library of *in vitro* transcribed and individually purified mRNAs spanning a range of structures and lengths. This library contains both model mRNAs and the natural *RPL41A* mRNA, as well as chimeric mRNAs containing both artificial sequence and regions of the *RPL41A* mRNA (Figure 2.4A). We followed the recruitment kinetics for each mRNA as a function of eIF4A (as described above) and determined the maximal rate ($k_{max\ 4A}$) as well as the concentration of eIF4A required to achieve the half-maximal rate ($K_{1/2\ 4A}$).

Figure 2.4. eIF4A stimulates recruitment of all mRNAs regardless of degree of structure. (A) Schematic of mRNAs used in the study. See "Key" in the figure for details. (B) Endpoints of mRNAs from (A) recruited to the PIC in presence (black) or absence (red) of saturating 5 μM eIF4A, listed in the same order as in A. (C) Maximal rate of mRNA recruitment ($k_{max\ 4A}$, min^{-1}) for the mRNAs in A. (D) Fold stimulation of the rate of mRNA recruitment by eIF4A. Numbers in parenthesis correspond to the mRNAs in (A). All data presented in the figure are mean values ($n \geq 2$) and error bars represent average deviation of the mean.

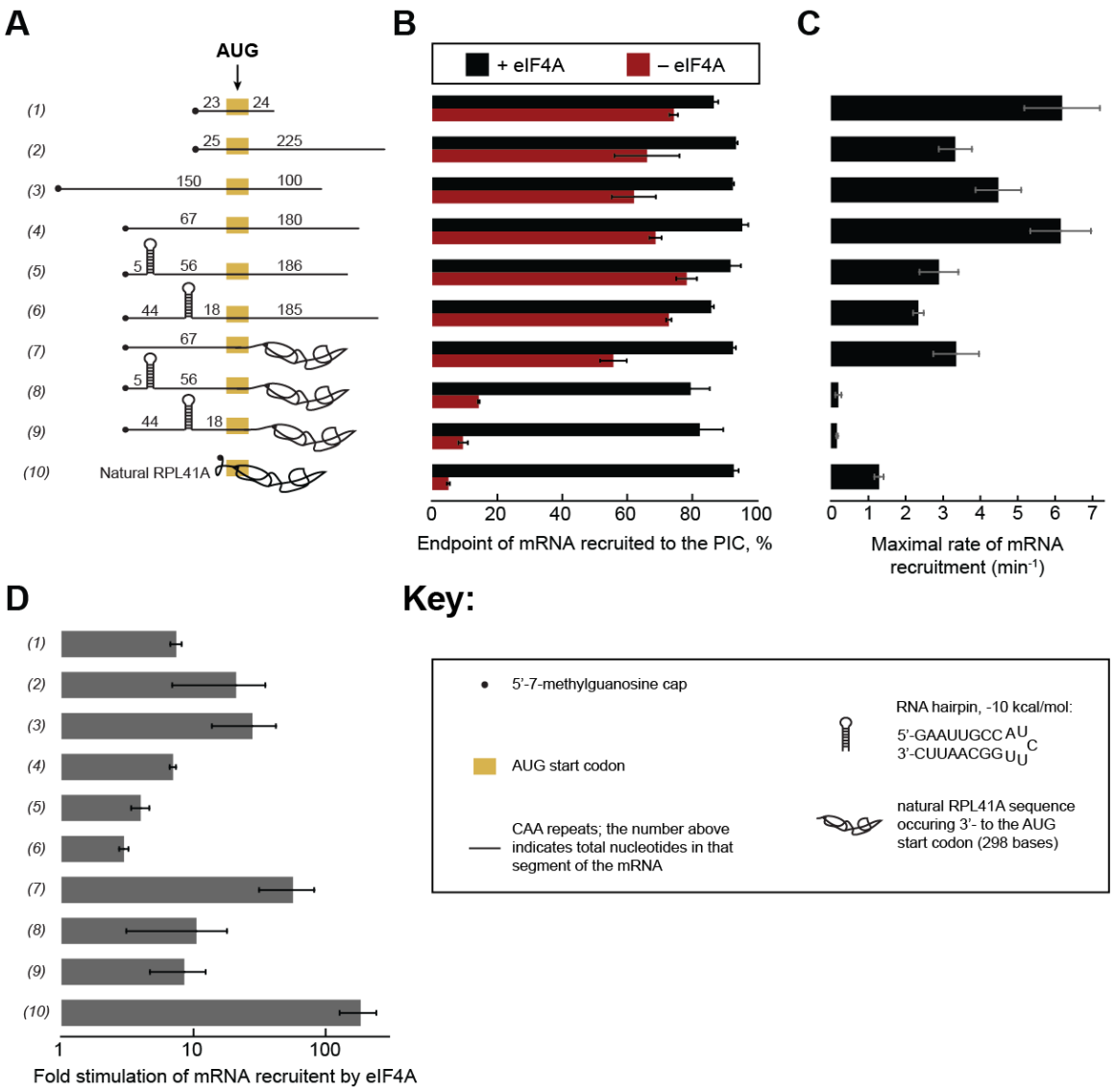
A
AUG
(1)
23
24
(2)
25
225
(3)
150
100
(4)
67
180
(5)
5
56
186
(6)
44
18
185
(7)
67
(8)
5
56
(9)
44
18
(10)
Natural RPL41A
B
+ eIF4A
– eIF4A
0
20
40
60
80
100
Endpoint of mRNA recruited to the PIC, %
C
0
1
2
3
4
5
6
7
Maximal rate of mRNA recruitment (min-1)
D
(1)
(2)
(3)
(4)
(5)
(6)
(7)
(8)
(9)
(10)
1
10
100
Fold stimulation of mRNA recruitent by eIF4A
Key:
5'-7-methylguanosine cap
AUG start codon
CAA repeats; the number above indicates total nucleotides in that segment of the mRNA
RNA hairpin, -10 kcal/mol:
5'-GAAUUGCC A U C
3'-CUUAACGG U U
natural RPL41A sequence occuring 3'- to the AUG start codon (298 bases)

Figure 2.5. eIF4A promotes rmRNA recruitment of structured and CAA-repeats mRNAs. (A-B) Observed rate of mRNA recruitment versus concentration of eIF4A. Data were fit to a hyperbolic equation allowing for a y-intercept > 0. Numbers in parentheses, to the right of the coordinate plain, correspond to mRNAs in Figure 2.4A and are colored for easier visualization of distinct curves. RNAs 2 and 3 are shown separately for clarity. (C) Zoom of mRNAs 8 and 9 from (A). (D) $k_{max\ 4A}$ and $K_{1/2\ eIF4A}$ from fits in panels A-C. All data presented in the figure are mean values ($n \geq 2$) and error is average deviation of the mean.

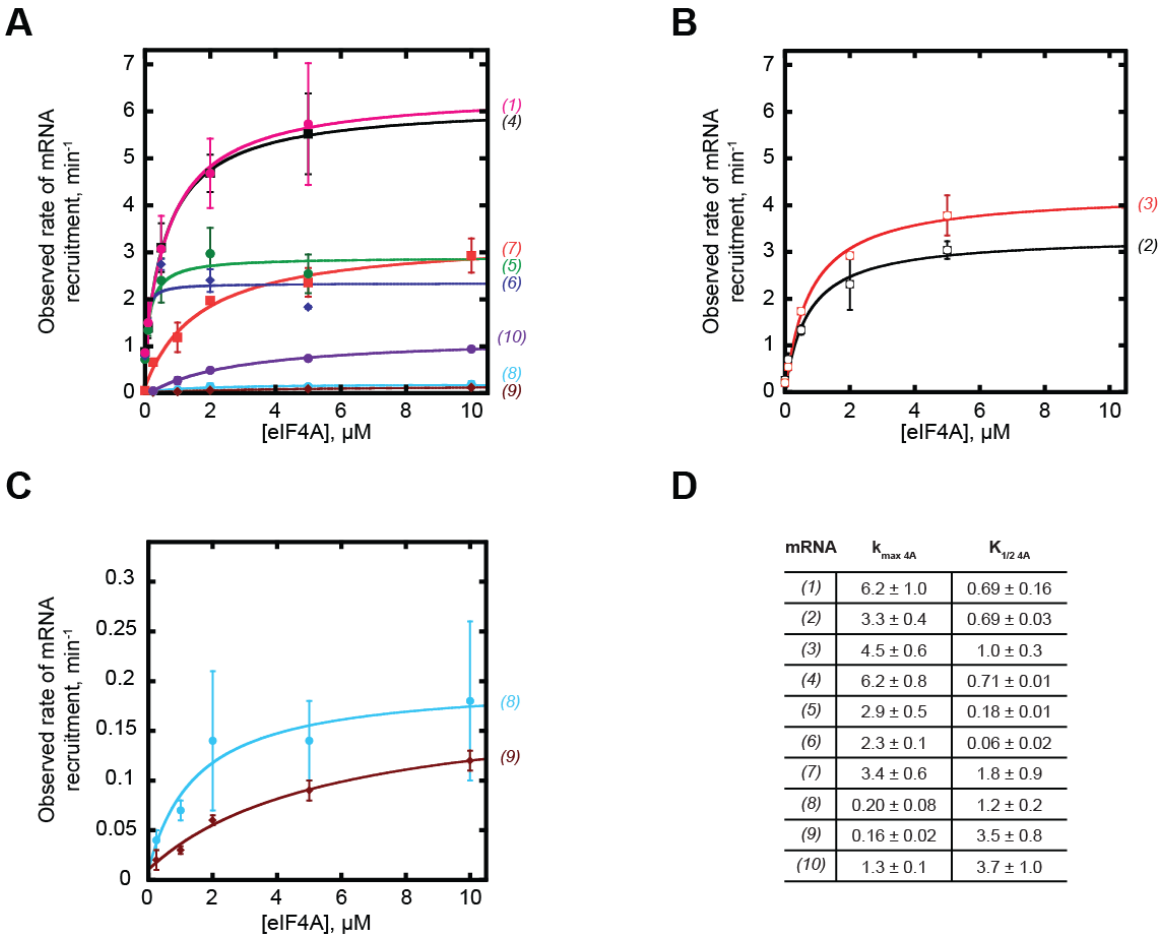

mRNA	$k_{max\ 4A}$	$K_{1/2\ 4A}$
(1)	6.2 ± 1.0	0.69 ± 0.16
(2)	3.3 ± 0.4	0.69 ± 0.03
(3)	4.5 ± 0.6	1.0 ± 0.3
(4)	6.2 ± 0.8	0.71 ± 0.01
(5)	2.9 ± 0.5	0.18 ± 0.01
(6)	2.3 ± 0.1	0.06 ± 0.02
(7)	3.4 ± 0.6	1.8 ± 0.9
(8)	0.20 ± 0.08	1.2 ± 0.2
(9)	0.16 ± 0.02	3.5 ± 0.8
(10)	1.3 ± 0.1	3.7 ± 1.0

The presence of saturating levels of eIF4A (as determined by $k_{max\ 4A}$ and $K_{m\ 4A}$ measurements, Figure 2.5) resulted in recruitment endpoints between 85%-95% with all mRNAs tested (Figure 2.4B, black bars). In the absence of eIF4A less than 10% of *RPL41A* was recruited (Figure 2.4B, RNA 10 red bar), consistent with the low levels of *RPL41A* recruitment we observed in the absence of ATP (Figure 2.1A). The $k_{max\ 4A}$ was 1.3 ± 0.1 min^{-1} (Figure 2.4C) and the $K_{1/2\ 4A}$ was measured to be 3.7 ± 1 μM (Figure 2.5). Due to the low extent of recruitment observed in the absence of eIF4A, timecourses with *RPL41A* mRNA could not be fit to a single-exponential kinetic model. Instead, comparison of estimated initial rates of recruitment of *RPL41A* revealed that recruitment proceeds more than two orders of magnitude more rapidly in the presence of saturating levels of eIF4A (Figure 2.4D) versus recruitment in the absence of eIF4A.

Consistent with our observation that the CAA 50mer mRNA is efficiently recruited even in the absence of ATP, we observed 74 ± 1 % recruitment of this mRNA in the absence of eIF4A as well (Figure 2.4A-B, RNA 1). Nonetheless, the addition of saturating eIF4A does increase this recruitment extent to 87 ± 1 %, consistent with our observation that the addition of ATP stimulates recruitment of this mRNA beyond the levels observed in the absence of ATP (Figure 2.1B). Beyond this modest stimulation of recruitment extent, saturating eIF4A accelerates the rate of CAA 50mer recruitment, yielding a $k_{max\ 4A}$ of 6.2 ± 1.0 min^{-1} (Figure 2.4C), a more than 7-fold increase (Figure 2.4D) as compared to the rate of CAA 50mer recruitment in the absence of eIF4A. As compared to *RPL41A* mRNA, this acceleration is achieved at lower levels of eIF4A ($K_{1/2\ 4A\ =}$ 0.69 ± 0.16 μM, Figure 2.5).

To compare the CAA 50mer with a longer mRNA, we increased the total length by an additional 200 nucleotides – that were all CAA repeats –making new mRNAs that were 250 nucleotides (250mer). We added all of the additional CAA repeats to the 3'-end (Figure

2.4A, RNA 2). With this mRNA, in the absence of eIF4A, we observed a 66 ± 10 % extent of recruitment, which was comparable to the CAA 50mer in the absence of eIF4A (Figure 2.4B, red bars RNA 1 vs. 2). The $k_{max\ 4A}$ was 3.3 ± 0.4 min^{-1}, less than 2-fold slower than that for CAA 50mer, and the $K_{1/2\ 4A}$ was 0.69 ± 0.03 μM, nearly identical to CAA 50mer. Importantly, eIF4A also stimulated the rate of recruitment for this mRNA by ~20-fold. To investigate how location of the AUG will influence the kinetics of mRNA recruitment with respect to eIF4A, we also made two similar CAA repeats mRNAs, 250 nucleotides in length, but the AUG start codon was 67 and 150 nucleotides away from the 5'-end, (Figure 2.4A, RNAs 3 and 4). The extent of recruitment (Figure 2.4B), $k_{max\ 4A}$ (Figure 2.4C), $K_{1/2\ 4A}$ (Figure 2.5), and fold stimulation of the rate of recruitment by eIF4A (Figure 2.4D) for both RNAs were similar to that of the CAA 50mer. Taken together, extending the CAA 50mer to 250 nucleotides in total length and location of the AUG within the extended mRNAs resulted in kinetics of recruitment comparable to that of the CAA 50mer. Notably, eIF4A accelerated the rate of mRNA recruitment for the 250mer mRNAs to a comparable degree as for the CAA 50mer (Figure 2.4D, RNA 1-4).

eIF4A is thought to remove RNA hairpins in the 5'-UTR to facilitate mRNA recruitment and scanning starting at the 5'-end so we added a single hairpin comprising 9 base pairs (-10 kcal/mol; see Figure 2.4, "Key") to the 5'-UTR of a 250mer, made of CAA repeats, either proximal or distal to the 5'-cap (Figure 2.4A, RNAs 5-6). To our surprise, in the absence of eIF4A, neither the cap-proximal and nor the cap-distal hairpins significantly influenced the extent of recruitment, achieving between 70 % and 80 %, comparable to the previously discussed CAA 50mer and 250mer RNAs lacking any significant structural elements. The $k_{max\ 4A}$ was 2.9 ± 0.5 min^{-1} and 2.3 ± 0.1 min^{-1} for 250mers with cap-proximal and cap-distal hairpins, respectively, which is ~2-fold lower than the CAA 50mer but ~2-

fold faster than the $k_{max\ 4A}$ for *RPL41A* (Figure 2.4C). As before, saturating eIF4A stimulated the rate of recruitment for both cap-proximal and cap-distal hairpin mRNAs but to a lesser degree than in the absence of the hairpin: between 3- and 4-fold (Figure 2.4D, RNA 5-6). Taken together, addition of a cap-proximal or a cap-distal hairpin in the 5'-UTR of a 250mer comprising CAA repeats throughout the rest of the sequence resulted in approximately slower mRNA recruitment as compared with the CAA 50mer but was faster than *RPL41A*.

eIF4A helicase is thought to act on the 5'-UTR, especially near the 5'-end; however, a chimeric mRNA, comprising CAA-repeats in the 5'-UTR and the natural sequence (with structural complexity) from *RPL41A* after the AUG start codon, had an endpoint of 55 ± 4 % recruitment in the absence of eIF4A (Figure 2.4A-B, RNA 7). Indeed, comparison with mRNAs possessing a hairpin in the 5'-UTR (Figure 2.4B, RNA 5-6) shows that the extent of recruitment was affected more by structural complexity 3'- to the AUG, rather than a stable hairpin in the 5'-UTR. In addition to a depressed extent of recruitment, the observed rate of mRNA recruitment in the absence of eIF4A was significantly lower for RNA 7 (~0.05 min^{-1}) than for RNAs 1-6 (~0.6-1 min^{-1}) (Figure 2.5A, RNAs 1-6 vs. 7), resembling the fully natural *RPL41A* mRNA. In contrast, the $k_{max\ 4A}$ for RNA 7 was 3.4 ± 0.6 min^{-1} (Figure 2.4C), within 2-fold of the rates observed with RNAs 1-6. Consequently, addition of a saturating level of eIF4A caused a greater (57-fold) increase in the rate of recruitment for RNA 7 than it did for RNAs 1-6. Also, the $K_{1/2\ 4A}$ was 1.8 ± 0.9 μM, approximately midway between the CAA 50mer (0.69 ± 0.16 μM) and *RPL41A* (3.7 ± 1 μM).

Lastly, combining a cap-proximal or a cap-distal hairpin and CAA repeats in the 5'-UTR together with natural *RPL41A* sequence after the AUG, was inhibitory to mRNA recruitment in the absence of eIF4A, resulting in endpoints observed with a natural *RPL41A*

of less than 20% (Figure 2.4B, RNAs 8 and 9). Also, the $k_{max\ 4A}$ for cap-proximal (RNA 8) and cap-distal (RNA 9) hairpins was 0.20 ± 0.08 min^{-1} and 0.16 ± 0.02 min^{-1}, respectively, and ~6-fold slower than the fully natural *RPL41A*. Thus, strict eIF4A dependence – observed with the natural *RPL41A* mRNA – was mimicked only when there was a hairpin in the 5'-UTR together with structural complexity 3'- to the AUG (Figure 2.4B, RNAs 1-7 vs. 8-9). Due to low endpoints in the absence of eIF4A, similar to *RPL41A*, mRNAs 8 -9 could not be fitted to a single exponential equation and fold stimulation by eIF4A was estimated from comparison of initial rates in the presence of saturating eIF4A versus no eIF4A (Figure 2.4D, 8-9). As for all other mRNAs, eIF4A stimulated the rate of recruitment 11-fold for RNA 8 and 9-fold for RNA 9. The $K_{1/2\ 4A}$ for cap-proximal (RNA 8) was 1.2 ± 0.2 μM and 3.5 ± 0.8 for cap-distal (RNA 9) (Figure 2.5C). RNA 8 may have resulted in a modestly lower $K_{1/2\ 4A}$ due to eIF4G•4E binding near the cap and removing structure by mass action.

In summary, presence of structure throughout the mRNA, rather than isolated hairpins in the 5'-UTR, was the primary determinant of imposing eIF4A dependence and had the biggest effect on the $k_{max\ 4A}$. Also, eIF4A promoted the rate of mRNA recruitment of all mRNAs tested, ranging from short low structure CAA repeats to natural *RPL41A*.

5'-7-methylguanosine cap imposes an eIF4A requirement for structured and unstructured mRNAs but does not affect ATPase

Having observed that eIF4A-dependent ATP hydrolysis is enhanced by eIF4G•4E in our experiments, we next inquired how the 5'-cap influences the requirement for eIF4A in mRNA recruitment. We have previously shown that the 5'-cap enforces the requirement for

numerous eIFs, including eIF4A, in mRNA recruitment (Mitchell et al., 2010). More recent work in the mammalian system demonstrated that the 5'-cap-eIF4E-eIF4G-eIF3-40S network of interactions promotes recruitment, while its disruption is inhibitory (Kumar et al., 2016). As above we monitored the kinetics of mRNA recruitment (30 nM PIC conditions) at various concentrations of eIF4A with mRNAs 1 (CAA 50mer), 4 (250 nt unstructured model), 7 (unstructured 5' UTR with natural sequence 3' of AUG), and 10 (*RPL41A*). For all four RNAs tested, the $k_{max\ 4A}$ was comparable to that measured in the presence of the cap. In contrast, in the absence of eIF4A, the rate of recruitment for uncapped versions of the unstructured model mRNAs 1 and 4 increased 3.7- and 2.5-fold, respectively, as compared to the observed rate of recruitment of 5' 7-methylguanosine-capped versions of the same mRNAs (Figure 2.6). This acceleration was even more pronounced for RNA 7, which contains natural mRNA sequence 3'- of the AUG. Uncapped RNA 7 was recruited at a 14-fold faster rate in the absence of eIF4A as compared to the same mRNA possessing a 5' 7-methylguanosine cap. Because the recruitment of more structurally complex mRNAs such as *RPL41A* and RNAs 8 and 9 (Figure 2.4A) depends so strongly on eIF4A, we were unable to compare the recruitment rates of uncapped and capped versions of these mRNAs in the absence of eIF4A. Nonetheless, the observation that capped mRNAs are recruited more slowly in the absence of eIF4A than identical uncapped mRNAs is consistent with our previous proposal that the 5'-cap enforces a stronger requirement for the full complement of initiation factors. This effect may be stronger for more structurally complex mRNAs because identification of the 5'-end may be more difficult, and thus depend more strongly on eIF4A, for more structurally heterogenous mRNAs.

Figure 2.6. 5'-7-methylguanosine cap inhibits mRNA recruitment in the absence of eIF4A. Observed rates of mRNA recruitment in the presence or absence of a 5'-cap. (See Key in Figure 2.4 for explanation of mRNA diagrams). All data presented in the figure are mean values and error bars represent average deviation of the mean. ND - not determinable due to a very low endpoint.

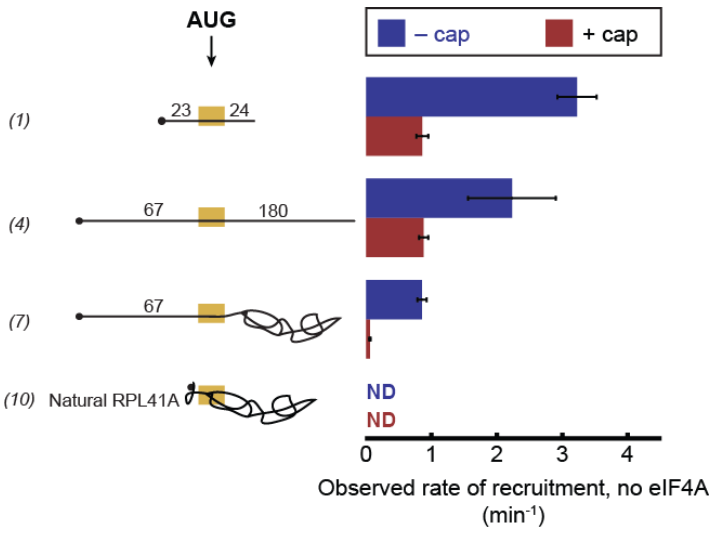

Discussion

Fifteen years ago it was suggested that an *in vivo* substrate for eIF4A is likely single stranded RNA (G. W. J. Rogers et al., 2002). Since then, high resolution crystal structures, genetic, and biochemical work provided critical insights into its mechanism of catalysis, alone and in the context of eIF4F (Harms et al., 2014; Hilbert et al., 2011; Lindqvist et al., 2008; Merrick, 2015; Oberer et al., 2005; Schütz et al., 2008). More recently, Next Generation Sequencing (i.e. Ribosome Profiling) allowed to holistically examine the effect of eIF4A on global translation (Sen et al., 2015) and biochemical techniques gave clues as to how eIF4A and eIF4F may interact with the rest of the recruitment machinery (Gao et al., 2016; Garcia-Garcia et al., 2015; Kumar et al., 2016). However, the mechanism of how an mRNA is unwound and bound by the PIC remains an open question. Our data demonstrate that ATP hydrolysis by eIF4A stimulates the recruitment of both natural *RPL41A* mRNA and a 50 nt model mRNA, and that the PIC stimulates the ATPase activity of eIF4A. Together, these observations suggest that eIF4A, eIF4F, or both interact with the PIC to promote mRNA recruitment. Further, we observed that eIF4A accelerates the recruitment for a wide variety of mRNAs, and that the degree of this acceleration does not only dependent on the amount of secondary structure in the 5'-UTR of an mRNA. Instead, the requirement for eIF4A is most pronounced for mRNAs containing some degree of structural complexity throughout their entire sequence. Surprisingly, eIF4A increases the rate of recruitment for unstructured model mRNAs comprising CAA repeats, regardless of length, in addition to being required for the recruitment of more structured mRNAs. We propose that eIF4A functions to relax the structural heterogeneity present in all mRNAs – owing to the entanglement of any polymer significantly longer than its persistence length (H. Chen et al., 2012) – perhaps to enable facile identification of the 5' cap structure by the

translational machinery. eIF4A could perform this role by interacting with the mRNA directly, or by remodeling the PIC mRNA entry channel.

The PIC stimulates eIF4A and eIF4F activity

In the current model of mRNA recruitment, eIF4F is localized to the 5'-end of the mRNA via the eIF4E-cap interaction, where it collaborates with eIF4B to prepare the mRNA for PIC binding. Consistent with this model, eIF4G and eIF4B were the only proteins known to stimulate eIF4A activity in translation initiation (Hinnebusch, 2014; Mitchell et al., 2011). And yet, given the natural propensity of an mRNA to form structure – either as a function of secondary structure elements or the structural complexity and entanglement inherent to all polymers – it is difficult to envision how the activated mRNP created upon mRNA interaction with eIF4F and eIF4B is handed over to the initiating ribosome without the mRNA reforming any structure. Moreover, recent work has demonstrated that eIF4B in fact binds the ribosome itself (Walker et al., 2013), thus blurring the lines between the PIC and the activated mRNP. In another proposed model, eIF4F and eIF4B could interact with the PIC, forming a "holo-PIC" (Aitken & Lorsch, 2012) that relaxes the mRNA and attaches to it simultaneously.

Our observation that the PIC stimulates eIF4A, both in the context of the eIF4F complex but also in the absence of eIF4G•4E, is consistent with the holo-PIC model. It is not clear if the mechanism of interaction between the PIC and eIF4A is the same as between the PIC and eIF4F. eIF4A is present at a higher intracellular concentration than eIF4G or eIF4E and it is possible to envision a scenario where the PIC directly interacts with eIF4A, while eIF4G – when present – also binds the mRNA and engages the eIF4A domains to promote more efficient catalysis.

Dissection of ATPase activity demonstrated that nearly all core components of the PIC are necessary for full acceleration of ATP hydrolysis, suggesting that the intact PIC is required for efficient interaction with eIF4A and eIF4F. The strongest defects we observe are in the absence of eIF4G•4E, eIF3, eIF2, and 40S. When eIF4G•4E was absent in combination with any of those factors, the stimulation of eIF4A activity by the PIC was completely abrogated. This further suggests that ATPase activity is stimulated only when the PIC is ready for translation initiation. It is also consistent with previous reports *in vivo* and *in vitro* demonstrating that eIF3 and eIF4G are critical for mRNA recruitment and are known to interact in the mammalian system (Jackson et al., 2010). Furthermore, all three proteins have previously been implicated in mRNA recruitment and scanning (Aitken et al., 2016; Cuchalová et al., 2010; Mitchell et al., 2010; Valásek, 2012), and structural data suggest that eIF3g and eIF3i are located near the mRNA entry channel of the 40S subunit, on either the solvent or intersubunit face (Aylett et al., 2015; des Georges et al., 2015; Llacer et al., 2015). The observation that these eIF3 subunits appear at distinct locations near the mRNA entry channel in complexes either containing or lacking mRNA has led to the speculation that they might participate in a large-scale rearrangement of the PIC important for either initial attachment to the mRNA or scanning along it (Llacer et al., 2015; Simonetti et al., 2016). Given our observation that these subunits, together with eIF4G, are important for full stimulation of eIF4A ATP hydrolysis, it is tempting to speculate that eIF4A might interact with these and other components of the PIC near the mRNA entry channel. At this location, eIF4A might interact directly with the mRNA to promote its loading into the PIC. Another possibility, however, is that eIF4A instead remodels the PIC near the entry channel in such a way as to facilitate mRNA insertion.

eIF4A promotes the rate of recruitment for all mRNAs regardless of structure and is required only for mRNAs containing structural complexity throughout their sequence

Owing to its identity as a helicase, and to the observations that it can unwind RNA duplexes *in vitro* (Alexandra Zoi Andreou et al., 2017; Garcia-Garcia et al., 2015; Lorsch & Herschlag, 1998; Özeş et al., 2011; Rajagopal et al., 2012; G. Rogers et al., 1999) and is required for 48S PIC formation on β-globin mRNA (Pestova & Kolupaeva, 2002), eIF4A has long been thought to promote mRNA recruitment by unwinding RNA structural elements. However, we observe that eIF4A accelerates the recruitment not just of the natural *RPL41A* mRNA or model mRNAs containing secondary structure elements, but also of unstructured CAA repeat model mRNAs of varying length. Together with the previous observations that eIF4A is a poor helicase, and that more potent helicases have recently been demonstrated to promote translation initiation (Gao et al., 2016; Parsyan et al., 2011; Sen et al., 2015), our observations point to a distinct role for eIF4A in promoting the recruitment of all mRNAs.

Figure 2.7. Proposed models for eIF4A in mRNA recruitment to the ribosome during translation initiation. (A) eIF4A keeps mRNA in a partially unwound state until PIC arrival, which stimulates ATPase activity 40-fold, ultimately causing eIF4A to dissociate from the mRNA. (B) eIF4A modulates the PIC to promote mRNA recruitment.

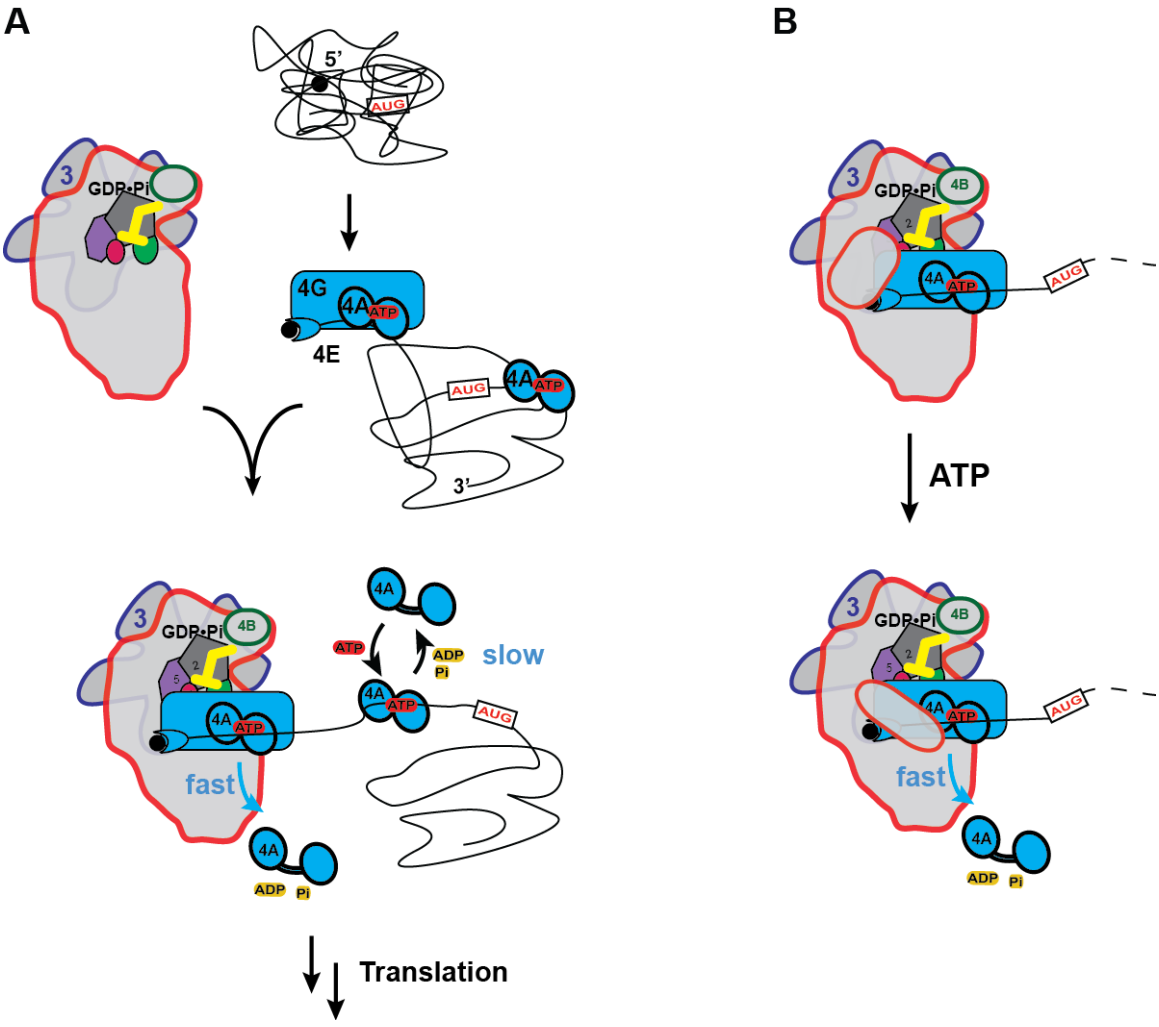

In fact, while eIF4A does accelerate the recruitment of otherwise unstructured mRNAs containing a stable hairpin (-10 kcal/mol) at different locations of their 5'-UTR, it is not required for recruitment of these mRNAs. In contrast, eIF4A was necessary for mRNAs containing these same 5'-UTR hairpins and natural sequence derived from *RPL41A* 3'- to the AUG. It is difficult to say if the PIC was able to directly bind (slot in) on the AUG, scanned through, or skipped over the hairpin during scanning. In contrast, the same hairpin strongly inhibited mRNA recruitment when the mRNA contained a natural (structured) sequence 3'- to the AUG. Together with our observation that ATP accelerates the recruitment of both *RPL41A* mRNA and CAA 50mer mRNA, these findings suggest that eIF4A-dependent ATP hydrolysis is responsible for relieving the global structural complexity present even in mRNAs lacking secondary structure elements, rather than unwinding defined hairpin elements. This activity might enable the disentanglement of the 5' end of the mRNA for identification by eIF4E. Another possible explanation for the requirement for eIF4A only in the presence of structural complexity 3' of the start codon is that the presence of structure throughout the mRNA occludes the start codon, preventing the PIC from slotting onto the mRNA downstream of the cap and forcing it to begin scanning at the eIF4E-5'-cap complex (Kumar et al., 2016), thus ensuring that it encounters the hairpin in the 5'-UTR. In the presence of all the factors, the 5'-cap promotes translation initiation (Kumar et al., 2016; Mitchell et al., 2010) and it is possible that it marks the beginning of the message for PICs that cannot bind to an AUG occluded by mRNA structure. Interestingly, these globally structured mRNAs – *RPL41A,* RNA 8, RNA 9 – are recruited at significantly reduced extents in the absence of eIF4A, whereas less complex mRNAs are efficiently recruited under these conditions (Figure 2.4B). This might reflect the fraction of mRNA inaccessible for PIC attachment in the absence of eIF4A activity.

Given that the 5'-cap enforces the requirement for the full complement of initiation factors in mRNA recruitment (Mitchell et al., 2010), we examined the effect of the 5'-cap on the role of eIF4A. The absence of the 5' cap resulted in the same maximal rate of recruitment as we observed in the presence of eIF4A for a particular mRNA. However, uncapped mRNAs were recruited more rapidly in the absence of eIF4A, as compared to identical capped mRNAs. This acceleration of uncapped mRNA recruitment was most pronounced for a model mRNA containing natural sequence 3'- of the start codon; more structurally complex mRNAs could not be tested owing to their requirement for eIF4A when capped. These results suggest that in the absence of a cap, PIC attachment may proceed on regions of low structural complexity. It is possible that PICs had more freedom to bind on uncapped mRNAs and due to presence of a single AUG, resulted in a faster observed rate of mRNA recruitment. In contrast, presence of structural complexity throughout the mRNA might occlude the 5'-end and the cap is a necessary signal for PIC attachment and mRNA recruitment.

The work presented here addresses the apparent contradiction between the fact that eIF4A is an essential protein responsible for promoting the translation of all mRNAs in vivo (Sen et al., 2015) and its status as one of the weaker helicases associated with translation initiation. It is curious that in the presence of similar but more robust DEAD-box RNA helicases in the cell, eIF4A is an essential protein. Biology is clearly capable of achieving more efficient helicase activity, thus the slow catalysis by eIF4A must be advantageous. Slow ATPase activity, an ability to interact with various components of the PIC, or some other quality gives eIF4A unique properties that other helicases cannot achieve. Our data suggest that eIF4A contributes to mRNA recruitment not by unwinding stable structural elements in the 5'-UTR but instead by relaxing the thermodynamically weaker global mRNA structure;

this structural complexity might include the heterogeneity inherent to any polymer longer than its persistence length (H. Chen et al., 2012), as well as sampling of metastable conformers stabilized by limited base-pairing interactions (Figure 2.7A). The effect of this relaxation might be to facilitate identification of the 5' cap structure by the PIC. In fact, our observation that the PIC stimulates eIF4A activity suggests that eIF4A or eIF4F might collaborate with the PIC within a larger holoPIC complex to couple mRNA relaxation, cap identification, and PIC attachment.

While it is possible that eIF4A interacts directly with mRNA another possibility is that it may be directly modulating or restructuring the PIC itself (Figure 2.7B). Several examples of DEAD-box helicases rearranging and modulating ribonucleoprotein complexes exist (Henn et al., 2012; Jankowsky, 2011; Patrick Linder & Jankowsky, 2011) including mammalian eIF4AIII critical in formation of Exon Junction Complexes (Andersen et al., 2006; Ballut et al., 2005) and DHX29, which binds and modulates the mammalian ribosome (Hashem et al., 2013; Pisareva, Pisarev, Komar, Hellen, & Pestova, 2008). Moreover, the bacterial ribosome has been demonstrated to possess helicase activity (Qu et al., 2011; Takyar, Hickerson, & Noller, 2005) and the residues responsible for this activity are preserved in the eukaryotic ribosome. In fact, we recently demonstrated that these residues in Rps3 – which occurs near the 40S latch and interacts with eIF3 – stabilize the PIC:mRNA interaction (Dong et al., 2017). It is thus tempting to speculate that eIF4A ATP hydrolysis might contribute to modulating this region, thus promoting PIC attachment or scanning.

If eIF4A does contribute to translation initiation as a component of the holoPIC, its presence at levels in vast excess to other translational components remains a mystery. Previous reports show that eIF4A prefers double-stranded RNA as a substrate, whereas eIF4F ATPase activity is maximized on single-stranded RNA (Rajagopal et al., 2012).

Perhaps excess eIF4A has an additional role when not bound to eIF4F or the PIC by binding to RNA unwound by more potent helicases such as Ded1, by (Firczuk et al., 2013; Gao et al., 2016). In such a role, the slow kinetics of eIF4A ATPase (2.41 ± 0.18 μM/min or 0.48 ± 0.04 min^{-1}), which are considerably slower than rates of initiation (approximately 10 min^{-1})(Palmiter, 1975) might prove advantageous. The stimulation of eIF4A by the PIC and eIF4G•4E that we observe increases this rate of ATPase more than 40-fold; scanning PICs could then promote rapid ATP hydrolysis by eIF4A molecules they encounter, resulting in their dissociation and recycling from the mRNA. Such an interaction might contribute to scanning processivity by ensuring that single-stranded mRNA is continuously presented to the PIC entry channel. In contrast, presence of structure or RNA-binding proteins (present from splicing, export, etc.) may inhibit scanning or cause an undesired pause and result in initiation on a near cognate codon (Y. V Svitkin, Ovchinnikov, Dreyfuss, & Sonenberg, 1996). Large cellular quantities of eIF4A could effectively compete with these proteins for the mRNA. Successive interactions between the PIC and eIF4A molecules downstream of it may work to bias the directionality of scanning (Spirin, 2009). Nonetheless, future studies *in vivo* and *in vitro* with mRNAs of high and low structure are necessary to further interrogate the mechanism whereby eIF4A contributes to translation initiation, as are high-resolution structural studies aimed at visualizing interactions between eIF4F and the PIC.

Material and Methods

Materials

ATP used in reactions and all nucleotides used for *in vitro* transcription were purchased from Affymetrix. All radionucleotides were purchased from PerkinElmer. All

nucleotide analogs and Pyruvate Kinase (900-1400 units/mL)/Lactic Dehydrogenase (600-1000 units/mL) mix from rabbit muscle were purchased from Sigma. NADH disodium salt was purchased from Calbiochem. Phosphoenolpyruvate potassium salt was purchased from Chem Impex International, Inc. RiboLock RNAse inhibitor was purchased from Thermo Fisher Scientific.

Reagent Preparation

Eukaryotic initiation factors used in these studies, including eIFs 1, 1A, 2, 3, 4A, 4B, 4E•4G, and 5, as well as mRNA and Met charged tRNAi were prepared as described previously (Acker et al., 2007; Mitchell et al., 2010; Walker et al., 2013; Aitken 2016). tRNAi was charged as described previously (Walker & Fredrick, 2008). Following charging, tRNA was separated from contaminating ATP (left over from the charging reaction) on a 5 mL General Electric (GE) desalting column equilibrated in 30 mM NaOAc pH 5.5. The tRNA and free nucleotide peaks were confirmed with individual standards that were worked up identically to a charging reaction. Eluted tRNA peak was precipitated with 3 volumes of 100% ethanol at –20°C overnight, pelleted, and resuspended in 30 mM NaOAc pH 5.5.

mRNA capping

mRNAs were capped exactly as described in Aitken et al., 2016. Briefly, RNAs 2-10 were 5 μM in the presence of 50 μM GTP, 0.67 μM α-^{32}P- GTP, 100 μM S-Adenosyl Methionine (SAM), 1 U/μl RiboLock, and 0.15 μM D1/D12 vaccinia virus capping enzyme. RNA 1 was 50 μM in the reaction in the presence of 100 μM GTP, while the other conditions were the same. Reactions were incubated at 37°C for 90 minutes and purified using the RNEasy RNA purification kit.

mRNA Recruitment Assay

In vitro mRNA recruitment assay was carried out as described previously with small modifications (Aitken et al., 2016; Walker et al., 2013). All reactions were carried out at 26°C in buffer containing 30 mM HEPES•KOH, pH 7.4, 100 mM KOAc, 3 mM $Mg(OAc)_2$, and 2 mM DTT. 15 μl reactions contained final concentrations of 500 nM GDPNP, 300 nM eIF2, 200 nM Met-tRNA(Met), 1 μM eIF1, 1 μM eIF1A, 30 nM 40S small subunit of the ribosome, 300 nM eIF3, 5 μM eIF4A, 50 nM eIF4G•eIF4E, 300 nM eIF4B, and 1 U/μL Ribolock RNase inhibitor (Thermo). To form the complex, GDPNP and eIF2 were incubated for 10 minutes, Met-tRNA(Met) was then added to the reaction and incubated an additional 7 minutes, forming the Ternary Complex (TC). The remainder of the components, except mRNA and ATP mix, were added and incubated for an additional 10 minutes to allow complex formation. Reactions were initiated with a mix containing final concentrations of 15 nM mRNA and ATP. Experiments varying eIF4A all had 5 mM ATP. Experiments varying ATP all had 5 μM eIF4A. To take timepoints, 2 μl reaction aliquots were combined with 1 μl of 0.02% bromophenol blue and xylene cyanol dye in 40% sucrose containing a final concentration of a 25-fold excess of a cold chase mRNA, identical to the labeled one used in the recruitment reaction. 2 μl of the chased reaction were immediately loaded and resolved on a native 4%, 37.5:1 crosslinking acrylamide gel using a Hoefer SE260 Mighty Small II Deluxe Mini Vertical Electrophoresis Unit, cooled to 22°C by a circulating water bath. Gels and running buffer contained 34 mM Tris Base, 57 mM HEPES, 1 mM EDTA, and 25 mM $MgCl_2$ (THEM). Gels were exposed overnight at –20°C, visualized on a GE Typhoon 9500 FLA, and quantified using Image Quant software. Data were plotted and fit using KaleidaGraph 4.5 software. Individual recruitment time courses were fit to a single

exponential curve: $y = A*(1-\exp(-k_{obs}*x))$, where x is time, A is amplitude, and k_{obs} is the observed rate. Observed rates were plotted against the concentration of the titrant and fit to a hyperbolic equation: $y = b+((k_{max}*x)/(K_{1/2}+x))$ where x is the concentration of the titrant, k_{max} is the maximal rate of mRNA recruitment when the reaction is saturated by the factor titrated, $K_{1/2}$ is the concentration of the factor required to achieve $½k_{max}$, and b is the y-intercept.

NADH-coupled ATPase Assay

The NADH-coupled ATPase assay was adapted from previously described methods with small modifications (Nørby, 1988; Bradley et al., 2012). All ATPase experiments were carried out in a 384-well Corning 3544 plate on a Tecan Infinite M1000PRO microplate reader at 26°C. Using a standard curve we determined that a 10 μL reaction with 1 mM NADH on a Corning 3544 microplate gives an absorbance of 1.23 Optical Density (OD) in the microplate reader. OD was measured every 20 seconds for 1 hour. OD was plotted vs. time for individual reactions and fit to y = mx + b where m is the slope, x is time in minutes, and b is the y-intercept. Thus m is OD of NADH/min. It follows that,

$$\frac{|m| \text{ OD of NADH/min}}{1.23 \text{ OD of NADH/1mM NADH}} = \text{mM NADH/min}$$

Note that the absolute value of m was used because the slope is a negative value due to loss of absorbance over time. NADH consumed is stoichiometric with ATP regenerated thus,

mM NADH/min = mM ATP/min

30 nM PIC. 10 μl reactions were set up at the same concentrations and as described in the mRNA Recruitment Assay above. In addition the reactions contained a Reporter Mix with final concentrations of 2.5 mM phosphoenolpyruvate, 1 mM NADH, and a 1/250 dilution

of the Pyruvate Kinase/Lactic Dehydrogenase enzymes mix from rabbit muscle. Reactions were initiated by addition of ATP. Changes in absorbance of 340 nm light were monitored over time.

0.5 μM PIC. Reactions were carried out identically as described in the "30 nM PIC" above except the final concentrations were as follows: 1 mM GDPNP, 500 nM eIF2, 500 nM Met-tRNA(Met), 1 μM eIF1, 1 μM eIF1A, 500 nM 40S small subunit of the ribosome, 500 nM eIF3, 5 μM eIF4A, 500 nM eIF4G•4E, 500 nM eIF4B, 5 mM ATP, 500 nM mRNA, and 1 U/μl RiboLock RNase inhibitor.

Chapter 3

An enzyme-coupled assay to study ATPase activity with high-throughput capabilities

Paul Yourik[1,2] and Jon R. Lorsch[2]

[1] Johns Hopkins University School of Medicine, Baltimore, MD

[2] Laboratory on the Mechanism and Regulation of Protein Synthesis, Eunice Kennedy Shriver National Institute of Child Health and Development, National Institutes of Health, Bethesda, MD

Abstract

ATP hydrolysis is a fundamental biological process in all life. Numerous approaches – each with advantages and disadvantages – to monitor ATP hydrolysis have been developed over the years. Here, we adapted the Pyruvate Kinase and Lactate Dehydrogenase enzyme-coupled ATPase assay, traditionally carried out in a 1 ml cuvette, for use in a microplate reader and used it to study eIF4A activity, alone and in the context of an *in vitro* reconstituted translation initiation system. The assay is highly sensitive, low cost, high throughput, employs a small reaction volume, and can be utilized for investigation of a wide range of other ATPases.

Introduction

Hydrolysis of adenosine triphosphate (ATP) is one of the most fundamental biochemical reactions occurring in all of life on earth. Enzymes often couple ATP hydrolysis with energetically unfavorable reactions to drive the equilibrium forward while the transfer of a phosphate group from ATP to a protein or another molecule can dramatically change the properties of those species (Voet & Voet, 2004). Numerous other uses of enzyme-catalyzed ATP hydrolysis (ATPase) exist in nature and it is clear that studying them can provide myriad insights into the mechanisms of biological function.

Decades of biochemical research resulted in novel approaches to investigate ATP hydrolysis, each with advantages and disadvantages. One of the most established and common methods to monitor ATP hydrolysis is to add [γ-^{32}P]-ATP or [α-^{32}P]-ATP, usually in trace amounts, together with non-radioactive ATP and monitor release of the inorganic phosphate or ADP. ATP can be resolved from adenosine diphosphate (ADP) and adenosine monophosphate (AMP) via thin layer chromatography or acrylamide gel electrophoresis (for an example see (Lorsch & Herschlag, 1998)). The method is robust, highly sensitive; however, it is usually low throughput and does not monitor reactions in real time. Also, use of radioactivity requires additional safety precautions, certifications, and regular use can be prohibitively expensive. Another approach relies on the *E. coli* Phosphate Binding Protein labeled with 7-Diethylamino-3-((((2-Maleimidyl)ethyl)amino)carbonyl)coumarin (PBP-MDCC) to measure appearance of inorganic phosphate (Pi) (Brune, Hunter, Corrie, & Webb, 1994). Binding of Pi by PBP-MDCC results in an increase in fluorescence that can be detected in a fluorometer. The assay is not radioactive and can be adapted for high throughput screens. However, Pi is abundant in biological systems and contamination can

skew results. A common solution is to use a "phosphate mop" to minimize background signal although researchers are still prohibited from use of phosphate buffers.

Detection of ADP can also be used to study ATPase activity. BellBrook Labs utilizes antibodies against ADP, producing a fluorescent signal, although the assay is not optimal for real time detection and is recommended for use up to 1 mM ATP, which may not be saturating for some enzymes (e.g. eIF4A). Another method detects ADP using the Pyruvate Kinase (PK) and Lactate Dehydrogenase (LDH) coupled assay (Bradley & De La Cruz, 2012). ADP is regenerated back to ATP and in the process oxidizes NADH, causing a loss of absorbance of 340 nm light. The assay is usually carried out in 1 mL cuvettes and monitored with a fluorometer, limiting throughput and prohibiting the use of reagents available in low quantities (e.g. certain eukaryotic translation initiation factors).

Here, we adapted the PK and LDH -coupled ATPase for use in a 384-well microplate (read by a Tecan microplate reader). The assay monitors numerous reactions in parallel – in real time – and requires a final volume of 10 μl per well, greatly decreasing the amount of reagent per reaction. It is cost effective, maintains a constant concentration of ATP (making it ideal for kinetic studies) and can – in theory – be coupled with other photometric techniques. We used the assay to study the ATPase activity of eIF4A, a slow DEAD-box protein, with a low affinity for ATP (Alexandra Z Andreou & Klostermeier, 2013; Lorsch & Herschlag, 1998). The assay accurately and reproducibly reported on the rate of ATP hydrolysis for eIF4A alone and in the presence of a host of translation initiation factors and the 40S small subunit of the ribosome.

Results

Adaptation of the pyruvate kinase and lactate dehydrogenase –coupled assay to monitor eIF4A ATPase activity in the context of the PIC

We addressed all of the problems in studying eIF4A ATPase activity described above using an enzyme-coupled ATPase Reporter Mix (RM) (Bradley & De La Cruz, 2012). The RM consists of pyruvate kinase (PK), lactate dehydrogenase (LDH), phosphoenolpyruvate (PEP), and reduced nicotinamide adenine dinucleotide (NADH). The ATPase (e.g. eIF4A) hydrolyzes ATP to ADP and PK transfers the phosphate moiety from PEP to ADP, generating pyruvate and ATP (Figure 3.1A). Regeneration of ATP ensures a constant concentration of ATP, creating more strict steady-state conditions, and LDH reduces pyruvate to lactate. Reduction of pyruvate oxidizes NADH, forming NAD+. That is, oxidation of NADH to NAD+ happens stoichiometrically with ATP hydrolysis. Importantly, NADH absorbs 340 nm light but NAD+ does not. We considered two possibilities for the readout of the assay: loss of NADH fluorescence (460 nm wavelength light) or loss of NADH absorbance (340 nm wavelength light). NADH was titrated in "Recon" reaction buffer (30 mM HEPES•KOH pH 7.4, 100 mM KOAc, 2 mM $Mg(OAc)_2$, 2 mM DTT) and fluorescence (Fig 3.1B) or absorbance (Figure 3.1C) was measured using clear bottom plates and a Tecan M1000Pro microplate reader in top-reading mode (see Methods). NADH absorbance was linear from 0 to 2.5 mM and florescence was linear from 0 to 1 mM NADH. Due to a wider linear range, we chose absorbance of NADH as the readout of the assay. The titration was repeated in the presence of the complete RM and ATP and yielded identical linear results (Figure 3.1C)

Figure 3.1. ATPase activity is monitored with an enzyme-coupled reporter. A. Schematic of enzyme-coupled ATPase assay. ATP is hydrolyzed to ADP. PK catalyzes the transfer of phosphate from PEP to ADP, generating ATP and pyruvate. LDH oxidizes pyruvate to lactate and in the process oxidizes NADH to NAD+. **B.** Relative fluorescence units (RFU) versus concentration of NADH in mM. NADH was excited with 340 nm light and fluorescence was monitored at 460 nm. Inset – a zoom of the x-axis between 0-0.5 mM NADH. **C.** NADH absorbance of 340 nm light versus NADH concentration in mM. NADH was titrated alone (black); in 1x Recon reaction buffer containing the rest of the RM (1 mM NADH, 2.5 mM PEP, 1/250 dilution of PK/LDH stock) (red); 1x Recon reaction buffer containing the same RM as in red and 2 mM ATP (green).

A

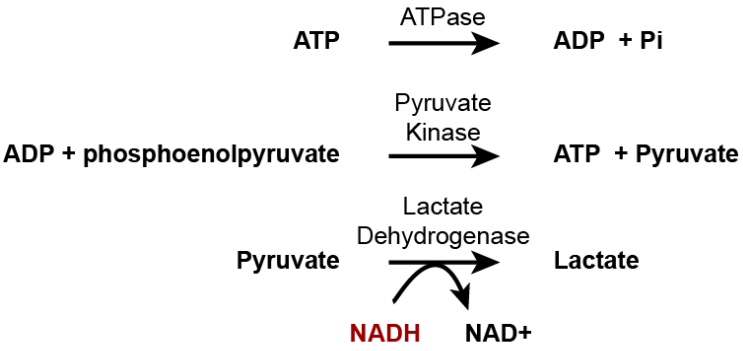
ATP
ATPase
ADP + Pi
ADP + phosphoenolpyruvate
Pyruvate Kinase
ATP + Pyruvate
Pyruvate
Lactate Dehydrogenase
Lactate
NADH
NAD+

B

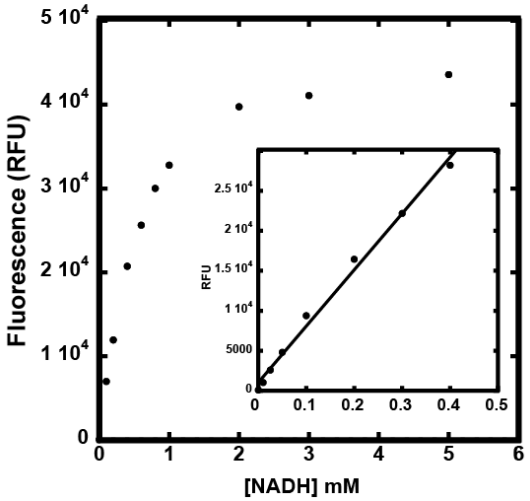
Fluorescence (RFU)
[NADH] mM
RFU

C

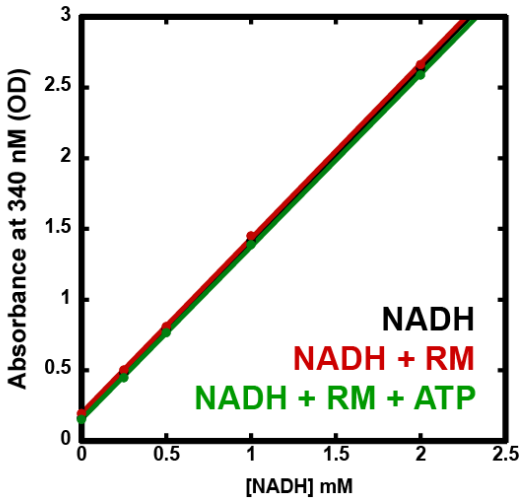
Absorbance at 340 nM (OD)
[NADH] mM
NADH
NADH + RM
NADH + RM + ATP

Having established the readout of the assay, next, we determined the optimal concentration of PK/LDH enzyme mix in the RM. The stock solution contained 600-1000 U/mL of PK together with 900-1400 U/mL of LDH from rabbit muscle. In order to successfully report on ATP hydrolysis activity, the rate of reactions carried out by the RM must be significantly faster than that of the ATPase. We titrated PK/LDH from 1/500 stock dilution to 1/20 stock dilution – in the presence of 1 mM ADP, 1 mM NADH, and 2.5 mM PEP – and monitored absorbance at 340 nm (Figure 3.2 A). 1/250 dilution of the PK and LDH stock converted the majority of ADP to ATP within 15 seconds and was used in subsequent assays. To access rapid kinetics, ADP was added using the Tecan M1000Pro injector. Modest increase in absorbance during the first 5 seconds (Figure 3.2A) was likely due to incomplete mixing.

The ATPase assay was originally developed for use in a spectrophotometer and adapting the assay to the plate reader presented several technical challenges when using a microplate. Nonspecific interactions between the proteins and the well of the plate ("sticking") can significantly interfere with the assay. Furthermore, ATPase reactions were all carried out at 26°C and due to low volumes, evaporation may skew the experimental results. Multiple 96-well and 384-well plates were screed for signal stability over time. Corning microplate 3544 (black 384 well plate, low volume, NBS surface, clear flat bottom) had superior performance and was selected for use in subsequent assays. Reaction volume was 10 μl/well, per manufacturer recommendations.

Having established basic assay parameters for reporting ATP hydrolysis, we tested the system with eIF4F – a heterotrimer consisting of the DEAD-box RNA helicase eIF4A, eIF4G, and eIF4E – for ATPase activity (Figure 3.2 B). To further demonstrate that 1/250 dilution of PK/LDH is not rate-limiting and accurately reports on ATP hydrolysis, we

monitored absorbance at 340 nm in the presence of 1/750, 1/250, and 1/83 final dilutions of PK and LDH stock solution in the RM. The results for all three dilutions were identical, providing further evidence that the RM conditions are not limiting, at least within 3-fold above or below the designated 1/250 dilution to be used in the assay. Also, when the PK and LDH mix, ATP, or eIF4F were left out of a reaction, absorbance at 340 nm did not change over 40 minutes (Figure 3.2B) suggesting that NADH oxidation strongly depends on the presence of both the RM and ATP hydrolysis.

Next, the assay was performed with various concentrations of ATP (0 – 5mM) and plotted versus time in minutes (Figure 3.2C). The data were described well by a linear equation, reflective of experimentally intended steady-state conditions. The slopes of individual reactions increased in magnitude with increasing concentration of ATP, while no absorbance changes were observed in the absence of ATP (Figure 3.2C, brown vs. all other traces). The units of the slope were OD per minute and had to be converted to ATP hydrolyzed per minute. The assay is traditionally carried out in a cuvette with a fixed path length, allowing use of Beer's Law, which was not possible in our experimental setup because a 384-well plate was used, thus a path length is not-defined. Instead, for each concentration of ATP, we consistently observed a point when all NADH was oxidized to NAD+ (absorbance ~ 0.23 OD) indicating the baseline signal in the assay (Figure 3.2C). Earlier titration of NADH showed that 1 mM NADH results in an absorbance reading of 1.46 OD (Figure 3.1C). Thus, 10 μl reactions with 1 mM NADH correspond to an absorbance of 1.23 OD. This constant was used to convert the slope of change of absorbance to ATP hydrolyzed:

$$\frac{OD\ of\ NADH/min}{1.23\ OD\ of\ NADH/\ 1\ mM\ NADH}$$

$= mM\ NADH/min,$

$= mM\ ATP/min$

ATP hydrolyzed is the velocity in mM ATP/min. It can be divided by the concentration of enzyme to obtain the rate min^{-1}. Either of these parameters can be plotted versus concentration of ATP and fit with the Michaelis-Menten equation. Numerous experimental replicates demonstrated that the results are highly sensitive, reproducible, have little noise, and a great dynamic range. We were able to accurately and reproducibly measure the rate of ATPase with eIF4A alone, eIF4F, as well as in the presence of the eukaryotic translation preinitiatin complex, spanning a range of rates differing by 40-fold (Figure 3.2 D) and the rate measured with eIF4A was comparable to previous reports (Rajagopal et al., 2012).

Figure 3.2. Change in absorbance of 340 nm light reports on ATP hydrolysis. A. Titration of PK and LDH mix to determine the lowest possible concentration that can be used in the RM to monitor ATPase activity for eIF4F. **B.** Increasing (pink) or decreasing (blue) the concentration of PK and LDH by 3-fold resulted in identical results as in the presence of a 1/250 dilution used in experimental assays (black). Also, leaving out PK and LDH (purple), ATP (red), or eIF4F (green) resulted in no changes in absorbance. **C.** Representative plot showing ATPase-dependent changes in absorbance with 0.5 μM eIF4F in the presence of 0.5 μM PIC, at various concentrations of ATP (indicated to the right of the plot) and a baseline of ~0.23 OD when all NADH has been converted to NAD+. **D.** Reaction velocities were plotted against the concentration of ATP for (cyan) 5 μM eIF4A V_{max} = 2.94 ± 0.4 μM/min, K_m = 2593 ± 250; (black) 5 μM eIF4A with 0.5 μM eIF4G and 0.5 μM eIF4E V_{max} = 12.2 ± 0.6 μM/min, K_m =212 ± 6 μM; (red) 5 μM eIF4A, 0.5 μM eIF4G, and 0.5 μM eIF4E in the presence of 0.5 μM PIC V_{max} = 41.3 ± 1.4 μM/min, K_m =309 ± 14 μM.

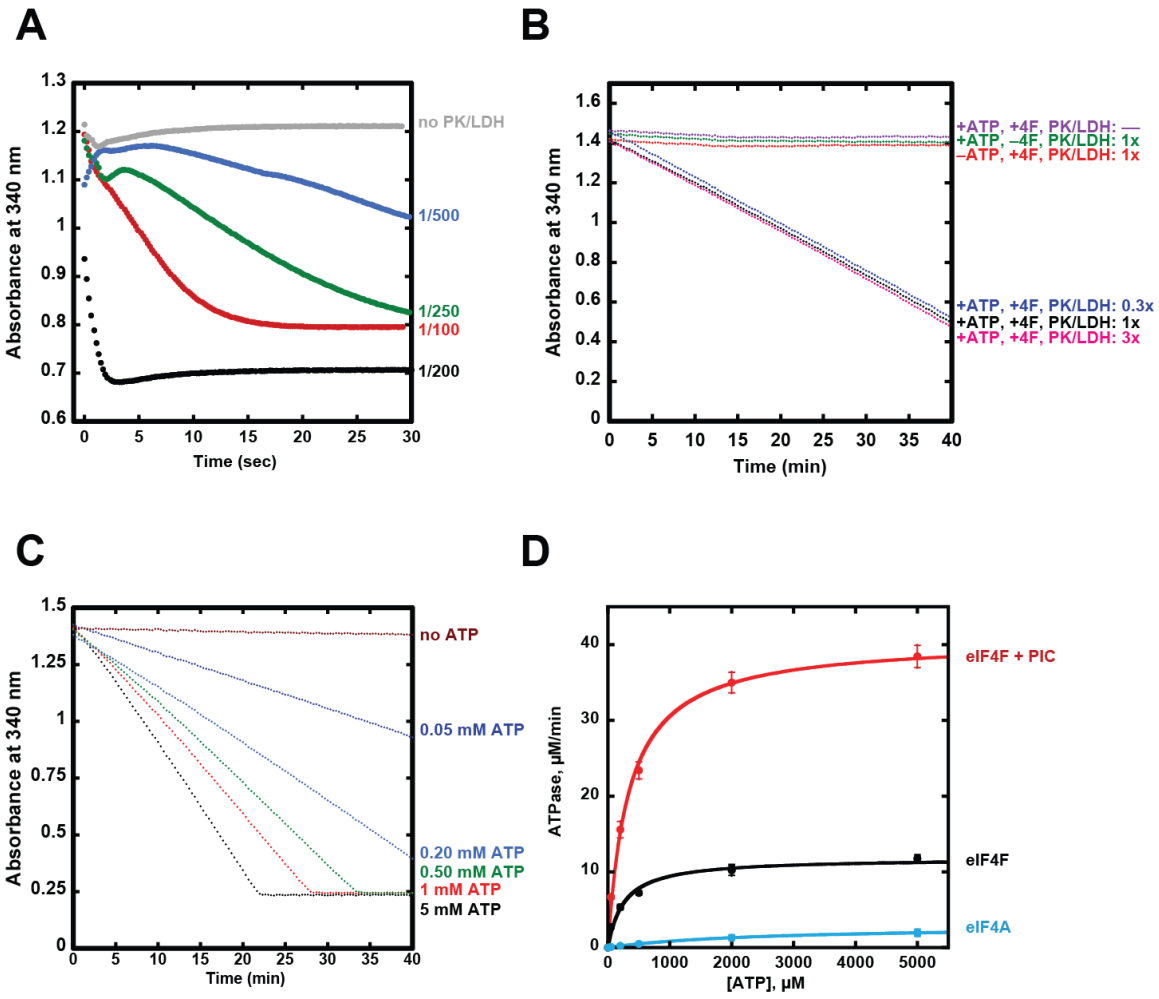
A
Absorbance at 340 nm
Time (sec)
no PK/LDH
1/500
1/250
1/100
1/200
B
Absorbance at 340 nm
Time (min)
+ATP, +4F, PK/LDH: —
+ATP, –4F, PK/LDH: 1x
–ATP, +4F, PK/LDH: 1x
+ATP, +4F, PK/LDH: 0.3x
+ATP, +4F, PK/LDH: 1x
+ATP, +4F, PK/LDH: 3x
C
Absorbance at 340 nm
Time (min)
no ATP
0.05 mM ATP
0.20 mM ATP
0.50 mM ATP
1 mM ATP
5 mM ATP
D
ATPase, μM/min
[ATP], μM
eIF4F + PIC
eIF4F
eIF4A

Discussion

As our understanding of translation initiation is evolving, new approaches are often needed to ask specific questions. In this work, we adapted a previously established ATPase assay to be used with an *in vitro* reconstituted translation initiation. The assay can also be used to study other ATPases. The readout of the assay is loss of absorbance at 340 nm, and because we adapted it to a 384 well plate, it is possible to perform one to hundreds of reactions, giving the assay high throughput capabilities. If the platereader has injectors, the assay can be adapted to monitor rapid kinetics; however, mixing may be an issue and would require further optimization. Also, performing the assay in a 384-well plate greatly reduces the amount of reagents required per reaction, and ATP hydrolysis is monitored in real time. The assay is photometric, eliminating all of the safety concerns and logistics required for use of radioactivity on a daily basis. Finally, using the PK/LDH –enzyme coupled assay reduces the cost by at least 100-fold.

Using the assay described here, we accurately and reproducibly measured ATPase activity ranging from less than 1 μM/min to in excess of 40 μM/min, highlighting the dynamic range of the assay (Figure 3.2D). The rates observed with eIF4A and eIF4F were comparable to previous reports (Rajagopal et al., 2012) and the trends observed in our experimental data were reproduced with [α-^{32}P]-ATP (not shown) further validating the enzyme-coupled ATPase assay.

Materials and Methods

Reagents

ATP used in reactions and all nucleotides used for *in vitro* transcription were purchased from Affymetrix. [α-^{32}P]-ATP and [γ-^{32}P]-ATP were purchased from PerkinElmer and MP Bio. Pyruvate Kinase (900-1400 units/mL)/Lactic Dehydrogenase (600-1000 units/mL) mix from rabbit muscle were purchased from Sigma. NADH disodium salt was purchased from Calbiochem. Phosphoenolpyruvate potassium salt was purchased from Chem Impex International, Inc. Corning 3544 microplates were purchased from Corning.

PIC formation

30 nM PICs and 0.5 μM PICs were assembled exactly as described previously to perform ATPase assays (Yourik et al., 2017) and in Methods of Chapter 2.

PK/LDH assay

A 10x Reporter Mix (RM) containing 25 mM PEP, 10 mM NADH, and 1/25 dilution of PK and LD was prepared in 1x reaction ("Recon") buffer. PICs at 2x of final desired concentration were assembled in the absence of mRNA and ATP as described in 30 nM PIC or 0.5 μM PIC above and incubated for 10 minutes at 26°C to allow PIC formation. Next, 6.75 μl of 2x PIC, 1.35 μl of 10x RM, 1.35 μl of mRNA at 10x of final desired concentration, and 0.68 μl of 1x Recon were combined. If multiple reactions are to be monitored, it is useful to scale up this mix for multiple reactions. Subsequently, 9 μl of the mix were combined with 3 μl of ATP that is 4x of final concentration to initiate the reaction.

10 μl of the initiated reaction were transferred to the microplate. It is possible to initiate the reaction with an injector instead; however, care must be taken to ensure thorough mixing.

Reactions were monitored using a Corning 3544 384-well plate in a Tecan M1000Pro microplate reader set to the following parameters:

Plate Definition: [COS 384fb_low volume] – Corning Flat Black

Temperature: On; 26°C

Shaking:

Duration = 3 sec

Mode = Orbital

Amplitude = 3 mM (Freq. 216 rpm)

Part of Plate (select wells of interest)

Kinetic Cycle:

Number of Cycles = 121

Kinetic Interval = 20 seconds

Absorbance:

Wavelength Measurement = 340;

Flashes:

Number of flashes = 25

Settle time = 0

Instrumentation

Tecan M1000 Pro microplate reader with Tecan injectors was used to carry out the ATPase assay. The instrument was controlled by iControl 1.10 software.

Appendix A

Specific domains of eIF4B contribute to utilization of ATP in mRNA recruitment

Paul Yourik,[1,2] Sarah E. Walker, and Jon R. Lorsch[2]

[1] Johns Hopkins University School of Medicine

Baltimore, MD

[2] Laboratory on the Mechanism and Regulation of Protein Synthesis

The Eunice Kennedy Shriver National Institute of Child Health and Human Development

Bethesda, MD

Previous studies demonstrated that eukaryotic translation initiation factor (eIF) 4B is critical for efficient mRNA recruitment to the eukaryotic translation preinitiation complex (PIC). Yeast eIF4B (yeIF4B) may have a functional interaction with eIF4A (Walker et al., 2013), the DEAD-box RNA helicase thought to hydrolyze ATP and remove RNA structure (Alexandra Z Andreou & Klostermeier, 2013), allowing PIC attachment near the 5'-end of the mRNA in a process called mRNA recruitment (see Chapter 1 for a more thorough review or (Mitchell et al., 2011)).

Here, we employed an *in vitro* reconstituted *S. cerevisiae* translation initiation system to ask how yeIF4B affects ATP dependence in mRNA recruitment (Acker et al., 2007; Mitchell et al., 2010; Walker et al., 2013). PICs were formed in the presence of saturating eIF4A using the same conditions as used previously to study mRNA recruitment (see 30 nM PIC Methods in Chapter 2) and reactions were initiated by addition of the natural mRNA *RPL41A* capped with a [^{32}P]-m7G 5'-cap and ATP. Reaction aliquots were resolved on a native acrylamide gel and fraction of mRNA incorporated into the PIC was plotted versus time and fit to a single exponential equation, describing the observed rate of mRNA recruitment. Observed rate of *RPL41A* recruitment to the PIC was measured at various concentrations of ATP in the presence or absence of yeIF4B (Figure A.1). In the presence of wild type eIF4B (WT), the maximal rate of recruitment achieved when the system was at a saturating level of ATP ($k_{max\ ATP}$), was 0.72 ± 0.1 min^{-1}, and the concentration of ATP required to achieve the half-maximal rate of recruitment ($K_{1/2\ ATP}$) was 606 ± 159 μM. In the absence of eIF4B, the concentration of eIF4A required to achieve the half-maximal rate of recruitment ($K_{1/2\ 4A}$) was previously demonstrated to be much higher versus in the presence of saturating eIF4B (Walker et al., 2013). In our hands the $K_{1/2\ 4A}$ was 3.7 ± 1 μM and ~10 μM in the presence and absence of eIF4B, respectively (not shown). To measure ATP

dependence in mRNA recruitment, in the absence of eIF4B, to saturate the system for the level of eIF4A, we used the highest experimentally available concentration of eIF4A (30 μM). In the absence of eIF4B, the $k_{max\ ATP}$ was slower by 3.6-fold (0.20 ± 0.01 min^{-1}) than in the presence of eIF4B and the $K_{1/2\ ATP}$ was elevated by 4.5-fold (2732 ± 454 μM) (Figure A.1 B-C).

Having established that absence of yeIF4B elevates the $K_{1/2\ ATP}$ and depresses the $k_{max\ ATP}$ in mRNA recruitment, we examined the individual contributions of its domains previously demonstrated to be important for mRNA recruitment (Walker et al., 2013). We purified variants of yeIF4B, lacking the N-terminal domain (NTD), the RNA-recognition motif (RRM), or a region of seven imperfect repeats (ΔRepeats) (Figure A.1A) as described previously (Walker et al., 2013). ATP was titrated in the presence of a saturating level of eIF4A (5 μM) and the rate of mRNA recruitment was measured as described above (Figure A.1B-C). Deletion of the NTD – critical for yeIF4B binding to the 40S – resulted in a 2.5-fold decrease in the $k_{max\ ATP}$ and a 4-fold increase in the $K_{1/2\ ATP}$ as compared to WT yeIF4B. Also, the RRM is dispensable for yeIF4B function in mRNA recruitment (Walker et al., 2013) and had a $k_{max\ ATP}$ of 0.70 ± 0.05 min^{-1} – comparable to WT – but the $K_{m\ ATP}$ (1731 ± 320 μM) was approximately 3-fold higher than WT (Figure A.1B-C). Lastly, the ΔRepeats did not significantly influence the $k_{max\ ATP}$ (0.55 ± 0.09 min^{-1}) nor the $K_{1/2\ ATP}$ (659 ± 131 μM) in the presence of saturating eIF4A (Figure A.1B-C).

Figure A.1. eIF4B influences the maximal rate and ATP dependence in mRNA recruitment. A. Domain structure of yeIF4B. yeIF4B has 4 main domains: N-terminal (NTD), RNA Recognition Motif (RRM), 7-Repeats, and C-terminal (CTD). **B-C.** Maximal rates (k_{max}) and $K_{1/2}$ for ATP were measured in mRNA recruitment with wild type eIF4B (WT), no eIF4B (–eIF4B), or mutants lacking either the 7-Repeats domain (ΔRepeats), the RRM (ΔRRM), or the NTD (ΔNTD). B shows the mean values ± average deviation and C shows the fits.

A

B

eIF4B variant	$K_{1/2\ ATP}$ (μM)	k_{max} (min^{-1})
WT	606 ± 159	0.72 ± 0.1
ΔRepeats	659 ± 131	0.55 ± 0.09
ΔRRM	1731 ± 320	0.70 ± 0.05
ΔNTD	2418 ± 158	0.29 ± 0.03
– eIF4B	2732 ± 454	0.20 ± 0.01

C

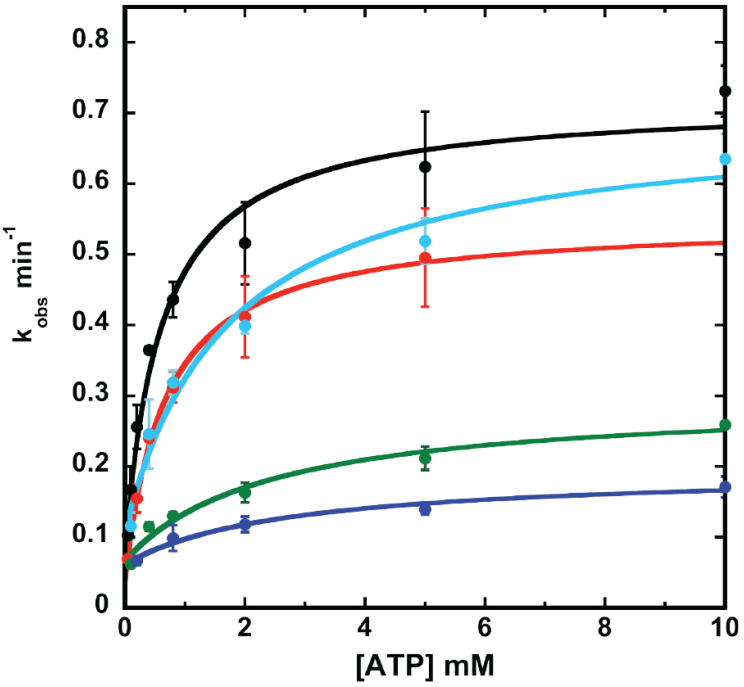

In our efforts to understand the mechanism of translation initiation, here, we focused on eIF4B, necessary for efficient mRNA recruitment to the PIC. A previous report demonstrated that eIF4B binds the 40S ribosomal subunit and may alter the structure of the mRNA entry channel (Walker et al., 2013). eIF4B did not affect the rate eIF4A-dependent ATP hydrolysis in the presence or absence of the PIC (see Chapter 2). In contrast, the yeIF4B mutant deficient in binding the 40S subunit (ΔNTD), increased the $K_{1/2\ ATP}$ in mRNA recruitment to the PIC by 4-fold over that measured with WT eIF4B. In fact, in the presence of a saturating concentration of eIF4A, the $K_{1/2\ ATP}$ was comparable to the $K_{1/2\ ATP}$ measured in the absence of eIF4B when there was a saturating concentration of eIF4A (Figure A.1 ΔNTD vs. –eIF4B). Taken together, when yeIF4B is not present or cannot bind to the PIC, mRNA recruitment is much less efficient and more ATP is required but the rate of ATP hydrolysis (catalyzed by eIF4A) is not influenced by eIF4B. One interpretation of the data is that eIF4B binding near the entry channel (Walker et al., 2013) allows the PIC to adopt an mRNA-receptive state, poised for efficient mRNA recruitment (Figure A.2). In the absence of eIF4B, the PIC is not receptive to recruitment so a higher concentration of ATP and eIF4A is required because the process is not efficient (Figure A.2, "mRNA-unreceptive state"). In contrast, in the presence of eIF4B, the PIC is poised for mRNA recruitment and the process is significantly more efficient (Figure A.2 "mRNA receptive state"). Also, a recent report suggests that yeIF4B 7-Repeats domain is critical for stimulating eIF4A helicase and ATPase activity (Alexandra Zoi Andreou et al., 2017), which may affect the ATP dependence in mRNA recruitment. Surprisingly, the $k_{max\ ATP}$ and $K_{1/2\ ATP}$ for the ΔRepeats was comparable to WT yeIF4B. It is possible that we did not see significant effects on ATP dependence with ΔRepeats because our studies were carried out in the presence of the PIC while the aforementioned study was not. Also, absence of the RRM increased the

$K_{1/2\ ATP}$ but did not change the $k_{max\ ATP}$, as compared to WT yeIF4B (Figure A.1). One interpretation of this result is that yeIF4B RRM may also be involved in the interaction with ribosomal or messenger RNA to mediate efficient mRNA recruitment to the PIC albeit these interactions are not as critical as binding and perhaps modulating the 40S subunit.

Figure A.2 Proposed role of eIF4B in mRNA recruitment to the ribosome. Top: PIC – eIF4B: in the absence of eIF4B, the PIC is fully functional but it is not poised to efficiently bind mRNA. Bottom: PIC +eIF4B: presence of eIF4B causes the PIC to adapt a conformation permitting efficient mRNA recruitment.

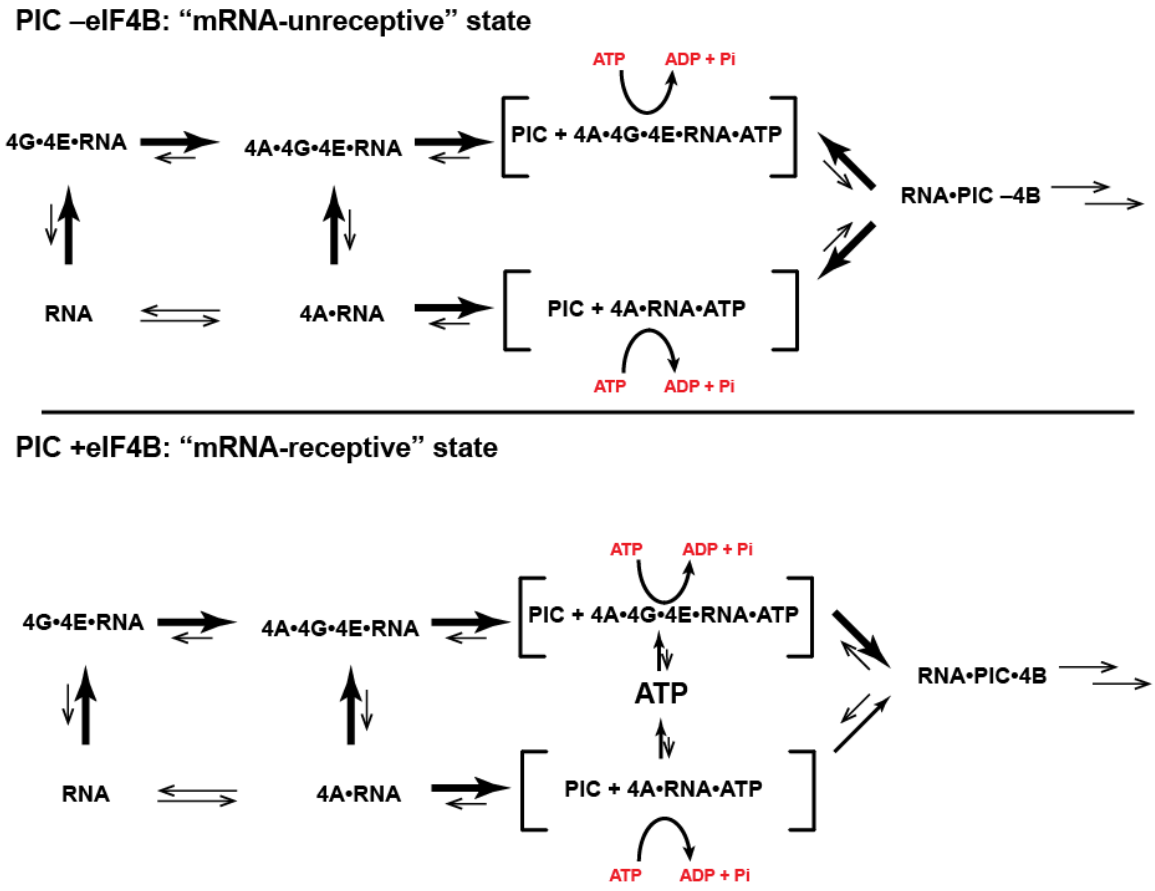

Appendix B

Investigation of eIF4A and eIF4F helicase activity in the context of translation initiation

Paul Yourik,[1,2] Colin Echeverría Aitken,[2] and Jon R. Lorsch[2]

[1] Johns Hopkins University School of Medicine, Baltimore, MD

[2] Laboratory on the Mechanism and Regulation of Protein Synthesis

The Eunice Kennedy Shriver National Institute of Child Health and Human Development

Bethesda, MD

mRNA has a natural tendency to fold forming Watson-Crick (WC) and non-WC interactions, probe numerous conformations, and seldom exists in an unwound single-stranded state (Halder & Bhattacharyya, 2013). Consequently, this structure must be unwound in order to facilitate attachment of the 43S translation preinitiation complex (PIC) and scanning of the mRNA for the start codon (Mitchell et al., 2011; Y. Y. V Svitkin et al., 2001). eIF4A is a DEAD-box RNA helicase thought to unwind structure to promote mRNA recruitment to the eukaryotic translation pre-initiation complex (PIC) (Hinnebusch, 2014). Paradoxically, multiple reports indicate that eIF4A is a weak helicase and its exact role in translation initiation is not completely understood (for a more thorough description see Chapter 1).

Here, using an *in vitro* reconstituted *S. cerevisiae* translation initiation system, we examined the helicase activity of eIF4A in parallel with mRNA recruitment. We show that an RNA oligomer annealed in the 5'-UTR of an RNA, close to the AUG start codon, is inhibitory to translation initiation but a weaker RNA duplex is removed in an eIF4A-independent manner by the PIC.

We monitored mRNA recruitment and helicase activity in parallel (Figure B.1 and Colin Echeverría Aitken, unpublished results) using three separate reactions. The substrate mRNA for all three reactions was 50 nucleotides long (50mer) and made of CAA repeats $(CAA)_n$ – possessing minimal structure (Shirokikh et al., 2010; Sobczak et al., 2010) – and one AUG codon in the middle of the mRNA. Also, the 5'-UTR contained a 13-nucleotide region of non-$(CAA)_n$ where an oligomer could be annealed (Figure B.1). For reactions (1) and (2) the 50mer was capped with a 5'- ^{32}P-7-methylguanosine (m^7G) cap. Next, the capped 50mer in (2) was annealed to a short unlabeled RNA oligomer 13 nucleotides in length (13mer) complementary to the non-$(CAA)_n$ region in the 5'-UTR, creating a region of double

stranded RNA (dsRNA) (Figure B.2A, 13mer). Lastly, the 50mer in reaction (3) was capped with a non-radioactive 5'-m7G and annealed to the same 13mer as in reaction (2) but the 13mer was labeled with a 5'-^{32}P. Thus, reaction (1) monitors mRNA recruitment in the absence of significant structure in the 5'-UTR, reaction (2) monitors recruitment in the presence of a region of double stranded (ds) RNA in the 5'-UTR, and reaction (3) monitors the annealed 13mer in the 5'-UTR annealed to an unlabeled capped 50mer mRNA (Figure B.1). Next, PICs were assembled as described previously (Walker et al., 2013) (or see Chapter 2 "30 nM PIC"), and initiated with one of the three aforementioned mRNA substrates (1-3). Reactions were quenched at different time-points by loading into a running native acrylamide gel and products were resolved by electrophoresis. Fraction of mRNA recruited to the PIC (reactions 1 and 2) migrated slower than free (not recruited) mRNA while the labeled 13mer oligomer removed from the 50mer (reaction 3) migrated faster than free mRNA. Fraction of mRNA recruited in reactions 1-2 and free 13mer in reaction 3 was quantified and plotted versus time. The 50mer without an annealed oligomer was recruited at a fast rate of approximately 4 min^{-1} (Figure B.2B, black). In contrast, the same mRNA with a 13mer annealed in the 5'-UTR was strongly inhibited (Figure B.2, blue) and achieved less than a 15% recruitment endpoint after 2 hours. Also, we observed that the annealed 13mer was not removed from the mRNA (Figure B.2, red). Taken together, a 13mer annealed in the 5'-UTR of an otherwise low-structured mRNA strongly inhibited mRNA recruitment and could not be removed by eIF4A.

Figure B.1. Scheme to simultaneously monitor mRNA recruitment and removal of an annealed RNA oligomer in the 5'-UTR. Three RNA substrates are investigated in parallel reactions to simultaneously monitor (1) mRNA recruitment of the CAA-repeats mRNA lacking significant structural elements (2) to monitor mRNA recruitment of the CAA-repeats mRNA in the presence of an annealed oligomer in the 5'-UTR (dsRNA), and (3) to monitor removal of the RNA oligomer from the 5'-UTR. Red squares indicate a ^{32}P-labeled nucleotide. Acrylamide gels are light blue and bands are drawn to indicate expected relative intensities over time. All reactions were carried out at 26°C and the gels were cooled by a circulating water bath to 16°C.

(Experimental scheme originally devised by Colin Echeverría Aitken.)

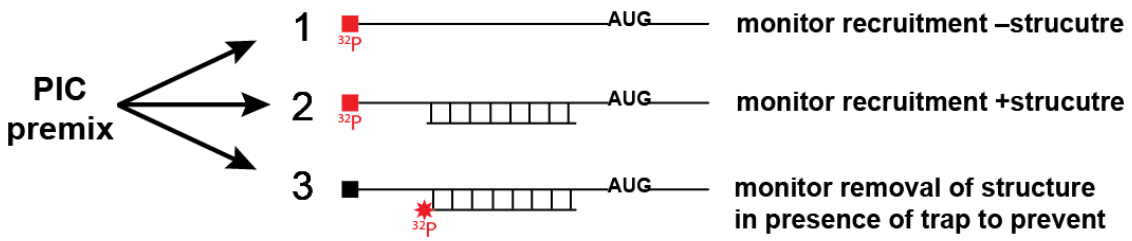
PIC
premix
1
AUG
monitor recruitment –strucutre
2
AUG
monitor recruitment +strucutre
3
AUG
monitor removal of structure
in presence of trap to prevent
reannealing

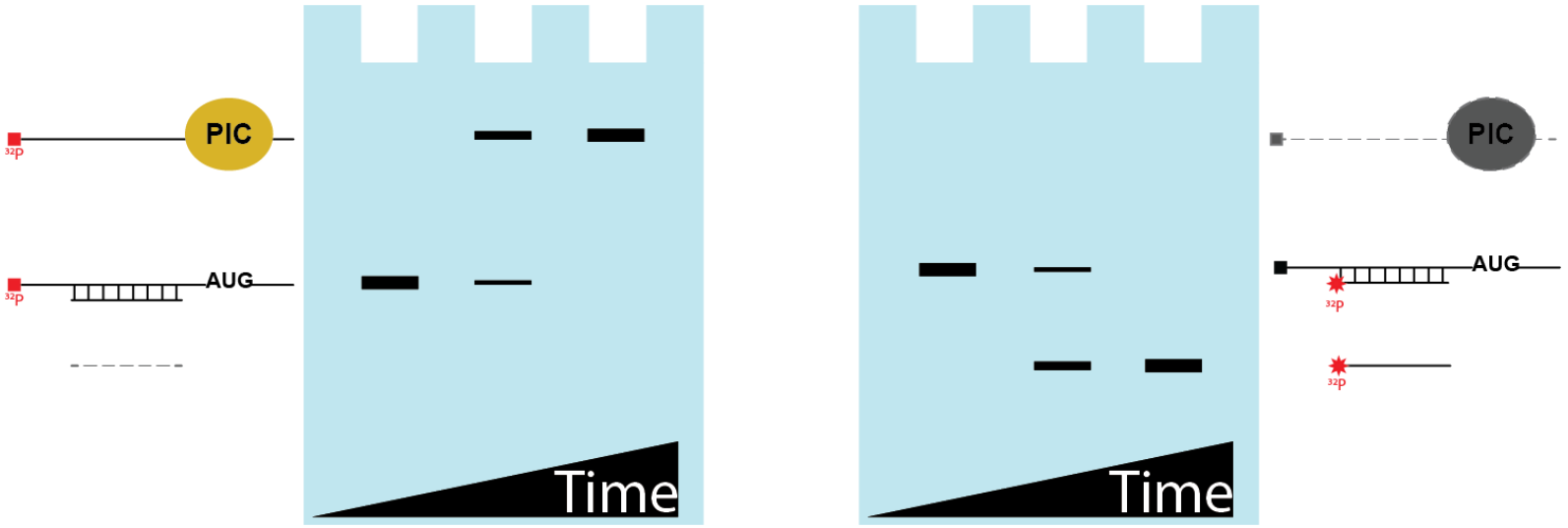
PIC
AUG
Time
PIC
AUG
Time

Having established that a 13mer is inhibitory to mRNA recruitment and cannot be removed by eIF4A in the context of the PIC, we annealed a 12mer RNA oligomer to decrease the duplex stability (Figure B.2A, 12mer). The 12mer was removed by the PIC but surprisingly, this was not strictly eIF4A-dependent (Figure B.2C). Indeed, the rate of 12mer removal was 0.058 ± 0.003 min^{-1} and 0.035 ± 0.004 min^{-1} in the presence and absence of eIF4A, respectively, while the duplex alone in the absence of any proteins remained annealed throughout the timecourse. Again, the 13mer was not removed to a significant extent by the PIC in the presence or absence of eIF4A (Figure B.2C). Taken together, our findings show that eIF4A is not able to remove an annealed 13mer in the 5'-UTR, which is inhibitory to translation initiation but a less stable 12mer is removed by the PIC at a comparable rate in the presence or absence of eIF4A, suggesting that the role of eIF4A is not to remove significant structural elements in translation initiation. In fact, previous work in bacteria demonstrated that the ribosome has helicase activity and those residues are conserved in eukaryotes (Qu et al., 2011; Takyar et al., 2005). Alternatively, an annealed oligomer might not be an accurate representation of a structural element for eIF4A and is thus not a substrate for the enzyme.

Figure B.2. Annealed 13mer is not removed by eIF4A and is inhibitory to translation initiation, while a 12mer is removed in the presence of the PIC, independent of eIF4A. A. Model mRNA used to monitor recruitment and helicase activity in parallel: 5'-GGACAACAA**CGAUUCAAUCGAG**CACGAAAUGAGAGCAACAACAACAACAA. The mRNA sequence complementary to the 12-mer or the 13-mer is indicated is red. The single AUG start codon is underlined. **B.** mRNA recruitment was monitored with the mRNA in (A) in the presence (blue) or absence (black) of an annealed 13mer oligomer. Recruitment in the absence of the annealed 13mer was ~4 min^{-1} and in the presence the reaction endpoint was too low to measure a rate (blue). Removal of the 13mer oligomer was also monitored in parallel (red) but no significant removal was observed. **C.** Helicase activity of eIF4A in the presence of the PIC. mRNA in (A) was annealed to a 12mer or a 13mer RNA oligomer. Removal of the 12mer with PIC in the presence of eIF4A (green, 0.058 ± 0.003 min^{-1}); PIC without eIF4A (cyan, 0.035 ± 0.004 min^{-1}); eIF4A alone (brown, 0.045 min^{-1}); or no protein at all (blue). Removal of the 13mer with PIC in the presence of eIF4A (black) or PIC without eIF4A (red). The data with the 13mer and 12mer only in the absence of protein could not be fit with an equation due to a very low endpoint. For all experiments except "eIF4A alone" (brown) n≥2 and the rates above are presented as mean ± average deviation.

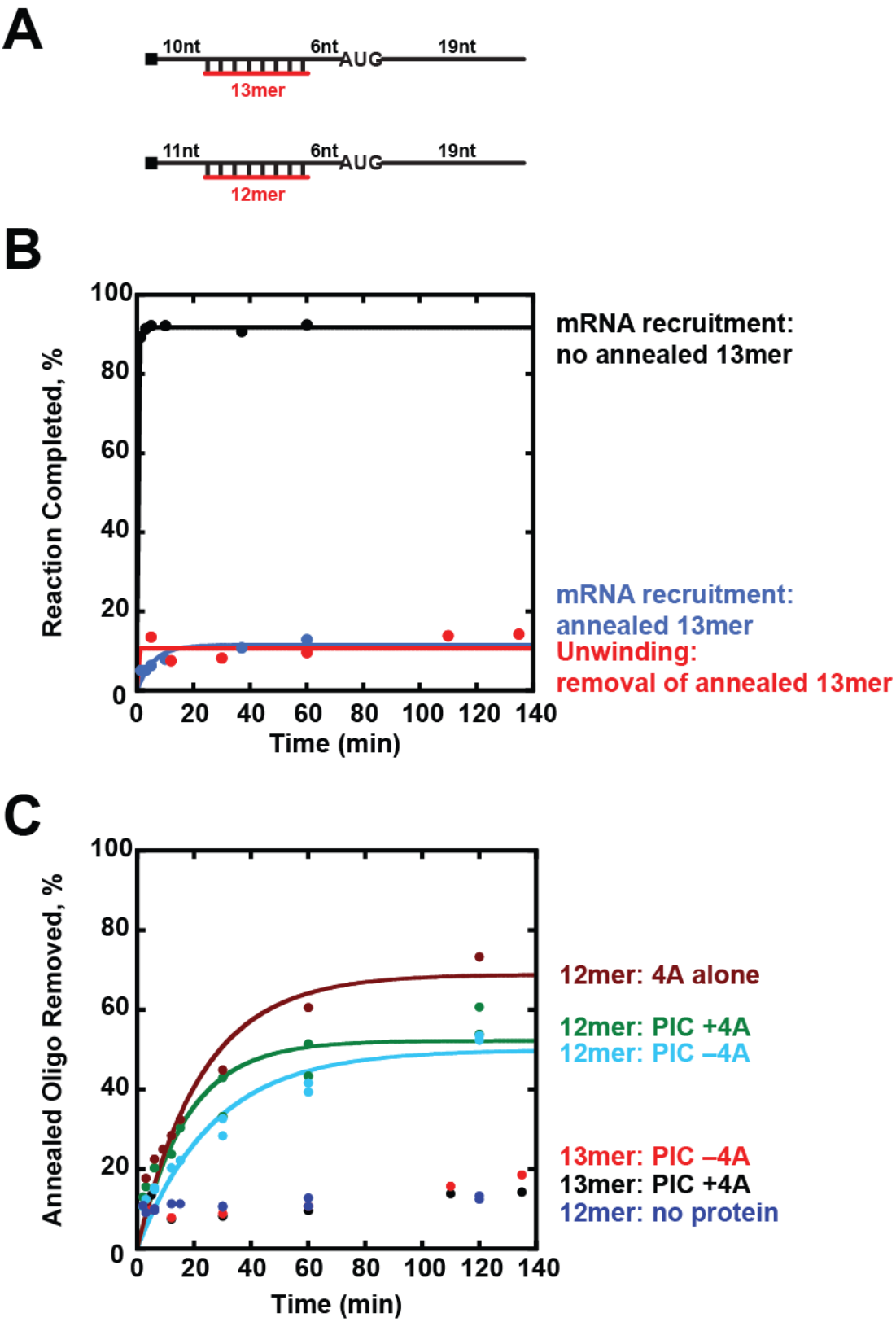
A
10nt
6nt
AUG
19nt
13mer
11nt
6nt
AUG
19nt
12mer
B
Reaction Completed, %
Time (min)
mRNA recruitment:
no annealed 13mer
mRNA recruitment:
annealed 13mer
Unwinding:
removal of annealed 13mer
C
Annealed Oligo Removed, %
Time (min)
12mer: 4A alone
12mer: PIC +4A
12mer: PIC –4A
13mer: PIC –4A
13mer: PIC +4A
12mer: no protein

Lastly, recent reports demonstrated that yeast eIF4B stimulates eIF4A helicase activity (Alexandra Zoi Andreou et al., 2017; Harms et al., 2014). We repeated the unwinding experiment as described in the study (Alexandra Z Andreou & Klostermeier, 2014) with the small modifications: the RNA oligomer that was removed was 5'-end-labeled with a ^{32}P, rather than 2-aminopurine (Figure B.3A) and unwound substrates were resolved on a native acrylamide gel cooled to 16°C by a circulating water bath (Figure B.3). Also, the concentration of all proteins was 1 μM, instead of 5 μM as used in Andreu & Klostermeier, 2014. Surprisingly, we did not observe any additional stimulation of unwinding by eIF4B. Furthermore, the rate of oligomer removal in the absence of eIF4A was slower but comparable to that in the presence of eIF4A (Figure B.3). It is possible that we did not observe stimulation by eIF4B because we used a full length eIF4G1, as opposed to the minimal domain required for eIF4A stimulation that was used in the study. Furthermore, there is a possibility that use of proteins at 1 μM yields different results than when used at 5 μM.

Figure B.3 eIF4B does not stimulate RNA helicase activity of eIF4F. A. Scheme to monitor removal of an RNA oligomer 9 nucleotides in length annealed to an RNA oligomer 32 nucleotides in length. The 32mer also had a 2-Aminopurine exactly as described in Andreu & Klostermeier, 2014. Reactions were loaded into a native acrylamide gel cooled to 16°C by a circulating water bath. **B-D.** Removal of 9mer was monitored over time with eIF4G•eIF4E as a negative control, eIF4F, and eIF4F with eIF4B all at 1 μM final concentration.

A

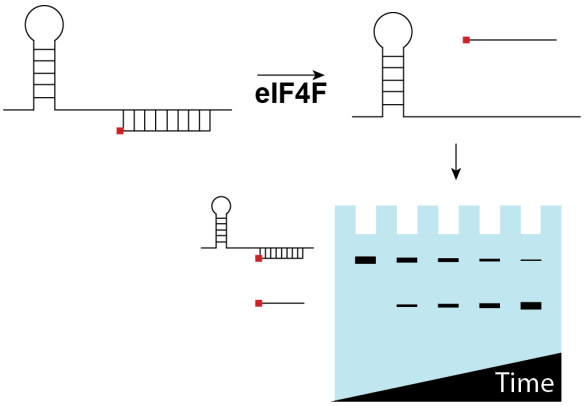

B

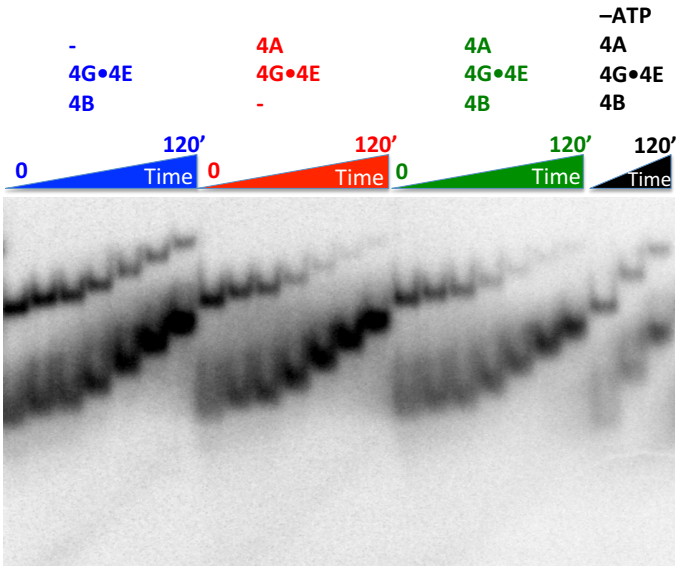

C

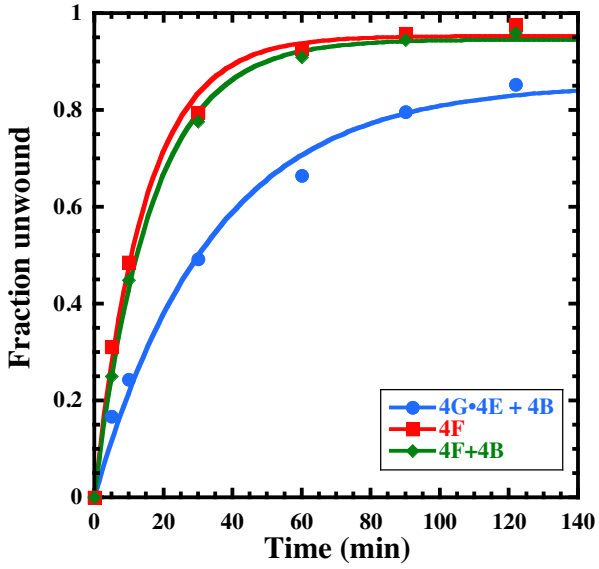

D

Protein	Rate sec^{-1}
4G•4E+4B	$4.8\ 10^{-4}$
4F	$11.5\ 10^{-4}$
4F+4B	$10.2\ 10^{-4}$

References

Acker, M. G., Kolitz, S. E., Mitchell, S. F., Nanda, J. S., & Lorsch, J. R. (2007). Reconstitution of yeast translation initiation. *Methods in Enzymology*, *430*(7), 111–45. http://doi.org/10.1016/S0076-6879(07)30006-2

Acker, M. G., Shin, B.-S., Nanda, J. S., Saini, A. K., Dever, T. E., & Lorsch, J. R. (2009). Kinetic analysis of late steps of eukaryotic translation initiation. *Journal of Molecular Biology*, *385*(2), 491–506. http://doi.org/10.1016/j.jmb.2008.10.029

Aitken, C. E., Beznosková, P., Vlčkova, V., Chiu, W.-L., Zhou, F., Valášek, L. S., … Lorsch, J. R. (2016). Eukaryotic translation initiation factor 3 plays distinct roles at the mRNA entry and exit channels of the ribosomal preinitiation complex. *eLife*, *5*, 1–37. http://doi.org/10.7554/eLife.20934

Aitken, C. E., & Lorsch, J. R. (2012). A mechanistic overview of translation initiation in eukaryotes. *Nature Structural & Molecular Biology*, *19*(6), 568–76. http://doi.org/10.1038/nsmb.2303

Algire, M. a, Maag, D., & Lorsch, J. R. (2005). Pi release from eIF2, not GTP hydrolysis, is the step controlled by start-site selection during eukaryotic translation initiation. *Molecular Cell*, *20*(2), 251–62. http://doi.org/10.1016/j.molcel.2005.09.008

Altmann, M., Müller, P. P., Wittmer, B., Ruchti, F., Lanker, S., & Trachsel, H. (1993). A Saccharomyces cerevisiae homologue of mammalian translation initiation factor 4B contributes to RNA helicase activity. *The EMBO Journal*, *12*(10), 3997–4003.

Andersen, C. B. F., Ballut, L., Johansen, J. S., Chamieh, H., Nielsen, K. H., Oliveira, C. L. P., … Andersen, G. R. (2006). Structure of the Exon Junction Core Complex with a Trapped DEAD-Box ATPase Bound to RNA. *Science*, *313*(5795), 1968–1972. http://doi.org/10.1126/science.1131981

Andreou, A. Z., Harms, U., & Klostermeier, D. (2017). eIF4B stimulates eIF4A ATPase and unwinding activities by direct interaction through its 7-repeats region. *RNA Biology*, *14*(1), 113–123. http://doi.org/10.1080/15476286.2016.1259782

Andreou, A. Z., & Klostermeier, D. (2013). The DEAD-box helicase eIF4A: paradigm or the odd one out? *RNA Biology*, *10*(1), 19–32. http://doi.org/10.4161/rna.21966

Andreou, A. Z., & Klostermeier, D. (2014). eIF4B and eIF4G Jointly Stimulate eIF4A ATPase and Unwinding Activities by Modulation of the eIF4A Conformational Cycle. *Journal of Molecular Biology*, *426*(1), 51–61.

http://doi.org/10.1016/j.jmb.2013.09.027

Aylett, C. H. S., Boehringer, D., Erzberger, J. P., Schaefer, T., & Ban, N. (2015). Structure of a Yeast 40S–eIF1–eIF1A–eIF3–eIF3j initiation complex. *Nat Struct Mol Biol*, *22*(3), 269–271. Retrieved from http://dx.doi.org/10.1038/nsmb.2963

Ballut, L., Marchadier, B., Baguet, A., Tomasetto, C., Séraphin, B., & Le Hir, H. (2005). The exon junction core complex is locked onto RNA by inhibition of eIF4AIII ATPase activity. *Nature Structural & Molecular Biology*, *12*(10), 861–869. http://doi.org/10.1038/nsmb990

Ben-Shem, A., Garreau de Loubresse, N., Melnikov, S., Jenner, L., Yusupova, G., & Yusupov, M. (2011). The structure of the eukaryotic ribosome at 3.0 Å resolution. *Science (New York, N.Y.)*, *334*(6062), 1524–9. http://doi.org/10.1126/science.1212642

Bhat, M., Robichaud, N., Hulea, L., Sonenberg, N., Pelletier, J., & Topisirovic, I. (2015). Targeting the translation machinery in cancer. *Nature Reviews. Drug Discovery*, *14*(4), 261–278. http://doi.org/10.1038/nrd4505

Bitterman, P. B., & Polunovsky, V. A. (2012). Attacking a nexus of the oncogenic circuitry by reversing aberrant eIF4F-mediated translation. *Molecular Cancer Therapeutics*, *11*(5), 1051–61. http://doi.org/10.1158/1535-7163.MCT-11-0530

Blum, S., Schmid, S. R., Pause, A., Buser, P., Linder, P., Sonenberg, N., & Trachsel, H. (1992). ATP hydrolysis by initiation factor 4A is required for translation initiation in Saccharomyces cerevisiae. *Proceedings of the National Academy of Sciences of the United States of America*, *89*(16), 7664–8. Retrieved from http://www.pubmedcentral.nih.gov/articlerender.fcgi?artid=49771&tool=pmcentrez&rendertype=abstract

Bradley, M. J., & De La Cruz, E. M. (2012). Analyzing ATP utilization by DEAD-Box RNA helicases using kinetic and equilibrium methods. *Methods in Enzymology*, *511*, 29–63. http://doi.org/10.1016/B978-0-12-396546-2.00002-4

Brune, M., Hunter, J. L., Corrie, J. E., & Webb, M. R. (1994). Direct, real-time measurement of rapid inorganic phosphate release using a novel fluorescent probe and its application to actomyosin subfragment 1 ATPase. *Biochemistry*, *33*(27), 8262–8271.

Caruthers, J. M., Johnson, E. R., & McKay, D. B. (2000). Crystal structure of yeast initiation factor 4A, a DEAD-box RNA helicase. *Proceedings of the National Academy of Sciences of the United States of America*, *97*(24),

13080–5. http://doi.org/10.1073/pnas.97.24.13080

Chen, H., Meisburger, S. P., Pabit, S. a., Sutton, J. L., Webb, W. W., & Pollack, L. (2012). Ionic strength-dependent persistence lengths of single-stranded RNA and DNA. *Proceedings of the National Academy of Sciences*, *109*(3), 799–804. http://doi.org/10.1073/pnas.1119057109

Chen, J., Choi, J., O'Leary, S. E., Prabhakar, A., Petrov, A., Grosely, R., … Puglisi, J. D. (2016). *The molecular choreography of protein synthesis: translational control, regulation, and pathways. Quarterly Reviews of Biophysics* (Vol. 49). http://doi.org/10.1017/S0033583516000056

Cuchalová, L., Kouba, T., Herrmannová, A., Dányi, I., Chiu, W.-L., & Valásek, L. (2010). The RNA recognition motif of eukaryotic translation initiation factor 3g (eIF3g) is required for resumption of scanning of posttermination ribosomes for reinitiation on GCN4 and together with eIF3i stimulates linear scanning. *Molecular and Cellular Biology*, *30*(19), 4671–86. http://doi.org/10.1128/MCB.00430-10

Das, S., & Das, B. (2016). eIF4G - An integrator of mRNA metabolism? *FEMS Yeast Research Advance Access Published*, *12*(May), 1–9. http://doi.org/10.1093/femsyr/fow087

des Georges, A., Dhote, V., Kuhn, L., Hellen, C. U. T., Pestova, T. V, Frank, J., & Hashem, Y. (2015). Structure of mammalian eIF3 in the context of the 43S preinitiation complex. *Nature*, *525*(7570), 491–495. Retrieved from http://dx.doi.org/10.1038/nature14891

Dever, T. E., & Green, R. (2012). The elongation, termination, and recycling phases of translation in eukaryotes. *Cold Spring Harbor Perspectives in Biology*, *4*(7). http://doi.org/10.1101/cshperspect.a013706

Dever, T. E., Kinzy, T. G., & Pavitt, G. D. (2016). Mechanism and regulation of protein synthesis in Saccharomyces cerevisiae. *Genetics*, *203*(1), 65–107. http://doi.org/10.1534/genetics.115.186221

Dong, J., Aitken, C. E., Thakur, A., Shin, B.-S., Lorsch, J. R., & Hinnebusch, A. G. (2017). Rps3/uS3 promotes mRNA binding at the 40S ribosome entry channel and stabilizes preinitiation complexes at start codons. *Proceedings of the National Academy of Sciences*, *114*(11), E2126–E2135. http://doi.org/10.1073/pnas.1620569114

Firczuk, H., Kannambath, S., Pahle, J., Claydon, A., Beynon, R., Duncan, J., … McCarthy, J. E. (2013). An in vivo control map for the eukaryotic mRNA translation machinery. *Molecular Systems Biology*, *9*(635), 635. http://doi.org/10.1038/msb.2012.73

Gao, Z., Putnam, A. A., Bowers, H. A., Guenther, U.-P., Ye, X., Kindsfather, A., … Jankowsky, E. (2016). Coupling between the DEAD-box RNA helicases Ded1p and eIF4A. *eLife*, *5*, 1–22.

http://doi.org/10.7554/eLife.16408

Garcia-Garcia, C., Frieda, K. L., Feoktistova, K., Fraser, C. S., & Block, S. M. (2015). Factor-dependent processivity in human eIF4A DEAD-box helicase. *Science*, *348*(6242), 1486–1488. http://doi.org/10.1126/science.aaa5089

Grifo, J. A., Tahara, S. M., Morgan, M. A., Shatkin, A. J., & Merrick, W. C. (1983). New initiation factor activity required for globin mRNA translation. *The Journal of Biological Chemistry*, *258*(9), 5804–5810. Retrieved from http://www.ncbi.nlm.nih.gov/pubmed/6853548

Gualerzi, C. O., & Pon, C. L. (2015). Initiation of mRNA translation in bacteria: Structural and dynamic aspects. *Cellular and Molecular Life Sciences*, *72*(22), 4341–4367. http://doi.org/10.1007/s00018-015-2010-3

Halder, S., & Bhattacharyya, D. (2013). RNA structure and dynamics: A base pairing perspective. *Progress in Biophysics and Molecular Biology*, *113*(2), 264–283. http://doi.org/10.1016/j.pbiomolbio.2013.07.003

Harms, U., Andreou, A. Z., Gubaev, A., & Klostermeier, D. (2014). eIF4B, eIF4G and RNA regulate eIF4A activity in translation initiation by modulating the eIF4A conformational cycle. *Nucleic Acids Research*, *42*(12), 7911–7922. http://doi.org/10.1093/nar/gku440

Hashem, Y., des Georges, A., Dhote, V., Langlois, R., Liao, H. Y., Grassucci, R. A., … Frank, J. (2013). Structure of the mammalian ribosomal 43S preinitiation complex bound to the scanning factor DHX29. *Cell*, *153*(5), 1108–19. http://doi.org/10.1016/j.cell.2013.04.036

Henn, A., Bradley, M. J., & De La Cruz, E. M. (2012). ATP utilization and RNA conformational rearrangement by DEAD-box proteins. *Annual Review of Biophysics*, *41*, 247–67. http://doi.org/10.1146/annurev-biophys-050511-102243

Hilbert, M., Kebbel, F., Gubaev, A., & Klostermeier, D. (2011). eIF4G stimulates the activity of the DEAD box protein eIF4A by a conformational guidance mechanism. *Nucleic Acids Research*, *39*(6), 2260–2270. http://doi.org/10.1093/nar/gkq1127

Hinnebusch, A. G. (2006). eIF3: a versatile scaffold for translation initiation complexes. *Trends in Biochemical Sciences*, *31*(10), 553–62. http://doi.org/10.1016/j.tibs.2006.08.005

Hinnebusch, A. G. (2014). The Scanning Mechanism of Eukaryotic Translation Initiation. *Annual Review of Biochemistry*, *83*, 779–812. http://doi.org/10.1146/annurev-biochem-060713-035802

Hinnebusch, A. G., & Lorsch, J. R. (2012). The Mechanism of Eukaryotic Translation Initiation: New Insights and Challenges. *Cold Spring Harbor Perspectives in Biology*. http://doi.org/10.1101/cshperspect.a011544

Hussain, T., Llácer, J. L., Fernández, I. S., Munoz, A., Martin-Marcos, P., Savva, C. G., … Ramakrishnan, V. (2014). Structural Changes Enable Start Codon Recognition by the Eukaryotic Translation Initiation Complex. *Cell*, *159*(3), 597–607. http://doi.org/10.1016/j.cell.2014.10.001

Jackson, R. J., Hellen, C. U. T., & Pestova, T. V. (2010). The mechanism of eukaryotic translation initiation and principles of its regulation. *Nature Reviews. Molecular Cell Biology*, *11*(2), 113–27. Retrieved from http://www.ncbi.nlm.nih.gov/pubmed/20094052

Jankowsky, E. (2011). RNA helicases at work: binding and rearranging. *Trends in Biochemical Sciences*, *36*(1), 19–29. http://doi.org/10.1016/j.tibs.2010.07.008

Jivotovskaya, A., Valášek, L., Hinnebusch, A. G., & Nielsen, K. H. (2006). Eukaryotic Translation Initiation Factor 3 (eIF3) and eIF2 Can Promote mRNA Binding to 40S Subunits Independently of eIF4G in Yeast. *Molecular and Cellular Biology*, *26*(4), 1355–1372. http://doi.org/10.1128/MCB.26.4.1355

Kolitz, S. E., & Lorsch, J. R. (2010). Eukaryotic initiator tRNA: finely tuned and ready for action. *FEBS Letters*, *584*(2), 396–404. http://doi.org/10.1016/j.febslet.2009.11.047

Korneeva, N. L., First, E. a, Benoit, C. a, & Rhoads, R. E. (2005). Interaction between the NH2-terminal domain of eIF4A and the central domain of eIF4G modulates RNA-stimulated ATPase activity. *The Journal of Biological Chemistry*, *280*(3), 1872–81. http://doi.org/10.1074/jbc.M406168200

Kozak, M. (1991). Structural features in eukaryotic mRNAs that modulate the initiation of translation. *Journal of Biological Chemistry*, *266*(30), 19867–19870.

Kramer, G., Konecki, D., Cimadevilla, J. M., & Hardesty, B. (1976). ATP requirement for binding of 125I-labeled globin mRNA to Artemia salina ribosomes. *Archives of Biochemistry and Biophysics*, *174*(1), 355–358. http://doi.org/http://dx.doi.org/10.1016/0003-9861(76)90356-8

Kumar, P., Hellen, C. U. T., & Pestova, T. V. (2016). Toward the mechanism of eIF4F-mediated ribosomal attachment to mammalian capped mRNAs. *Genes Dev*, *30*(13), 1573–1588. http://doi.org/10.1101/gad.282418.116

Laursen, B. S., Sørensen, H. P., Mortensen, K. K., & Sperling-Petersen, H. U. (2005). Initiation of protein synthesis in bacteria. *Microbiology and Molecular Biology Reviews : MMBR*, *69*(1), 101–23. http://doi.org/10.1128/MMBR.69.1.101-123.2005

LeFebvre, A. K., Korneeva, N. L., Trutschl, M., Cvek, U., Duzan, R. D., Bradley, C. A., … Rhoads, R. E. (2006). Translation Initiation Factor eIF4G-1 Binds to eIF3 through the eIF3e Subunit. *The Journal of*

Biological Chemistry, *281*(32), 22917–22932. http://doi.org/10.1074/jbc.M605418200

Linder, P., & Fuller-Pace, F. V. (2013). Looking back on the birth of DEAD-box RNA helicases. *Biochimica et Biophysica Acta*, *1829*(8), 750–755. http://doi.org/10.1016/j.bbagrm.2013.03.007

Linder, P., & Jankowsky, E. (2011). From unwinding to clamping - the DEAD box RNA helicase family. *Nature Reviews. Molecular Cell Biology*, *12*(8), 505–16. http://doi.org/10.1038/nrm3154

Linder, P., Lasko, P. F., Ashburner, M., Leroy, P., Nielsen, P. J., Nishi, K., … Slonimski, P. P. (1989). Birth of the D-E-A-D box. *Nature*. http://doi.org/10.1038/337121a0

Linder, P., & Slonimski, P. P. (1989). An essential yeast protein, encoded by duplicated genes TIF1 and TIF2 and homologous to the mammalian translation initiation factor eIF-4A, can suppress a mitochondrial missense mutation. *Proceedings of the National Academy of Sciences of the United States of America*, *86*(7), 2286–90. Retrieved from http://www.pubmedcentral.nih.gov/articlerender.fcgi?artid=286897&tool=pmcentrez&rendertype=abstract

Lindqvist, L., Imataka, H., & Pelletier, J. (2008). Cap-dependent eukaryotic initiation factor-mRNA interactions probed by cross-linking. *RNA*, *14*(5), 960–9. http://doi.org/10.1261/rna.971208

Liu, F., Putnam, A., & Jankowsky, E. (2008). ATP hydrolysis is required for DEAD-box protein recycling but not for duplex unwinding. *Proceedings of the National Academy of Sciences*, *51*(105), 20209–20214. Retrieved from http://www.pnas.org/content/105/51/20209.short

Llacer, J. L., Hussain, T., Marler, L., Aitken, C. E., Thakur, A., Lorsch, J. R., … Ramakrishnan, V. (2015). Conformational Differences between Open and Closed States of the Eukaryotic Translation Initiation Complex. *Molecular Cell*, *59*(3), 399–412. http://doi.org/10.1016/j.molcel.2015.06.033

Lorsch, J. R., & Herschlag, D. (1998). The DEAD box protein eIF4A. 1. A minimal kinetic and thermodynamic framework reveals coupled binding of RNA and nucleotide. *Biochemistry*, *37*(8), 2180–93. http://doi.org/10.1021/bi972430g

Lorsch, J. R., & Herschlag, D. (1999). Kinetic dissection of fundamental processes of eukaryotic translation initiation in vitro. *The EMBO Journal*, *18*(23), 6705–6717. http://doi.org/10.1093/emboj/18.23.6705

Lu, W.-T., Wilczynska, A., Smith, E., & Bushell, M. (2014). The diverse roles of the eIF4A family: you are the company you keep. *Biochemical Society Transactions*, *42*(1), 166–72. http://doi.org/10.1042/BST20130161

Maag, D., Fekete, C. a, Gryczynski, Z., & Lorsch, J. R. (2005). A conformational change in the eukaryotic

translation preinitiation complex and release of eIF1 signal recognition of the start codon. *Molecular Cell*, *17*(2), 265–75. http://doi.org/10.1016/j.molcel.2004.11.051

Majumdar, R., Bandyopadhyay, A., & Maitra, U. (2003). Mammalian translation initiation factor eIF1 functions with eIF1A and eIF3 in the formation of a stable 40 S preinitiation complex. *Journal of Biological Chemistry*, *278*(8), 6580–6587. http://doi.org/10.1074/jbc.M210357200

Merrick, W. C. (2015). eIF4F: A Retrospective. *Journal of Biological Chemistry*, *290*(40), 24091–24099. http://doi.org/10.1074/jbc.R115.675280

Milón, P., & Rodnina, M. V. (2012). Kinetic control of translation initiation in bacteria. *Critical Reviews in Biochemistry and Molecular Biology*, *47*(January), 334–48. http://doi.org/10.3109/10409238.2012.678284

Mitchell, S. F., & Lorsch, J. R. (2008). Should I stay or should I go? Eukaryotic translation initiation factors 1 and 1A control start codon recognition. *The Journal of Biological Chemistry*, *283*(41), 27345–9. http://doi.org/10.1074/jbc.R800031200

Mitchell, S. F., Walker, S. E., Algire, M. A., Park, E., Hinnebusch, A. G., & Lorsch, J. R. (2010). The 5′-7-Methylguanosine Cap on Eukaryotic mRNAs Serves Both to Stimulate Canonical Translation Initiation and to Block an Alternative Pathway. *Molecular Cell*, *39*(6), 950–62. http://doi.org/10.1016/j.molcel.2010.08.021

Mitchell, S. F., Walker, S. E., Rajagopal, V., Aitken, C. E., & Lorsch, J. R. (2011). Recruiting knotty partners: The roles of translation initiation factors in mRNA recruitment to the eukaryotic ribosome. In *Ribosomes. Springer Vienna* (pp. 155–169). Retrieved from http://link.springer.com/chapter/10.1007/978-3-7091-0215-2_13

Nanda, J. S., Cheung, Y.-N., Takacs, J. E., Martin-Marcos, P., Saini, A. K., Hinnebusch, A. G., & Lorsch, J. R. (2009). eIF1 controls multiple steps in start codon recognition during eukaryotic translation initiation. *Journal of Molecular Biology*, *394*(2), 268–85. http://doi.org/10.1016/j.jmb.2009.09.017

Nanda, J. S., Saini, A. K., Muñoz, A. M., Hinnebusch, A. G., & Lorsch, J. R. (2013). Coordinated Movements of Eukaryotic Translation Initiation Factors eIF1, eIF1A, and eIF5 Trigger Phosphate Release from eIF2 in Response to Start Codon Recognition by the Ribosomal Preinitiation Complex. *The Journal of Biological Chemistry*, *288*(8), 5316–29. http://doi.org/10.1074/jbc.M112.440693

Nielsen, K. H., Behrens, M. a, He, Y., Oliveira, C. L. P., Jensen, L. S., Hoffmann, S. V, … Andersen, G. R. (2011). Synergistic activation of eIF4A by eIF4B and eIF4G. *Nucleic Acids Research*, *39*(7), 2678–89.

http://doi.org/10.1093/nar/gkq1206

Oberer, M., Marintchev, A., & Wagner, G. (2005). Structural basis for the enhancement of eIF4A helicase activity by eIF4G. *Genes & Development*, *19*(18), 2212–23. http://doi.org/10.1101/gad.1335305

Özeş, A. R., Feoktistova, K., Avanzino, B. C., & Fraser, C. S. (2011). Duplex unwinding and ATPase activities of the DEAD-box helicase eIF4A are coupled by eIF4G and eIF4B. *Journal of Molecular Biology*, *412*(4), 674–87. http://doi.org/10.1016/j.jmb.2011.08.004

Palmiter, R. D. (1975). Quantitation of parameters that determine the rate of ovalbumin synthesis. *Cell*, *4*(3), 189–197. http://doi.org/http://dx.doi.org/10.1016/0092-8674(75)90167-1

Park, E.-H., Walker, S. E., Lee, J. M., Rothenburg, S., Lorsch, J. R., & Hinnebusch, A. G. (2011). Multiple elements in the eIF4G1 N-terminus promote assembly of eIF4G1•PABP mRNPs in vivo. *The EMBO Journal*, *30*(2), 302–16. http://doi.org/10.1038/emboj.2010.312

Park, E.-H., Walker, S. E., Zhou, F., Lee, J. M., Rajagopal, V., Lorsch, J. R., & Hinnebusch, A. G. (2013). Yeast eukaryotic initiation factor 4B (eIF4B) enhances complex assembly between eIF4A and eIF4G in vivo. *The Journal of Biological Chemistry*, *288*(4), 2340–54. http://doi.org/10.1074/jbc.M112.398537

Parsyan, A., Svitkin, Y., Shahbazian, D., Gkogkas, C., Lasko, P., Merrick, W. C., & Sonenberg, N. (2011). mRNA helicases: the tacticians of translational control. *Nature Reviews. Molecular Cell Biology*, *12*(4), 235–45. http://doi.org/10.1038/nrm3083

Passmore, L. A., Schmeing, T. M., Maag, D., Applefield, D. J., Acker, M. G., Algire, M. a, … Ramakrishnan, V. (2007). The eukaryotic translation initiation factors eIF1 and eIF1A induce an open conformation of the 40S ribosome. *Molecular Cell*, *26*(1), 41–50. http://doi.org/10.1016/j.molcel.2007.03.018

Peck, M. L., & Herschlag, D. (1999). Effects of oligonucleotide length and atomic composition on stimulation of the ATPase activity of translation initiation factor elF4A. *RNA (New York, N.Y.)*, *5*(9), 1210–1221. http://doi.org/10.1017/S1355838299990817

Pelletier, J., Graff, J., Ruggero, D., & Sonenberg, N. (2015). Targeting the eIF4F Translation Initiation Complex: A Critical Nexus for Cancer Development. *Cancer Research*, *75*(2), 250–263. http://doi.org/10.1158/0008-5472.CAN-14-2789

Pelletier, J., & Sonenberg, N. (1985). Insertion mutagenesis to increase secondary structure within the 5' noncoding region of a eukaryotic mRNA reduces translational efficiency. *Cell*, *40*(March), 515–526. http://doi.org/10.1016/0092-8674(85)90200-4

Pestova, T. V, & Kolupaeva, V. G. (2002). The roles of individual eukaryotic translation initiation factors in ribosomal scanning and initiation codon selection. *Genes & Development*, *16*(22), 2906–22. http://doi.org/10.1101/gad.1020902

Pisareva, V. P., Pisarev, A. V, Komar, A. A., Hellen, C. U. T., & Pestova, T. V. (2008). Translation initiation on mammalian mRNAs with structured 5'UTRs requires DExH-box protein DHX29. *Cell*, *135*(7), 1237–50. http://doi.org/10.1016/j.cell.2008.10.037

Qu, X., Wen, J.-D., Lancaster, L., Noller, H. F., Bustamante, C., & Tinoco, I. (2011). The ribosome uses two active mechanisms to unwind messenger RNA during translation. *Nature*, *475*(7354), 118–121. http://doi.org/10.1038/nature10126

Rajagopal, V., Park, E.-H., Hinnebusch, A. G., & Lorsch, J. R. (2012). Specific Domains in Yeast Translation Initiation Factor eIF4G Strongly Bias RNA Unwinding Activity of the eIF4F Complex toward Duplexes with 5'-Overhangs. *The Journal of Biological Chemistry*, *287*(24), 20301–12. http://doi.org/10.1074/jbc.M112.347278

Rogers, G., Richter, N., & Merrick, W. (1999). Biochemical and Kinetic Characterization of the RNA Helicase Activity of Eukaryotic Initiation Factor 4A. *Journal of Biological Chemistry*, *274*(18), 12236–12244. Retrieved from http://www.jbc.org/content/274/18/12236.short

Rogers, G. W. J., Komar, A. A., & Merrick, W. C. (2002). eIF4A: The Godfather of the DEAD Box Helicases. *Progress in Nucleic Acid Research and Molecular Biology*, *72*, 307–331.

Rogers, G. W., Lima, W. F., & Merrick, W. C. (2001). Further characterization of the helicase activity of eIF4A. Substrate specificity. *The Journal of Biological Chemistry*, *276*(16), 12598–608. http://doi.org/10.1074/jbc.M007560200

Rogers, G. W., Richter, N. J., Lima, W. F., & Merrick, W. C. (2001). Modulation of the Helicase Activity of eIF4A by eIF4B, eIF4H, and eIF4F. *Journal of Biological Chemistry*, *276*(33), 30914–30922. http://doi.org/10.1074/jbc.M100157200

Roux, P. P., & Topisirovic, I. (2012). Regulation of mRNA Translation by Signaling Pathways. *Cold Spring Harbor Perspectives in Biology*. http://doi.org/10.1101/cshperspect.a012252

Schütz, P., Bumann, M., Oberholzer, A. E., Bieniossek, C., Trachsel, H., Altmann, M., & Baumann, U. (2008). Crystal structure of the yeast eIF4A-eIF4G complex: an RNA-helicase controlled by protein-protein interactions. *Proceedings of the National Academy of Sciences*, *105*(28), 9564–9.

http://doi.org/10.1073/pnas.0800418105

Sen, N. D., Zhou, F., Ingolia, N. T., & Hinnebusch, A. G. (2015). Genome-wide analysis of translational efficiency reveals distinct but overlapping functions of yeast DEAD-box RNA helicases Ded1 and eIF4A. *Genome Research*, *25*, 1196–1205. http://doi.org/10.1101/gr.191601.115.25

Shibuya, T., Tange, T. Ø., Sonenberg, N., & Moore, M. J. (2004). eIF4AIII binds spliced mRNA in the exon junction complex and is essential for nonsense-mediated decay. *Nature Structural & Molecular Biology*, *11*(4), 346–51. http://doi.org/10.1038/nsmb750

Shirokikh, N. E., Agalarov, S. C., & Spirin, A. S. (2010). Chemical and enzymatic probing of spatial structure of the omega leader of tobacco mosaic virus RNA. *Biochemistry. Biokhimiia*, *75*(4), 405–411. http://doi.org/10.1134/S0006297910040024

Simonetti, A., Querido, J. B., Myasnikov, A. G., Mancera-Martinez, E., Renaud, A., Kuhn, L., & Hashem, Y. (2016). eIF3 Peripheral Subunits Rearrangement after mRNA Binding and Start-Codon Recognition. *Molecular Cell*, *63*(2), 206–217. http://doi.org/10.1016/j.molcel.2016.05.033

Sobczak, K., Michlewski, G., De Mezer, M., Kierzek, E., Krol, J., Olejniczak, M., … Krzyzosiak, W. J. (2010). Structural diversity of triplet repeat RNAs. *Journal of Biological Chemistry*, *285*(17), 12755–12764. http://doi.org/10.1074/jbc.M109.078790

Spirin, A. S. (2009). How does a scanning ribosomal particle move along the 5'-untranslated region of eukaryotic mRNA? Brownian Ratchet model. *Biochemistry*, *48*(45), 10688–92. http://doi.org/10.1021/bi901379a

Svitkin, Y. V, Ovchinnikov, L. P., Dreyfuss, G., & Sonenberg, N. (1996). General RNA binding proteins render translation cap dependent. *The EMBO Journal*, *15*(24), 7147–55. Retrieved from http://www.pubmedcentral.nih.gov/articlerender.fcgi?artid=452541&tool=pmcentrez&rendertype=abstract

Svitkin, Y. Y. V, Pause, A., Haghighat, A., Pyronnet, S., Witherell, G., Belsham, G. J., & Sonenberg, N. (2001). The requirement for eukaryotic initiation factor 4A (eIF4A) in translation is in direct proportion to the degree of mRNA 5' secondary structure. *RNA*, *7*, 382–394. Retrieved from http://rnajournal.cshlp.org/content/7/3/382.short

Takyar, S., Hickerson, R. P., & Noller, H. F. (2005). mRNA helicase activity of the ribosome. *Cell*, *120*(1), 49–58. http://doi.org/10.1016/j.cell.2004.11.042

Valásek, L. S. (2012). "Ribozoomin" – translation initiation from the perspective of the ribosome-bound eukaryotic initiation factors (eIFs). *Current Protein & Peptide Science*, *13*(4), 305–30. Retrieved from http://www.pubmedcentral.nih.gov/articlerender.fcgi?artid=3434475&tool=pmcentrez&rendertype=abstract

Voet, D., & Voet, J. G. (2004). *Biochemistry* (3rd ed.). Hoboken.

von der Haar, T., & McCarthy, J. E. G. (2002). Intracellular translation initiation factor levels in Saccharomyces cerevisiae and their role in cap-complex function. *Molecular Microbiology*, *46*(2), 531–44. Retrieved from http://www.ncbi.nlm.nih.gov/pubmed/12406227

Walker, S. E., & Fredrick, K. (2008). Preparation and evaluation of acylated tRNAs. *Methods*, *44*(2), 81–86. http://doi.org/10.1016/j.ymeth.2007.09.003

Walker, S. E., Zhou, F., Mitchell, S. F., Larson, V. S., Valasek, L., Hinnebusch, A. G., & Lorsch, J. R. (2013). Yeast eIF4B binds to the head of the 40S ribosomal subunit and promotes mRNA recruitment through its N-terminal and internal repeat domains. *RNA (New York, N.Y.)*, *19*(2), 191–207. http://doi.org/10.1261/rna.035881.112

Wells, S. E., Hillner, P. E., Vale, R. D., & Sachs, a B. (1998). Circularization of mRNA by eukaryotic translation initiation factors. *Molecular Cell*, *2*(1), 135–40. Retrieved from http://www.ncbi.nlm.nih.gov/pubmed/9702200

Woese, C. R., & Fox, G. E. (1977). Phylogenetic structure of the prokaryotic domain: the primary kingdoms. *Proceedings of the National Academy of Sciences of the United States of America*, *74*(11), 5088–5090. Retrieved from http://www.ncbi.nlm.nih.gov/pmc/articles/PMC432104/

Yusupov, M. M., Yusupova, G. Z., Baucom, a, Lieberman, K., Earnest, T. N., Cate, J. H., & Noller, H. F. (2001). Crystal structure of the ribosome at 5.5 A resolution. *Science (New York, N.Y.)*, *292*(5518), 883–896. http://doi.org/10.1126/science.1060089

Paul Yourik April 2017

Educational History

PhD	2017	Program in Biochemistry, Cellular and Molecular Biology Mentors: Jon R. Lorsch and James T. Stivers	Johns Hopkins University School of Medicine
B.S.	2010	Biochemistry	The Ohio State University

Professional Experience

Intramural Research Training Fellow	10/2013 – present	*Eunice Kennedy Shriver* National Institute of Child Health and Human Development
Doctoral Student Summer Research Intern	06/2016 – 092016	MedImmune
Doctoral Student Intern	03/2011 – 06/2011	Procter and Gamble
Research Contractor	02/2011 – 03/2011	Prestige Technical Services, Procter and Gamble
Undergraduate Researcher	09/2010 – 12/2010	The Ohio State University
Undergraduate Summer Intern	06/2010 – 09/2010	Procter and Gamble
Undergraduate Researcher	09/2009 – 06/2009	The Ohio State University
Undergraduate Summer Intern	06/2009 – 09/2009	Procter and Gamble
Undergraduate Researcher	04/2008 – 02/2009	The Ohio State University

Awards

2016	Summer Intern Poster Fair: 3rd Place	MedImmune
2015	Poster Award for Excellence in Research	Twentieth Annual Meeting of the RNA Society
2013	Graduate Research Fellowship Honorable Mention	National Science Foundation
2012	Graduate Research Fellowship Honorable Mention	National Science Foundation

2011	Irene Rosenfeld Scientific Achievement Award	The Ohio State University Department of Biochemistry
2010	Graduation with Research Distinction in Biochemistry	The Ohio State University
2010	3rd place in Biological Sciences	The Ohio State University Denman Undergraduate Research Forum
2010	Best Poster Award	The Ohio State University Biological, Physical, and Mathematical Sciences Fair

Publications

Yourik P, Aitken CE, Zhou F, Gupta N, Hinnebusch AG, Lorsch JR (2017) RNA helicase eIF4A is stimulated by the translation pre-initiation complex and promotes mRNA loading into the ribosomal entry channel regardless of structure. Manuscript in preparation for submission.

Munoz AM, **Yourik P**, Lorsch JR, Walker SE (2017) Active Yeast Ribosome Preparation Using Monolithic Anion Exchange Chromatography. RNA Biology. 14: 188-196.

Poster Presentations

Yourik P, Hofele R, Heidbrink-Thompson J (2016) Cross-linking mass spectrometry for characterization of protein interaction. Summer Intern Poster Fair, Gaithersburg, MD, August 19, 2016.

Yourik P, Aitken CE, Walker SE, Lorsch JR (2015) Probing the mechanism of eIF4F and ATP in translation initiation: a downstream target of oncogenic signaling pathways. Johns Hopkins University – MedImmune Science Day, Gaithersburg, MD, September 24, 2015.

Yourik P, Aitken CE, Walker SE, Lorsch JR (2015) Probing the mechanism of ATP utilization in mRNA recruitment to the eukaryotic ribosome. Twentieth Annual Meeting of the RNA Society, Madison, WI, May 28, 2015.

Yourik P, Lorsch JR (2015) Probing the mechanism of ATP utilization in mRNA recruitment to the eukaryotic ribosome. National Institutes of Health RNA Biology Conference, Bethesda, MD, March 11, 2015.

Yourik P, Lorsch JR (2014) Probing the mechanism of ATP utilization in mRNA recruitment to the eukaryotic ribosome. Cold Spring Harbor Laboratory Meeting on Translational Control, Cold Spring Harbor, NY, September 4, 2014.

Yourik P, Aitken CE, Walker SE, Lorsch JR (2014) Probing the mechanism of ATP and eIF4A in mRNA recruitment to the eukaryotic ribosome. National Institute of Child Health and Human Development Annual Retreat, Washington, DC, April 21, 2014.

Patents

2014	Dishwashing composition with improved protection against aluminum corrosion. (pending)

Leadership

2013 – 2016	NIH Fellows Committee Career Development Panel NICHD Representative
2014 – 2015	NIH Graduate Student Council Officer: Treasurer
2012 – 2013	Biophysics Research for Baltimore Teens Instructor and laboratory co-mentor
2011 – 2012	Incentive Mentoring Program Volunteer